Title
Morphology, Function, and Evolution of the Gills of High-Performance Fishes

Author
Wegner, Nicholas C.

Publication Date
2009

Peer reviewed

UNIVERSITY OF CALIFORNIA, SAN DIEGO

Morphology, function, and evolution of the gills of high-performance fishes

A dissertation submitted in partial satisfaction of the

requirements for the degree Doctor of Philosophy

in

Marine Biology

by

Nicholas Craig Wegner

Committee in charge:

Professor Jeffrey B. Graham, Chair

Professor Philip A. Hastings

Professor Matthew J. McHenry

Professor Frank L. Powell

Professor Richard H. Rosenblatt

2009

INFORMATION TO USERS

The quality of this reproduction is dependent upon the quality of the copy submitted. Broken or indistinct print, colored or poor quality illustrations and photographs, print bleed-through, substandard margins, and improper alignment can adversely affect reproduction.
In the unlikely event that the author did not send a complete manuscript and there are missing pages, these will be noted. Also, if unauthorized copyright material had to be removed, a note will indicate the deletion.

ProQuest LLC
789 East Eisenhower Parkway
P.O. Box 1346
Ann Arbor, MI 48106-1346

The Dissertation of Nicholas Craig Wegner is approved, and it is acceptable in quality and form for publication on microfilm and electronically:

_____

_____

_____

_____

_____
Chair

University of California, San Diego

2009

EPIGRAPH

"He was a very big Mako shark, built
to swim as fast as the fastest fish in the sea
and everything about him was beautiful…"

Ernest Hemingway

Old Man and the Sea

TABLE OF CONTENTS

LIST OF FIGURES

Chapter 1

Chapter 2

Chapter 3

Chapter 4

Appendix Chapter

LIST OF TABLES

Chapter 1

Chapter 2

Chapter 3

Chapter 4

Appendix Chapter

ACKNOWLEDGEMENTS

The research conducted for this dissertation was only possible through the help of many friends and colleagues. I am indebted to my advisor Jeffrey Graham, who provided me with the opportunity to attend Scripps Institution of Oceanography and work in the field of fish physiology. It is clear that he is deeply committed to my success as a scientist and I thank him for his constructive advice with respect to my research and in the scientific writing process. It has been a pleasure to work with him over the past few years, and I look forward to continued collaboration in the years to come. One of Jeff's greatest assets is his ability to work jointly with other scientists in related fields in order to answer complex questions, and to this end I thank him for his help in the selection of a committee which has given me helpful and constructive feedback. In addition, I wish to personally thank past and present members of the Graham laboratory, including Chugey Sepulveda, Dan Cartamil, Scott Aalbers, Kristina Bull, N.C. Lai, and Andy Nosal, who have helped in many aspects of my research. This, of course, is not an exhaustive list. Each chapter of the dissertation has an acknowledgements section that details the help of those involved and the various funding sources which made it all possible.

DISSERTATION MATERIAL PUBLISHED, SUBMITTED, OR IN PREPARATION FOR PULICATION

Chapter 1, in full, was submitted for publication as:

Wegner NC, Sepulveda CA, Bull KB, Graham JB. In press. Gill morphometrics in relation to gas transfer and ram ventilation in high-energy demand teleosts: Scombrids and billfishes. J Morph. The dissertation author is the primary investigator and author of this paper.

Chapter 2, in full, is currently being prepared for submission for publication as: Wegner NC, Sepulveda CA, Aalbers SA, Graham JB. Structural adaptations for ram ventilation: Gill fusions in scombrids and billfishes. Journal to be determined. The dissertation author is the primary investigator and author of this paper.

Chapter 3, in full, is currently being prepared for submission for publication as: Wegner NC, Sepulveda CA, Olson, KR, Hyndman KA, Graham JB. Functional morphology of the gills of the shortfin mako, *Isurus oxyrinchus*, a lamnid shark. J Morph. The dissertation author is the primary investigator and author of this paper.

Chapter 4, in full, is currently being prepared for submission for publication as: Wegner NC, Lai NC, Bull KB, Graham JB. Ram ventilation in the shortfin mako, *Isurus oxyrinchus*: Oxygen utilization and the branchial pressure gradient. J Exp Biol. The dissertation author is the primary investigator and author of this paper.

The appendix chapter, in full, was published as: Wegner NC, Sepulveda CA, Graham JB. 2006. Gill specializations in high-performance pelagic teleosts, with reference to striped marlin (*Tetrapturus audax*) and wahoo (*Acanthocybium solandri*). Bull Mar Sci 79:747-759. The dissertation author is the primary investigator and author of this paper.

CURRICULUM VITAE

EDUCATION

2004 Bachelor of Science
General Biology
University of California, San Diego

2009 Doctor of Philosophy
Marine Biology
Scripps Institution of Oceanography
University of California, San Diego

PUBLICATIONS

Wegner NC, Sepulveda CA, Bull KB, Graham JB. (In press) Gill morphometrics in relation to gas transfer and ram ventilation in high-energy demand teleosts: Scombrids and billfishes. J Morph.

Graham, JB and **Wegner, NC**. (In press) Breathing air in water and in air: The air-breathing fishes. *In* Respiratory Physiology of Vertebrates: Life With and Without Oxygen (GE Nilsson ed.) Cambridge University Press.

Seymour, RS, **Wegner, NC**, and Graham, JB. (2008) Body size and the air-breathing organ of the Atlantic tarpon *Megalops atlanticus*. Comp Bio Physiol A. 150:282-287.

Graham, JB, Lee, HL, and **Wegner, NC.** (2007) Transition from water to land in an extant group of fishes: Air breathing and the acquisition sequence of adaptations for amphibious life in oxudercine gobies. *In* Fish Respiration and Environment (MN Fernandes et al., eds.) Science Publishers: Enfield. p. 255-288

Wegner, NC, Sepulveda, CA, and Graham, JB. (2006) Gill specializations in high-performance pelagic teleosts, with reference to striped marlin (*Tetrapturus audax*) and wahoo (*Acanthocybium solandri*). Bull Mar Sci 79:747-760.

Sepulveda, CA, **Wegner, NC**, Bernal, D, and Graham, JB. (2005) The red muscle morphology of the thresher sharks (family Alopiidae). J Exp Biol 208:4255-4261.

SELECTED AWARDS

Achievement Rewards for College Scientists (ARCS) Scholarship, Los Angeles Chapter (2007-2009)
Samuel H. Gruber Award for Outstanding Student Oral Presentation (2008)
American Elasmobranch Society Student Travel Award (2008)
Art Proceeds Peterson Fellowship (2007)
Haymet-Kennel Student Lecture Award (2007)
Tuna Conference Scholarship (2007)
Edna Bailey Sussman Foundation Award (2006, 2007)
Seagrant Traineeship (2004-2007)
Research Assistance Award, Amer. Inst. of Fisheries Research Biologists (2006)
California Diving & Aquatic Studies Scholarship (2005)
Research funding from the Tuna Industry Endowment Fund (2005)

FIELDS OF STUDY

Respiratory specializations in high-performance fishes
Adaptations for air breathing in fishes
Fish habitat utilization and movement patterns
Shark muscle morphology

ABSTRACT OF THE DISSERTATION

Morphology, function, and evolution of the gills of high-performance fishes

by

Nicholas Craig Wegner

Doctor of Philosophy in Marine Biology

University of California, San Diego, 2009

Jeffrey B. Graham, Chair

This dissertation describes gill specializations related to fast, continuous swimming in tunas, bonitos, and mackerels (family Scombridae), the billfishes (Istiophoridae, Xiphiidae) and the shortfin mako, *Isurus oxyrinchus* (Lamnidae). These fishes all require gill adaptations for increased gas exchange to meet

relatively high aerobic demands and for added rigidity to withstand the forceful branchial flow produced by ram ventilation. Preliminary research for this dissertation, included as an appendix chapter and published as Wegner et al. (2006), examined gill specializations in the striped marlin, *Kajikia audax* (formerly *Tetrapturus audax*), and the wahoo, *Acanthocybium solandri*, and sets the stage for Chapters 1-4. Chapter 1 documents changes in scombrid and billfish gill morphometrics which augment gill surface area above that of other fish groups and increase branchial resistance to slow and streamline ram-ventilatory flow. Many scombrids and billfishes also have gill fusions which provide support and secure the spatial relationship of filaments and lamellae. Chapter 2 details the structure, function, and distribution of these fusions within different species; they are most complex in large tunas and billfishes, which are obligate ram ventilators, but are absent in mackerels, which utilize active ventilation at slower swimming speeds. Chapter 3 investigates the convergence of mako and tuna gill structure in relation to high aerobic demands and ram ventilation and shows that although makos have relatively larger gill surface areas and shorter diffusion distances than those of other shark species, these features are not as specialized as those of tunas. This work suggests that differences in the gill design of elasmobranchs and teleosts may limit mako gill surface area and ultimately constrain mako aerobic performance in comparison to tunas. Chapter 4 tests this hypothesis with *in vivo* studies of gill function in makos swimming in a water tunnel. Mako gills are similar to those of tunas in terms of oxygen utilization, the total pressure gradient driving the

ventilatory stream, and flow conditions along the respiratory surfaces. However, the interbranchial septum, an intrinsic feature of the shark gill, greatly contributes to mako branchial resistance, and this is compensated by changes to gill dimensions that ultimately limit gill surface area.

INTRODUCTION

A number of fishes including the tunas and some of their relatives (family Scombridae), the billfishes (Istiophoridae, Xiphiidae), and the lamnid sharks (Lamnidae) are often described as "high-performance" based on their capacities for an elevated rate of aerobic metabolism and for relatively fast, continuous swimming (Dickson, 1995; Bernal et al., 2001; Graham and Dickson, 2004). These fishes ventilate their gills by ram ventilation, a mechanism in which the forward momentum of continuous swimming is the driving force for water flow through the branchial chamber (Brown and Muir, 1970; Roberts, 1975). The gills of high-performance fishes accordingly require structural support to ensure that the force of the ram-ventilatory flow stream does not alter the normal orientation of the gill epithelium with respect to flow and thus reduce efficacy. These fishes also have gill specializations for augmenting respiratory gas transfer required by their high aerobic demands. Tunas, for example, have much larger gill surface areas than those of most other fishes (Muir and Hughes, 1969; Palzenberger and Pohla, 1992) and possess fusions on the gill filaments and lamellae which increase rigidity (Muir and Kendall, 1968; Muir, 1969; Johnson, 1986; Wegner et al., 2006). Although much is known about tuna gill specialization, there are few comparative data on gill surface areas and other adaptations for increased gas exchange or the occurrence of fusions or related modifications in the gills of other high-performance fish species.

This dissertation fills these voids by examining the evolution and diversity of gill specialization in the Scombridae, and, by comparing scombrid gills to those of billfishes and lamnid sharks, it documents the breadth of the functional convergence in gill specialization for high performance. The studies contained in this dissertation answer two main questions: 1. How do the gills of these different groups compare to tunas for specializations required by ram ventilation and for meeting increased oxygen demands associated with high aerobic performance? 2. How do marked intrinsic differences in the gill design of teleosts (scombrids and billfishes) and elasmobranchs (lamnid sharks) affect water-flow dynamics and gas exchange during ram ventilation?

The dissertation is a four-part comparative study. Chapter 1 describes the gill morphometrics in three non-tuna scombrids and two billfishes in comparison to tunas and examines features of gill design related to high rates of gas transfer and the high-pressure branchial flow associated with fast, continuous swimming. Chapter 2 investigates specializations in scombrids and billfishes for maintaining gill structural integrity during ram ventilation by tracing the type and pattern of gill-supporting fusions through the scombrid and billfish clades. Chapter 3 examines the gill structure of the shortfin mako (*Isurus oxyrinchus*), a lamnid shark, in order to determine the extent to which lamnid gills differ from those of other shark species and show convergence with tunas in specializations for augmenting gas transfer and increasing gill rigidity for ram ventilation. Finally, Chapter 4 examines mako ram ventilation while swimming in a water tunnel, in which measurements were made of the

transbranchial pressure gradient in relation to swimming speed, and a polarographic O_2 sensor was used to obtain a synoptic view of branchial O_2 utilization.

LITERATURE CITED

Bernal D, Dickson KA, Shadwick RE, Graham JB. 2001. Review: Analysis of the evolutionary convergence for high performance swimming in lamnid sharks and tunas. Comp Biochem Physiol 129:695-726.

Brown CE, Muir BS. 1970. Analysis of ram ventilation of fish gills with application to skipjack tuna (*Katsuwonus pelamis*). J Fish Res Bd Canada 27:1637-1652.

Dickson KA. 1995. Unique adaptations of the metabolic biochemistry of tunas and billfishes for life in the pelagic environment. Environ Biol Fishes 42:65-97.

Graham JB, Dickson KA. 2004. Tuna comparative physiology. J Exp Biol 207:4015-4024.

Johnson GD. 1986. Scombroid phylogeny: An alternative hypothesis. Bull Mar Sci 39:1-41.

Muir BS. 1969. Further observations on gill modifications of oceanic fishes. Copeia 1969:629.

Muir BS, Hughes GM. 1969. Gill dimensions for three species of tunny. J Exp Biol 51:271-285.

Muir BS, Kendall JI. 1968. Structural modifications in the gills of tunas and some other oceanic fishes. Copeia 1968:388-398.

Palzenberger M, Pohla H. 1992. Gill surface area of water-breathing freshwater fish. Rev Fish Biol Fisheries 2:187-196.

Roberts JL. 1975. Active branchial and ram gill ventilation in fishes. Biol Bull Mar Biol Lab, Woods Hole 148:85-105.

Wegner NC, Sepulveda CA, Graham JB. 2006. Gill specializations in high-performance pelagic teleosts, with reference to striped marlin (*Tetrapturus audax*) and wahoo (*Acanthocybium solandri*). Bull Mar Sci 79:747-759.

CHAPTER 1: GILL MORPHOMETRICS IN RELATION TO GAS TRANSFER AND RAM VENTILATION IN HIGH-ENERGY DEMAND TELEOSTS: SCOMBRIDS AND BILLFISHES

ABSTRACT

This comparative study of the gill morphometrics in scombrids (tunas, bonitos, and mackerels) and billfishes (marlins, swordfish) examines features of gill design related to high rates of gas transfer and the high-pressure branchial flow associated with fast, continuous swimming. Tunas have the largest relative gill surface areas of any fish group, and although the gill areas of non-tuna scombrids and billfishes are smaller than those of tunas, they are also disproportionally larger than those of most other teleosts. The morphometric features contributing to the large gill surface areas of these high- energy demand teleosts include: 1. a relative increase in the number and length of gill filaments that have, 2. a high lamellar frequency (i.e., the number of lamellae per length of filament), and 3. lamellae that are long and low in profile (height), which allows a greater number of filaments to be tightly packed into the branchial cavity. Augmentation of gill area through these morphometric changes represents a departure from the general mechanism of area enhancement utilized by most teleosts, which lengthen filaments and increase the size of the lamellae. The gill design of scombrids and billfishes reflects the combined requirements for ram ventilation and elevated energetic demands. The high lamellar frequencies and long lamellae increase branchial resistance to water flow which slows and streamlines the ram ventilatory stream. In general, scombrid and billfish gill surface areas correlate

with metabolic requirements and this character may serve to predict the energetic demands of fish species for which direct measurement is not possible. The branching of the gill filaments documented for the swordfish in this study appears to increase its gill surface area above that of other billfishes and may allow it to penetrate oxygen-poor waters at depth.

INTRODUCTION

Fish gill structure varies in relation to activity level and habitat use. Correspondingly, fishes with high metabolic requirements or inhabiting hypoxic environments generally have gill specializations facilitating gas transfer (Hughes, 1966; 1970; Hughes and Morgan, 1973; De Jager and Dekkers, 1975; Graham, 2006; Mandic et al., 2009). Gill dimensions, including the length and abundance of gill filaments, the number of respiratory lamellae on the filaments, and lamellar bilateral surface area, are altered by selective factors to augment gill surface area and increase oxygen uptake from the water. Research on gill morphology and ventilatory mechanics suggests that teleost gill morphometrics balance the optimization of gas exchange to meet metabolic demands with the limitation of branchial resistance to minimize the energetic costs associated with the biphasic buccal-branchial pump system used to actively ventilate the gills (Hughes, 1966; Hughes and Morgan, 1973). Accordingly, Hughes (1966) theorized that gill surface area could be optimally increased by long gill filaments with large lamellae and this has subsequently been documented in numerous groups of fishes, including some African swamp teleosts

living in hypoxic waters (Chapman, 2007) and some marine species living within the oxygen minimum layer (Graham, 2006).

While the gill morphometrics recruited to increase gill surface area appear consistent in a number of species, other fishes are unlikely to conform to these "rules of assembly." Specifically, fast, continuously swimming teleosts such as scombrids (tunas, bonitos, and mackerels) and billfishes (marlins and swordfish) differ from other teleosts by having metabolic demands that are greater than those of other fishes (Brill, 1979; 1987; Brill and Bushnell, 1991; Dewar and Graham, 1994; Korsmeyer and Dewar, 2001), and by utilizing ram ventilation, the mechanism in which the forward momentum of continuous swimming is the driving force for ventilatory water flow through the gills (Roberts, 1975; Freadman, 1981; Roberts and Rowell, 1988). While tuna gill morphometrics has been studied (Muir and Hughes, 1969), a more comprehensive sampling of pelagic teleosts, ranging in aerobic capacity, is needed for insight into the selective effects of metabolic demand and ram ventilation on gill area and dimensions.

Tunas (family Scombridae) differ from other pelagic teleosts including other scombrids (mackerels, Spanish mackerels, wahoo, bonitos) in having a unique anterior and central positioning of the red (aerobic) swimming musculature coupled with counter-current heat exchangers (*retia mirabilia*) that allows for the retention of body heat produced through continuous swimming and ultimately increases muscle-power output and other metabolic functions (Carey and Teal, 1966; Altringham and Block, 1997; Graham and Dickson, 2001). The conservation of metabolically produced heat

in the red muscle, eye and brain, and in some species, the viscera, its concomitant effects on the different tissues, and the high somatic and gonadal growth rates of tunas, all increase their metabolic demands above that of other fishes (Korsmeyer and Dewar, 2001). Oxygen acquisition in tunas is augmented through disproportionately large gill surface areas, which are as much as an order of magnitude larger than those of other marine teleosts (Muir and Hughes, 1969; Palzenberger and Pohla, 1992). Additional tuna gill specializations include thin diffusion distances and an unconventional diagonal blood-flow pattern that appears to optimize gas transfer (Muir, 1970; Muir and Brown, 1971; Olson et al., 2003; Wegner et al., 2006). A series of unique fusions connecting the gill filaments and lamellae function to support tuna gills against the forces of ram ventilation (Muir and Kendall, 1968; Johnson, 1986; Wegner et al., 2006).

Within the Scombridae, the sequence of evolutionary changes (from mackerel, less derived, to tunas, most derived) has been well documented in terms of gross muscle and skeletal morphology (Graham and Dickson, 2000; Collette et al., 2001) locomotor adaptations (Magnuson, 1978; Westneat and Wainwright, 2001), swimming biomechanics (Donley and Dickson, 2000; Altringham and Shadwick, 2001; Dowis et al., 2003), thermoregulation (Graham and Dickson, 2000; 2001), and energetics (Sepulveda and Dickson, 2000; Korsmeyer and Dewar, 2001; Sepulveda et al., 2003). However, the evolutionary progression of changes in gill morphometry remains generally unstudied. Limited gill surface area measurements for some non-tuna scombrids have been published (Gray, 1954; Steen and Berg, 1966; Hughes, 1970;

1972), but the small sample size and limited body-size range of the specimens examined preclude accurate interspecies comparison. With the exception of gill area estimates for the dolphinfish, *Coryphaena hippurus* (Hughes, 1970), even less is known for non-scombrid, high-energy demand teleosts. As a result, there has been little consideration of how groups such as the billfishes (families Xiphiidae, Istiophoridae) relate to tunas in terms of gill morphometry. Although billfishes lack the red-muscle endothermy of tunas, they possess a number of features related to fast and continuous swimming (Dobson et al., 1986; Davie, 1990; Dickson, 1995), including gill-supporting fusions that appear to rival tunas in structural complexity (Johnson, 1986; Wegner et al., 2006).

This study examines the gill morphometry of five active pelagic teleosts (three non-tuna scombrids and two billfish species) for comparison with tunas, and investigates the rules of assembly governing the optimization of gill design in these fishes to meet requirements for high rates of gas transfer and ram ventilation.

METHODS

Total gill surface areas were determined for three non-tuna scombrid species: Eastern Pacific bonito, *Sarda chiliensis* (n=8, 0.2 - 6.4 kg), wahoo, *Acanthocybium solandri* (n=8, 2.1 - 24.2 kg), and Pacific chub mackerel, *Scomber japonicus* (n=8, 95 - 740 g), and two species of billfish: Striped marlin, *Kajikia audax* (n=7, 8.0 - 70.0 kg), and swordfish, *Xiphias gladius* (n=4, 22.0 - 125.1 kg). Gill areas were also determined for one skipjack tuna, *Katsuwonus pelamis* (3.4 kg), and one yellowfin

tuna, *Thunnus albacares* (4.3 kg) in order to verify that the analytical methods used in this study yielded results that were consistent with previous work (Muir and Hughes, 1969).

Gill collection

Specimens were collected by hook and line off the coasts of Southern California and Hawaii, USA and Baja California, Mexico. Fish were euthanized immediately upon capture by surgically severing the spinal cord in accordance with Protocol S00080 of the University of California, San Diego Institutional Animal Care and Use Committee. Fish mass was determined by electronic scale or, when direct measurement was not possible, by using weight-length regression equations for the different species (Chatwin, 1959; Ponce-Díaz et al., 1991; DeMartini et al., 2000; Beerkircher, 2005).

Freshly euthanized specimens were placed ventral side up in a V-shaped cradle and the gills were irrigated with aerated sea water. The gills received one of two treatments. 1. Gills from approximately one half of the specimens were immediately excised and placed in 10% formalin buffered in seawater. 2. Gills from the remaining specimens were perfused with vascular casting solution (Mercox, Ladd Research, Williston, VT) according to methods described in Wegner et al. (2006). For this treatment, the heart was exposed by midline incision, cannulated, and specimens were perfused with heparinized teleost saline (Brill and Dizon, 1979) followed by the casting solution. Perfusions were conducted at physiological pressures (70-100

mmHg) consistent with those used in a previous study of tuna gill casting (Olson et al., 2003) in order to prevent rupturing and possible over-inflation of the gill blood vessels. Following perfusion, irrigation of the gills with sea water continued until complete polymerization of the casting solution (<15 min following injection), at which point the four gill arches from one side of each fish were placed into 10% formalin buffered in seawater. The other four arches were macerated in 15-20% KOH to remove all of the tissue from the casts.

Total gill surface area

Gill surface areas were estimated using methods established by Muir and Hughes (1969) and Hughes (1984b), and calculated by the equation:

$$A = L_{fil} \cdot 2n_{lam} \cdot A_{lam}$$

where A is total gill surface area, L_{fil} is the total length of all of the gill filaments, n_{lam} is lamellar frequency [the mean number of lamellae per unit length on one side of a filament (this is multiplied by two to account for the lamellae on both sides of each filament)], and A_{lam} is the mean bilateral surface area of a lamella.

For each specimen, all of the filaments on the four gill arches from one side of the head were counted. In specimens having more than 300 filaments per gill hemibranch, the filaments where divided into bins of 40 and the length of the medial filament (i.e., 20^{th}, 60^{th}, 100^{th}, etc.) was determined and assumed to represent the average filament length for that bin. For individuals with fewer than 300 filaments per hemibranch, a bin size of 20 was used. Filament lengths were measured using fixed

(or cast and subsequently fixed) material. Macerated vascular casts were not used to make this measurement because the casting solution did not always penetrate to the tip of each filament and would thus cause underestimation of length. Total filament length was calculated by combining the length determinations for each bin on each arch from one side of the head and then doubling this quantity to account for the filaments of the four gill arches on the other side of the head that were not measured.

Preliminary morphometric comparisons for all gill arches revealed that filaments on the third arch were most representative of average lamellar frequency and bilateral surface area, and further examination revealed that the anterior and posterior hemibranchs of gill arch three did not differ significantly with respect to these dimensions. Accordingly, all lamellar frequency and bilateral surface area data were obtained from the anterior hemibranch of the third gill arch. The medial filament of each bin from this hemibranch was removed from the arch, rinsed in deionized water, dehydrated in ethanol (20-25% increments over 24 hours), and critical-point dried to facilitate the acquisition of digital images and the removal of intact lamellae from the base, middle, and tip of each filament. Digital images were acquired using a camera mounted on a light microscope and analyzed using NIH Image J computer software to determine lamellar frequencies and areas. Vascular-cast filaments from the third gill arch were also sampled, photographed using a light microscope, and analyzed. Comparison of cast and critical-point-dried lamellae revealed that some shrinkage of lamellar bilateral surface area occurred during the drying process. For specimens not perfused with vascular casting solution, lamellar areas were thus adjusted by a species-

specific correction factor that was determined by comparing cast and non-cast lamellae.

Lamellar blood flow

Cast gill material was also examined for comparison with previous studies which have described a unique diagonal pattern of blood flow through the lamellae of some scombrids and billfishes (Muir, 1970; Muir and Brown, 1971; Olson et al., 2003; Wegner et al., 2006). Twenty cast lamellae from each specimen were randomly sampled and viewed under low-vacuum mode using an FEI Quanta 600 scanning electron microscope. Acquired digital images of the lamellae were analyzed using Image J; the angle of blood flow relative to the lamellar long axis was measured midway along the length of each lamella.

Statistical Analysis

For each species, total gill surface area (A) and corresponding gill dimensions (L_{fil}, n_{lam}, A_{lam}) were plotted in relation to body mass and linear regression equations were calculated. Regression lines for the different species were compared using 10,000 bootstrap replications (R v2.7.0) of the raw data, and statistical difference between species was determined if less than 5% of the resultant regression replicas intersected within the overlapping body-mass range of the species being compared. Species that did not overlap in mass were not compared statistically. The scaling exponents of the regressions were also compared to predictions assuming isometric

scaling of gill growth using 95% confidence intervals. Finally, the angles of lamellar blood flow were compared between species using a one-way ANOVA in conjunction with a Tukey test.

RESULTS

Gill surface area

Figure 1 shows the total gill surface area in relation to body mass for the species examined in this study together with data for tunas (Muir and Hughes, 1969) and other marine teleosts (Hughes, 1970; Palzenberger and Pohla, 1992). Estimates of total gill surface area for the 3.4 kg skipjack tuna and 4.2 kg yellowfin tuna made in this study fit on the regressions determined for the same species by Muir and Hughes (1969) (Note: Muir and Hughes reported bluefin tuna, *Thunnus thynnus*, and yellowfin tuna data together as a single bluefin-yellowfin tuna regression). The consistency of data between the two reports confirms the morphometric methods used in this study and verifies that the skipjack tuna has the largest relative gill surface area of any teleost species examined to date. When compared over their shared ranges of body mass, skipjack tuna have significantly larger gill surface areas than those of bluefin-yellowfin tuna, eastern Pacific bonito, and wahoo. Bluefin-yellowfin tuna have significantly larger gill areas than those of bonito, wahoo, swordfish (when fish mass is greater than 29.93 kg), and striped marlin. Bonito gill areas are significantly larger than those of wahoo throughout the majority of their overlapping weight range ($P < 0.05$ when fish mass is greater than 2.72 kg), but are not significantly greater than

those of Pacific chub mackerel. Wahoo gill areas do not differ significantly from those of striped marlin and appear less than those of swordfish (however, the later relationship is not significant due to the small swordfish sample size). Swordfish have larger gill areas than those of striped marlin for the majority of their overlapping weight range ($P < 0.05$ when fish mass is greater than 34.78 kg).

The scaling exponents of gill surface area to body mass for the species examined range from 0.74 to 0.97, which is within the range found in other teleosts (Hughes, 1972; De Jager and Dekkers, 1975; Palzenberger and Pohla, 1992). These scaling exponents are higher than that predicted by geometric similarity assuming isometric gill growth (0.67); the 95% confidence intervals for bluefin-yellowfin tuna (0.7576 - 1.0070), bonito (0.7549 - 0.9185), wahoo (0.8066 - 1.1176), and mackerel (0.7440 - 1.1920) all fall above this prediction.

Total filament length

Regressions for total filament length and body mass are shown in Figure 2. Skipjack tuna total filament length is not larger than that of bluefin-yellowfin tuna, but is significantly greater than that of both bonito and wahoo. Bluefin-yellowfin tuna total filament length is also significantly larger than that of bonito and wahoo, but does not differ statistically from that of striped marlin. Bonito total filament length does not differ significantly from that of wahoo or mackerel for most of their overlapping range of body mass.

Total filament length in swordfish appears greater than in bluefin-yellowfin tuna, wahoo, and striped marlin (Fig. 2); however, because of the limited swordfish sample size, total filament length is only significantly different with respect to striped marlin ($P < 0.05$ when fish mass is greater than 42.19 kg). The high total filament length of swordfish results from a unique branching of the gill filaments (Fig. 3). Although filament branching in the swordfish occurs throughout each gill hemibranch, it is most elaborate on filaments originating near the acute angle formed by the ceratobranchial-epibranchial joint of the gill arch (Fig. 3A,C). The small number of filaments emanating from the gill arch at this location branch extensively to fill the area created as the filaments radiate outward. The widespread filament branching observed in swordfish was not present in the other pelagic teleosts examined (e.g., Fig. 3B,D for striped marlin). Although a few isolated cases of filament branching were observed in striped marlin, these often appear to be associated with filament regeneration following gill damage and are not inherent structural features of the gill that increase surface area.

The scaling exponents for total filament length in the scombrids and billfishes examined extend from 0.26 - 0.48, which range is similar to that found in other teleosts (0.28 - 0.52) (Hughes, 1972; Palzenberger and Pohla, 1992).

It is important to further note that the gill dimension "total filament length" has two constituent parts: the average length of the gill filaments (average filament length) and their total number (total filament number). For each species, regressions for the two components were determined in relation to body mass, and these are shown in

Table 1. Wahoo average filament length is significantly less than that of skipjack tuna, bluefin-yellowfin tuna, bonito, and striped marlin. Other interspecies comparisons do not show any significant differences. For total filament number, bonito have significantly fewer filaments than skipjack tuna, bluefin-yellowfin tuna, and wahoo. Examination of the regression lines shows that like bonito, mackerel also possess fewer filaments than the other pelagic teleosts examined; however, because the body-mass range of mackerel does not overlap with that of the other teleosts, this difference was not quantified statistically. Swordfish were not included in these analyses because the unique branching of the gill filaments prevents accurate comparison with other species.

Lamellar frequency

Regressions in Figure 4 compare the number of lamellae per mm of filament as a function of body mass. Skipjack tuna lamellar frequency per mm is not significantly different from that of bluefin-yellowfin tuna or bonito, but is greater than that of wahoo ($P < 0.05$ when fish mass is less than 6.22 kg). The lamellar frequency in bluefin-yellowfin tuna is significantly greater than in swordfish and striped marlin ($P < 0.05$ for most of their shared weight range), but lower than in bonito. In addition to bluefin-yellowfin tuna, the lamellar frequency of bonito also is significantly greater than that of wahoo and striped marlin, but is significantly less than that of mackerel. Wahoo lamellar frequency is greater than that of swordfish and striped marlin ($P <$

0.05 for most of their overlapping body-mass range). Swordfish have a significantly lower lamellar frequency than that of striped marlin.

The scaling exponents for lamellar frequency and body mass for the pelagic teleosts examined range from -0.089 to 0.006, which falls within the range determined for other bony fishes (Hughes, 1972; Palzenberger and Pohla, 1992).

Lamellar area

Regressions for lamellar bilateral surface area in relation to body mass are shown in Figure 5. The average lamellar surface area of skipjack tuna is significantly larger than that of bluefin-yellowfin tuna and wahoo ($P < 0.05$ for most of the overlapping range of body mass), but does not differ significantly from that of bonito. Bluefin-yellowfin tuna lamellar area is significantly larger than that of wahoo and striped marlin, but is not statistically different from that of bonito or swordfish. Bonito lamellar area is greater than that of wahoo for most of their shared weight range, but does not differ significantly from that of mackerel. The average bilateral lamellar area of wahoo does not differ significantly from that of striped marlin and is significantly less than that of swordfish. Swordfish lamellar area is significantly greater than that of striped marlin.

The scaling exponents of lamellar area and body mass range from 0.41 to 0.58 for the pelagic teleosts examined and fall within the range reported for other teleosts (Hughes, 1972; Palzenberger and Pohla, 1992).

Lamellar shape and blood flow

The lamellae of the examined pelagic teleosts are rectangular and have a high aspect ratio (i.e., they are several times longer than they are high). This differs from the lamellae of most other teleosts, which have a lower aspect ratio and are frequently triangular or semicircular (Hughes, 1970; Hughes and Morgan, 1973). Associated with the high aspect ratio of scombrid and billfish lamellae are lamellar blood-flow patterns that usually differ from those of other fishes; these are shown in Figure 6 and some of the related features are quantified in Table 2. The pattern of lamellar blood flow observed for the tunas in this study is consistent with previous reports (Muir, 1970; Muir and Brown, 1971; Olson et al., 2003; Wegner et al., 2006), and the yellowfin tuna blood-flow pattern is shown in Figure 6A. Blood entering tuna lamellae proceeds into a series of outer marginal channels (OMCs) extending along the lamellar lateral edge and is then directed (by the unique placement of lamellar pillar cells) diagonally across the lamellae at an angle of 50 - 60° relative to the lamellar long axis; efferent blood is collected by an inner marginal channel (IMC). In the eastern Pacific bonito (Fig. 6B), the angle of diagonal flow with respect to the lamellar axis is reduced in comparison to that of tunas. Also, the diagonal flow does not extend across the entire lamellar height, and therefore, blood is not collected by a single inner marginal channel. Wahoo lamellar blood flow does not show a diagonal progression, but rather advances parallel to the lamellar long axis (Fig. 6C) and is thus similar to that of most fishes. The Pacific chub mackerel lamellar blood-flow pattern (Fig. 6D) is similar to that of bonito; however, the angle of diagonal flow is further

reduced from that of tunas (approximately 20°) and is less than that reported by Muir and Brown (1971) for a single specimen of Atlantic chub mackerel, *Scomber scombrus* (approximately 35°). The swordfish lamellar blood-flow pattern (Fig. 6E) is also similar to that of bonito. Although the angle is less than that of skipjack tuna and yellowfin tuna (Table 2), striped marlin lamellar blood flow is similar to that of tunas in that diagonal flow extends across the entire lamellar height and is collected in an inner marginal channel (Fig. 6F).

DISCUSSION

This study confirms the large gill surface areas of tunas and shows that the gill areas of non-tuna scombrids and billfishes, while not as high as those of tunas, are larger than those of most other fish species. The morphometric parameters underlying the large gill surface areas of tunas include: 1. a high total filament length resulting from a large number of long gill filaments, 2. a high lamellar frequency, and 3. lamellae that, although not larger in area than those of other species, have a high-aspect ratio (i.e., they are long but not high) and are thus optimally shaped for the close-proximity packing of gill filaments. The non-tuna scombrids and billfishes examined utilize these same features to increase gill surface area, however, to a lesser extent than tunas. This section compares the gill morphometry of the scombrid and billfish species studied and examines the influence of both ram ventilation and metabolic demand in the sculpting of gill dimensions.

Scombrids

The species examined in this study represent four scombrid tribes (Scombrini = mackerels, Scomberomorini = Spanish mackerels and wahoo, Sardini = bonitos, and Thunnini = tunas), and Figure 7 shows their phylogenetic relationship. Previous research comparing these tribes has readily demonstrated the sequential increase in adaptations for high-performance swimming from mackerels to tunas (Magnuson, 1978; Collette et al., 2001; Graham and Dickson, 2001; Korsmeyer and Dewar, 2001). However, while tunas have larger gill surface areas than other scombrids, there is not a progressive increase in this feature within the clade; the gill areas of mackerel and bonito are similar, and the wahoo has a relatively smaller gill surface area than that of the mackerel (Fig. 1), despite its closer relationship to tunas (Fig. 7). Likewise, there are not emergent patterns for graded changes in the gill-area dimensions among the genera examined. For example, bonito and mackerel show little difference in their gill morphometrics (Figs. 2,4,5).

Tuna gill surface area is augmented above that of their scombrid relatives by a higher total filament length (Fig. 2). This results from relatively more gill filaments than in both bonito and mackerel, and longer gill filaments than in wahoo (Table 1). Figure 8 shows how the lamellar shape of tunas decreases interfilament spacing and allows for a high filament number. In addition, because tunas are obligate ram ventilators, and thus do not use the opercular chambers to induce branchial flow, this may allow them to more fully utilize this space to increase filament length. Although less than that of tunas, the other scombrid species examined also have a relatively

higher total filament length than that of most other teleosts. Bonito and mackerel gill filaments are as long as those of tunas, but are not as numerous (Table 1). In contrast, the long and slender head of the wahoo (Fig. 7) allows for a high filament number, but limits filament length (Table 1).

A common feature in the gills of all scombrids is a high lamellar frequency. Concomitant with this is a short interlamellar spacing (which minimizes physiological dead space) and a reduction in the thickness of the lamellae. Scombrid lamellar thickness is only about 5-6 μm (Wegner et al., 2006) and is associated with a thin respiratory epithelium (water-blood barrier distance) of only 0.5 – 1.2 μm (Hughes, 1970; Wegner et al., 2006), which can be more than an order of magnitude less than that of other fishes (range 2–11 μm) (Piiper, 1971; Hughes and Morgan, 1973). Thus, in addition to allowing for a high lamellar frequency, the close spacing and reduction in lamellar thickness also decrease diffusion distances for gas exchange.

The lamellae of scombrids are also long and low in profile, and this is associated with an atypical diagonal blood-flow pattern through the lamellae of tunas, bonito, and mackerel. This diagonal pattern differs from that of other fishes, including the wahoo, in which blood flows parallel to and along the lamellar long axis (compare Fig. 6A,B,D with 6C, and Fig. 8A with 8B) (Muir, 1970; Muir and Brown, 1971; Olson et al., 2003; Wegner et al., 2006). The diagonal pattern has been suggested as a mechanism that reduces the length of the lamellar blood pathway to that required for oxygen loading (i.e., blood channels running along the entire length of a lamella would be longer than necessary for complete gas exchange) (Muir, 1970; Muir and

Brown, 1971; Olson et al., 2003; Wegner et al., 2006). Thus, the larger number of short, in-parallel blood vessels resulting from diagonal flow increases gas-exchange efficiency by more closely matching blood-resident and oxygen-loading times and permits the entire length of the lamella to function for gas exchange despite its long shape. In addition, because the diagonal blood channels are significantly shorter than lamellar length, this adaptation also reduces vascular resistance through the gills (Muir, 1970; Muir and Brown, 1971). The angles of diagonal blood flow in the lamellae of bonito (31.9 ± 6.7°) and mackerel (20.1 ± 7.2°) are much less than those of tunas (48.5 ± 10.3° for yellowfin and 61.5 ± 6.3° for skipjack) (Fig. 6, Table 2). The decrease in the angle of diagonal flow results in a longer blood pathway through the lamellae, consequently increasing blood residence times, and likely indicates a reduced capacity for non-tuna scombrids to uptake oxygen in comparison to tunas.

Billfishes

Swordfish and striped marlin are convergent with scombrids for the general features of gill design (i.e., high total filament lengths, a relatively high lamellar frequency, and long lamellae with diagonal blood flow) that augment gill surface area. However, the extent to which the morphometrics are utilized differs slightly; both swordfish and striped marlin have lower lamellar frequencies than any of the scombrids examined (Fig. 4), which is compensated by relatively high total filament lengths (Fig. 2).

Swordfish gill surface area is markedly larger than that of striped marlin (Fig. 1). Morphometric comparisons reveal that although striped marlin lamellar frequency is significantly greater (Fig. 4), swordfish gill area is augmented by both a larger lamellar bilateral surface area (Fig. 5) and a higher total filament length (Fig. 2). The larger total filament length in the swordfish is derived from the unique branching of the gill filaments (Fig. 3). In addition to augmenting gill area, branching also appears to even the spacing between adjacent filaments. This is particularly apparent near the cerato-epibranchial joint where, with the acute intersection angle of the two bones, a relatively small number of filaments branch extensively to fill the expanding sector of the branchial cavity extending out from the gill arch (Fig. 3A,C). The resulting consistency in interfilament spacing likely encourages the uniform distribution of water flow between the filaments and to the lamellae. In contrast, the filaments leaving the cerato-epibranchial joint in the other pelagic teleosts examined (as seen for the striped marlin in Fig. 3B,D) are spaced close together near their origin, but separate as they radiate outward. Although this progressive increase in interfilament spacing away from the arch does not seem to result in morphological dead space [i.e., the lamellae appear to fully occupy this area (Fig. 3D)], water flow between the filaments may be less evenly distributed.

Although gill morphometric data are needed for other billfish species, the swordfish appears unique in having branching filaments and thus likely has the largest relative gill surface area among all billfishes (blue marlin, *Makaira nigricans*, shortbill spearfish, *Tetrapturus angustirostris*, and roundscale spearfish, *Tetrapturus georgii*,

all lack the extensive filament branching of the swordfish; Wegner, unpublished). The higher gill surface area of the swordfish may reflect differences from other billfishes in terms of metabolic demand, habitat utilization, or both. Although little is known about billfish metabolic requirements, swordfish differ greatly from other billfish species in terms of habitat exploitation. Tagging data show that swordfish spend most of the daylight hours at depth, often in excess of 400 m (Carey, 1990; Sepulveda et al., in review), while most other billfishes appear to be much more surface oriented (Block et al., 1992; Brill et al., 1993; Prince and Goodyear, 2006). In many regions, the depth at which swordfish spend significant time correlates with the oxygen minimum layer (OML) where oxygen content can be below 0.5 ml l^{-1} (Conkright et al., 1998; Bograd et al., 2008). In contrast, both blue marlin and sailfish (*Istiophorus platypterus*) in the Eastern Tropical Pacific appear to be limited to the top 100 m of the water column where dissolved oxygen levels are greater than 3.5 ml l^{-1} (Prince and Goodyear, 2006). The large gill area of the swordfish may thus facilitate respiration in the OML and allow this species to exploit resources unavailable to other billfishes.

Gill morphometrics and ram ventilation

The gill dimensions contributing to the large gill surface areas of both scombrids and billfishes do not conform to predictions by Hughes (1966) that gill surface area is optimally increased by long gill filaments and large (tall) lamellae. Hughes based his predictions on the concept that gill morphometrics are a balance between optimizing gill surface area and minimizing gill resistance to water flow in

order to conserve energy associated with actively pumping water through the gills. However, in scombrids and billfishes, the need to propel sufficient water over the gills, a fundamental paradigm of active ventilation, is reversed: these ram-ventilators have sufficient water flow; the need is to ensure the slow and uniform passage of water over the exchange surfaces and to maintain gill structural integrity in face of the high-pressure ventilatory stream.

While most scombrids and billfishes have relatively long gill filaments as predicted by Hughes (1966), total filament length is also increased in these fishes by numerous, tightly packed filaments. The close proximity of neighboring filaments necessarily requires a low lamellar height (Fig. 8), and the pelagic teleosts examined thus lack the large and tall lamellae predicted by Hughes (1966). In addition to allowing for extra gill filaments, the long rectangular shape of scombrid and billfish lamellae offers the following advantages: 1. it allows for a longer axis for lamellar attachment to the gill filament, which likely increases lamellar rigidity opposing the forceful branchial flow associated with ram ventilation, 2. the low profile of the lamellae requires less structural support than tall lamellae, and thus the thickness of the lamellar epithelium can be reduced to decrease diffusion distances, 3. short diffusion distances allow lamellar blood to quickly load oxygen and thus vascular resistance can be minimized through short diagonal blood channels (discussed above), and 4. lamellar shape in conjunction with lamellar spacing increases gill resistance, which is likely necessary to slow and streamline branchial flow to create optimal conditions for gas exchange in the interlamellar spaces.

The lamellae are the primary site of gill resistance (Hughes, 1966; Brown and Muir, 1970), and according to Poiseuille's equations for water flow, this resistance is a function of both the length and width of the interlamellar channels (Fig. 8). In order to minimize resistance, and as predicted by Hughes (1966), many active-ventilating teleosts have relatively tall lamellae (which are not long) and wide interlamellar spaces. However, scombrids and billfishes have both narrow (due to high lamellar frequencies) and long interlamellar channels (Fig. 8) which increase gill resistance, and this appears to slow the ram ventilatory stream and optimize water residence times at the exchange surfaces. In swimming skipjack tuna, water entering the mouth is slowed by 200x to interlamellar velocities ranging from 0.13 to 0.75 cm/s (Brown and Muir, 1970; Stevens and Lightfoot, 1986), which speeds fall within the range reported for teleosts that rely upon active ventilation (Lauder, 1984).

In large scombrids (tunas of the genus, *Thunnus,* wahoo) and billfishes, water flow through the gills also encounters resistance in the form of filament fusions (shown in Figure 3C for swordfish and 3D for striped marlin). These fusions are thought to provide added structural support to long gill filaments in order to counteract the tendency of the ram-ventilatory stream to deform the gills (Muir and Kendall, 1968; Johnson, 1986; Wegner et al., 2006). However, filament fusions may also function to help streamline water flow and encourage its uniform distribution to the gill lamellae. The fusions which, in most species line both the leading and trailing edges of the gill filaments, essentially encase the respiratory lamellae, and the resulting pores between juxtaposed fusions likely restrict both the speed and volume

of water entering the lamellar channels (Muir and Kendall, 1968). This mechanism for streamlining branchial flow appears to lessen the need for a high lamellar frequency, and accordingly, a negative correlation is seen between lamellar frequency and the proliferation of filament fusions in the species examined; filament fusions are most extensive in swordfish (Fig. 3C), followed by striped marlin (Fig. 3D), and are less prevalent in wahoo and bluefin and yellowfin tunas. Correspondingly, lamellar density is lowest in swordfish (16-18 mm^{-1}), somewhat greater in striped marlin (20-24 mm^{-1}), and further increased in wahoo (27-29 mm^{-1}) and bluefin-yellowfin tuna (24-33 mm^{-1}). Lamellar frequency peaks (30-36 mm^{-1}) in skipjack tuna, bonito, and mackerel, which all lack filament fusions.

The selective pressures operating on the evolution of gill morphometrics in scombrids and billfishes thus appear to be a balance between the optimization of both gill resistance to provide favorable flow conditions through the lamellae and gill surface area to meet metabolic demands. However, unlike most teleosts in which resistance is thought to be minimized, scombrid and billfish evolution appears to have selected for higher gill resistance in order to streamline the high-speed ventilatory flow produced by ram ventilation, whether through high lamellar densities, filament fusions, or a combination of both. The negative correlation of lamellar frequency and the prevalence of filament fusions suggests that the high density of the gill lamellae may be more important in slowing and streamlining branchial flow induced by ram ventilation than it is in increasing gill surface area. This may explain why many marine teleosts which utilize ram ventilation while feeding or when swimming at

faster speeds (e.g. menhaden, herring, bluefish, and some jack species) have high lamellar frequencies (Gray, 1954; Hughes, 1966; Piiper, 1971) despite metabolic demands that are assumedly less than those of scombrids and billfishes. Likewise, bonito and mackerel lamellar frequencies are as high as or greater than those of tunas (Fig. 4), despite much smaller gill surface areas (Fig. 1).

Gill area and metabolic demand

While a high lamellar frequency appears linked to the use of ram ventilation, gill surface area as a whole tends to correlate with metabolic demand. Table 3 shows the relationship between gill area and standard metabolic rate (SMR) in the scombrids and billfishes for which data are available. The ratio of SMR to gill surface area appears fairly consistent (100-250 $mgO_2\ h^{-1}\ m^{-2}$) within the species examined and argues for a direct correlation of gill surface area with metabolic requirements. The SMRs of Pacific chub mackerel and eastern Pacific bonito are similar (Sepulveda and Dickson, 2000; Sepulveda et al., 2003) and are matched by comparable gill areas. Tunas, having higher SMRs, possess correspondingly larger gill surface areas.

The general consistency of the ratio of SMR to gill area within the scombrids and billfishes examined provides insight into the metabolic requirements of large pelagic fishes for which SMR cannot be determined directly. Because of their size, pelagic habitat, and dependence on ram ventilation, many high-energy demand teleosts (i.e., certain tunas, the wahoo, and billfishes) cannot easily be caught at sea and returned to the laboratory for experimental determination of energetic

requirements. Gill area measurements may thus serve as a proxy to estimate SMR which is an important parameter in energetic, growth, and fisheries modeling. The similarity in the relative gill surface areas of billfishes and non-tuna scombrids suggests comparable aerobic demands for these two groups. However, the correlation between SMR and gill surface area may be altered by factors such the exploitation of hypoxic habitats (De Jager and Dekkers, 1975; Mandic et al., 2009). The utilization of the oxygen minimum layer by the swordfish may have been a key evolutionary driving force that led to its large gill surface area in comparison to other billfishes and does not necessarily indicate higher aerobic demands in swordfish than in its relatives. Additional insight into the effects of metabolic demand and habitat utilization on the gill dimensions of pelagic fishes would be gained by examining bigeye tuna, *Thunnus obesus*, which also frequents the oxygen minimum layer and should have metabolic requirements similar to those of other tunas.

In addition to the effects of exploiting hypoxic habitats, the relationship of SMR and gill area can be compounded by scaling. In many teleosts, the scaling exponents of gill surface area to body mass and SMR to body mass are similar (average 0.75-0.85) (Hughes, 1984a; Palzenberger and Pohla, 1992), and this correlation has been suggested as the reason that the scaling exponent of gill surface area is often greater than that predicted by geometric similarity assuming isometric growth of the gills (scaling exponent = 0.67). However, the scaling exponents for SMR to body mass for skipjack tuna (0.50) (Brill, 1979) and yellowfin tuna (0.57-0.60) (Brill, 1987; Dewar and Graham, 1994) are significantly less than those of gill

surface area to body mass (skipjack tuna = 0.85, bluefin-yellowfin tuna = 0.86). Consequently, the ratio of SMR to gill surface area varies as a function of body mass. Although these scaling effects may not change the general conclusions that can be drawn on how scombrid and billfish standard metabolic rates compare, the disparity in the scaling exponents of gill area and SMR in skipjack tuna and yellowfin tuna suggests other factors influence gill size. Hughes (1984a) and others have suggested that gill area may scale more consistently with routine or active metabolic rates, and for fish groups such as scombrids and billfishes this seems more appropriate as these fishes are continuous swimmers and never experience "rest" conditions.

Table 1.1: Regression equations for average filament length and total filament number in relation to body mass for the species examined.

Species	Average filament length		Total filament number	
	Regression	R^2	Regression	R^2
Skipjack Tuna	$y = 0.2221x^{0.2804}$	0.945	$y = 2532.30x^{0.1075}$	0.904
Bluefin-Yellowfin Tuna	$y = 0.1366x^{0.3360}$	0.977	$y = 4097.51x^{0.0458}$	0.406
Eastern Pacific Bonito	$y = 0.1193x^{0.3476}$	0.979	$y = 1341.02.x^{0.1277}$	0.926
Wahoo	$y = 0.0734x^{0.3667}$	0.973	$y = 3156.89x^{0.0714}$	0.463
Pacific Chub Mackerel	$y = 0.1208x^{0.3453}$	0.936	$y = 2036.75x^{0.0758}$	0.656
Striped Marlin	$y = 0.2304x^{0.2824}$	0.956	$y = 6295.58x^{0.0040}$	0.005

Note: Regressions for skipjack tuna and bluefin-yellowfin tuna were calculated using data from Muir and Hughes (1969).

Table 1.2: Angle of lamellar blood flow (measured relative to the lamellar long axis) and related features (distribution of blood to the lamellae by outer marginal channels, collection of blood in an inner marginal channel) in the pelagic teleosts examined.

Species	(n)	Weight range (kg)	Mean blood-flow angle ± SD	OMCs	IMC
Skipjack Tuna	1	3.4	61.5 ± 6.3	Yes	Yes
Yellowfin Tuna	1	4.3	48.5 ± 10.3	Yes	Yes*
Eastern Pacific Bonito	4	0.2 - 1.9	31.9 ± 6.7	Yes	No
Wahoo	3	12.8 - 19.4	0	No	No
Pacific Chub Mackerel	5	0.1 - 0.7	20.1 ± 7.2	Yes	No
Swordfish	3	20.0 - 125.1	29.9 ± 6.3	Yes	No
Striped Marlin	3	8.0 - 56.8	36.3 ± 6.7	Yes	Yes

Note: Abbreviations: IMC, inner marginal channel; OMC, outer marginal channel; SD, standard deviation. All interspecies comparisons of blood-flow angle are significantly different with the exception of eastern Pacific bonito and swordfish. *In some of the small yellowfin tuna lamellae sampled diagonal blood flow did not extend across the entire lamellar height, and therefore was not collected by an inner marginal channel.

Table 1.3: Comparison of gill surface areas ($mm^2\ g^{-1}$) and standard metabolic rates (SMR, $mgO_2\ kg^{-1}\ h^{-1}$) for the high-energy demand teleosts in this study at a body mass of 1 kg (determined from gill area to body mass and SMR to body mass regressions).

Species	Gill area ($mm^2\ g^{-1}$)	SMR ($mgO_2\ kg^{-1}\ h^{-1}$)	SMR / Gill area ($mgO_2\ h^{-1}\ m^{-2}$)
Skipjack Tuna	1846[1]	412[2]	223.2
Yellowfin Tuna	1327[1]	286[3]	215.5
Eastern Pacific Bonito*	933 (1080)[4]	161[5]	149.1
Wahoo	342[4]	-	-
Pacific Chub Mackerel	1110[4]	132[6]	118.9
Swordfish	856[4]	-	-
Striped Marlin	746[4]	-	-

Note: SMR data from the literature were determined for skipjack tuna at 23.5-25.5 °C and for yellowfin tuna at 25 °C. Bonito and mackerel SMRs were thus adjusted to 25 °C using a Q_{10} of 2. Sources: [1]Muir and Hughes (1969). [2]Brill (1979). [3]Brill (1987). [4]Present study. [5]Sepulveda et al. (2003). [6]Calculated from Sepulveda and Dickson (2000). *Sepulveda et al. (2003) made metabolic measurements on a limited size range of bonito and did not find a significant relationship between metabolic rate and body size; SMR data were thus pooled for all specimens (average body mass = 1191 g). For accurate determination of the SMR to gill area ratio, gill area was calculated for a fish of this size (shown in parentheses), and the SMR to gill area ratio reflects this body mass.

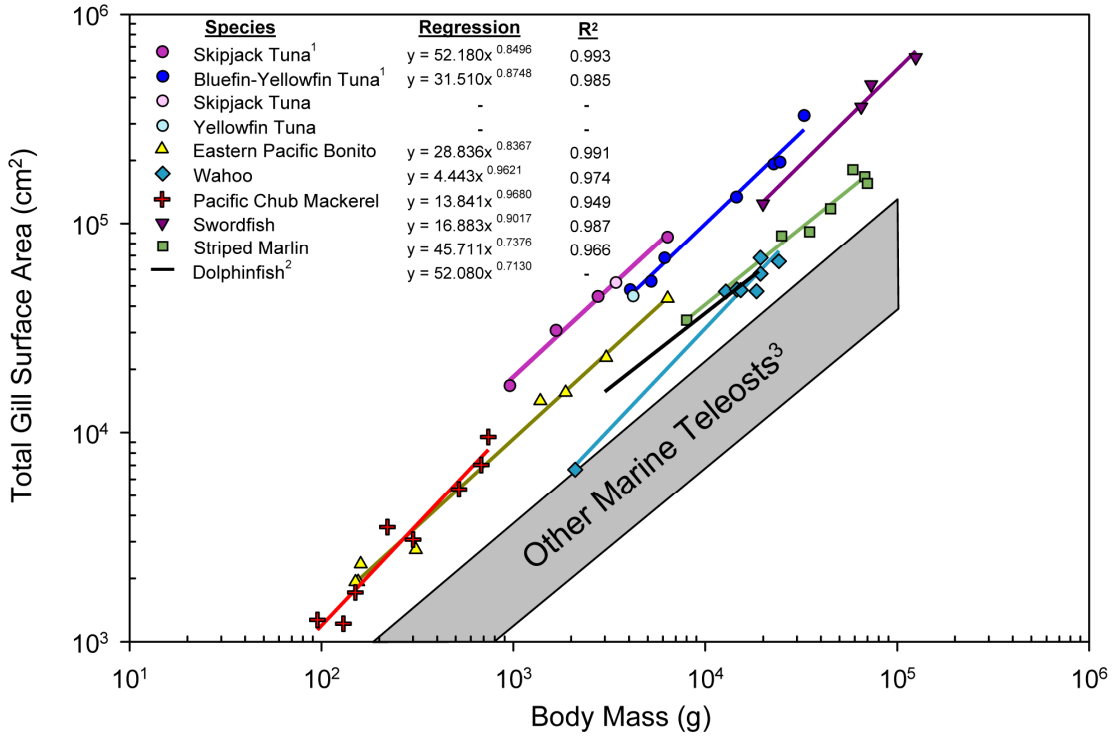

Figure 1.1: Linear regressions showing the relationship of total gill surface area (cm^2) and body mass (g) for the scombrids and billfishes examined in this study. Also included for comparison are gill area regressions for three species of tuna, dolphinfish, and a range of values compiled for other marine teleosts. Sources: [1]Muir and Hughes (1969). [2]Hughes (1970). [3]Palzenberger and Polha (1992).

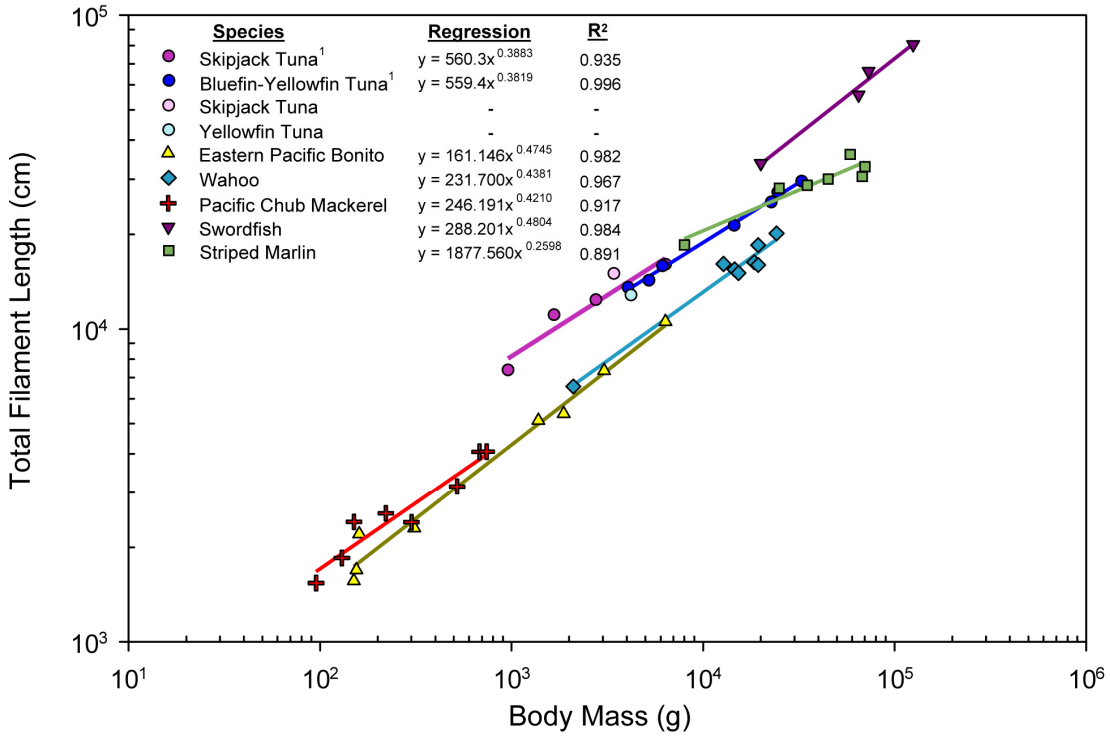

Figure 1.2: Linear regressions relating total gill filament length (cm) to body mass (g) for the high-energy demand teleosts examined in this study together with data for three species of tuna from [1]Muir and Hughes (1969).

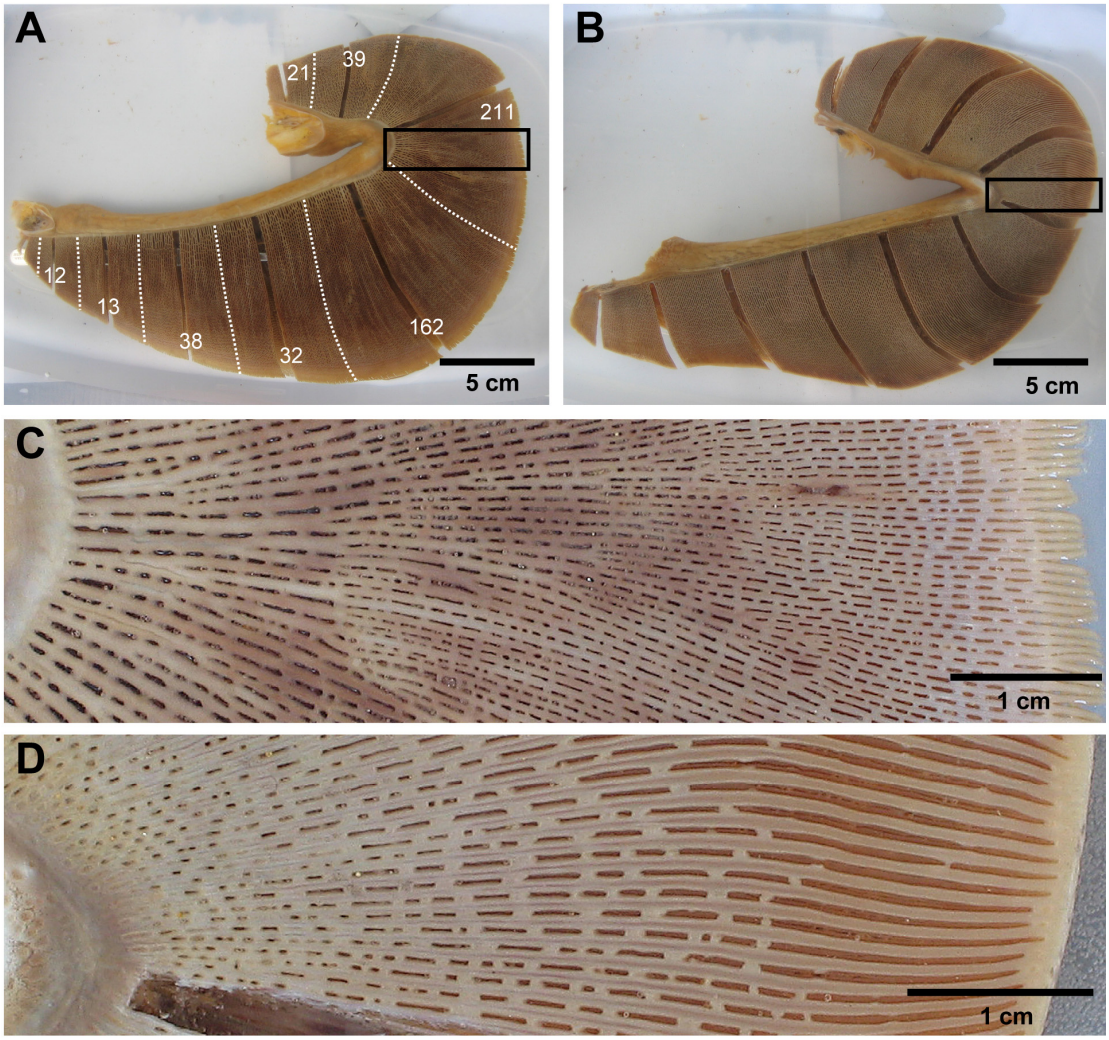

Figure 1.3: Comparison of the anterior hemibranch of the 3rd gill arch in **A:** a 64.9 kg swordfish and **B:** a 67.8 kg striped marlin. Dotted white lines on the swordfish gill arch distinguish bins of 40 filaments, and the number of branching events in each bin is listed. The medial filaments of each bin (dark areas) were removed for gill area measurements on the lamellae (i.e., determination of lamellar frequency and bilateral surface area). **C:** Enlarged view of the box in **A** showing the details of swordfish filament branching. **D:** Enlarged image of box in **B** detailing the non-branching filaments of striped marlin.

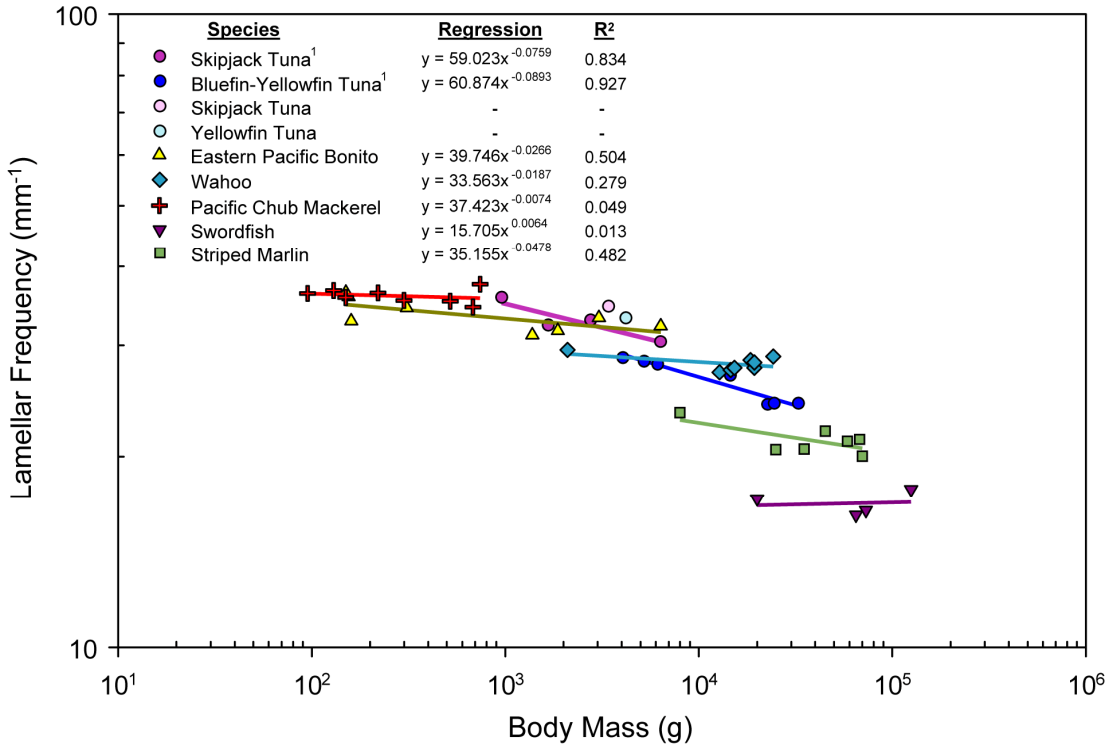

Figure 1.4: Linear regression functions for lamellar frequency (average number of lamellae per millimeter on one side of a gill filament) and body mass (g) for the pelagic teleosts examined. Also shown are data for three species of tuna from [1]Muir and Hughes (1969).

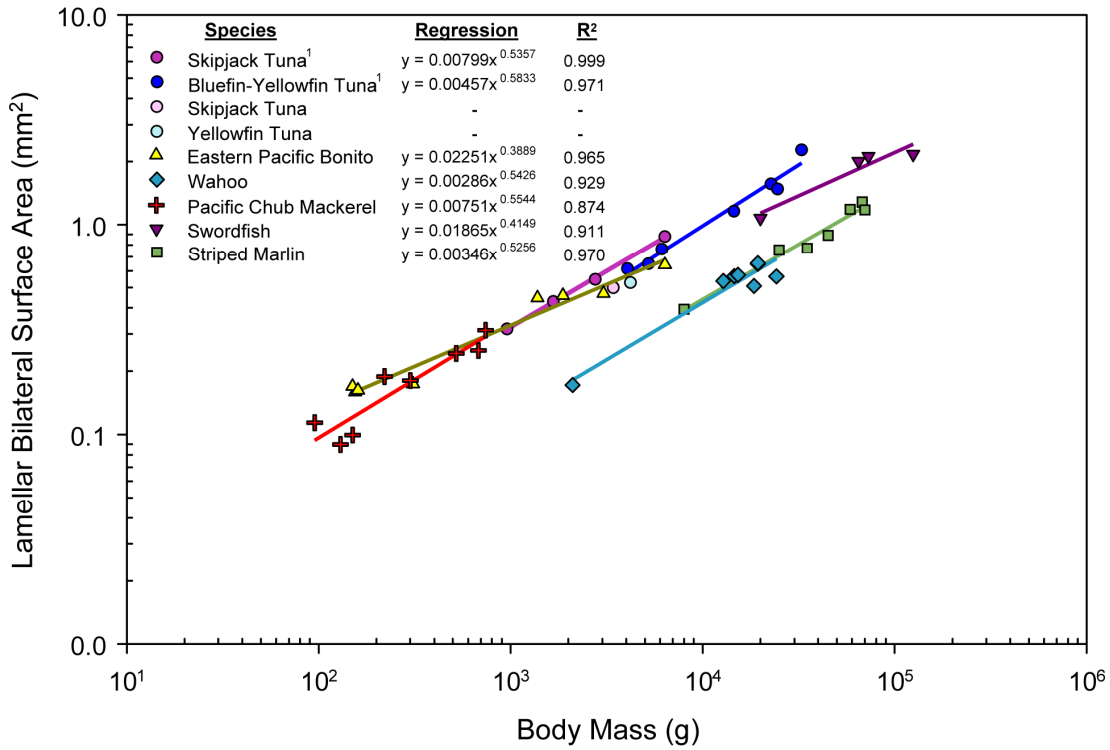

Figure 1.5: Linear regressions for lamellar bilateral surface area (mm^2) and body mass (g) for the scombrids and billfishes in this study. Data for three species of tuna are from [1]Muir and Hughes (1969).

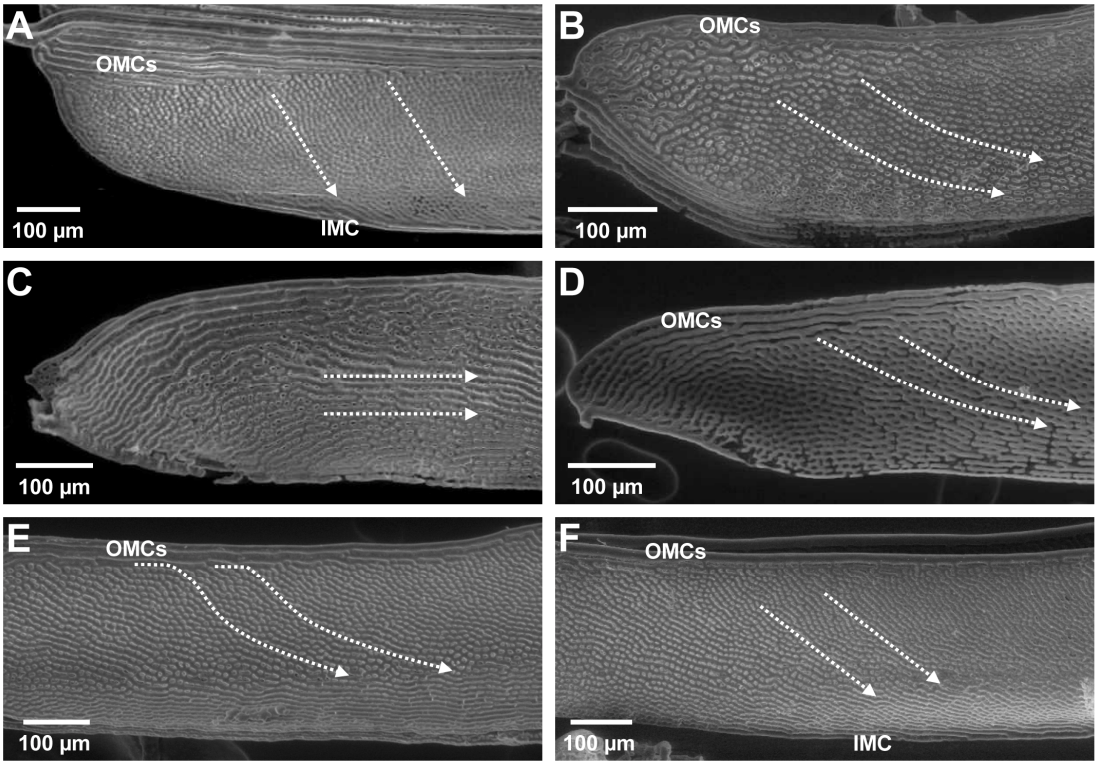

Figure 1.6: Microvascular-cast gill lamellae from **A:** a 4.2 kg yellowfin tuna, **B:** a 1.87 kg eastern Pacific bonito, **C:** a 15.3 kg wahoo, **D:** a 0.74 kg Pacific chub mackerel, **E:** a 20.0 kg swordfish, and **F:** a 45.0 kg striped marlin. Dotted arrows indicate the pathway of blood flow. Water flow is from right to left in all images. Abbreviations: IMC, inner marginal channel; OMC, outer marginal channel.

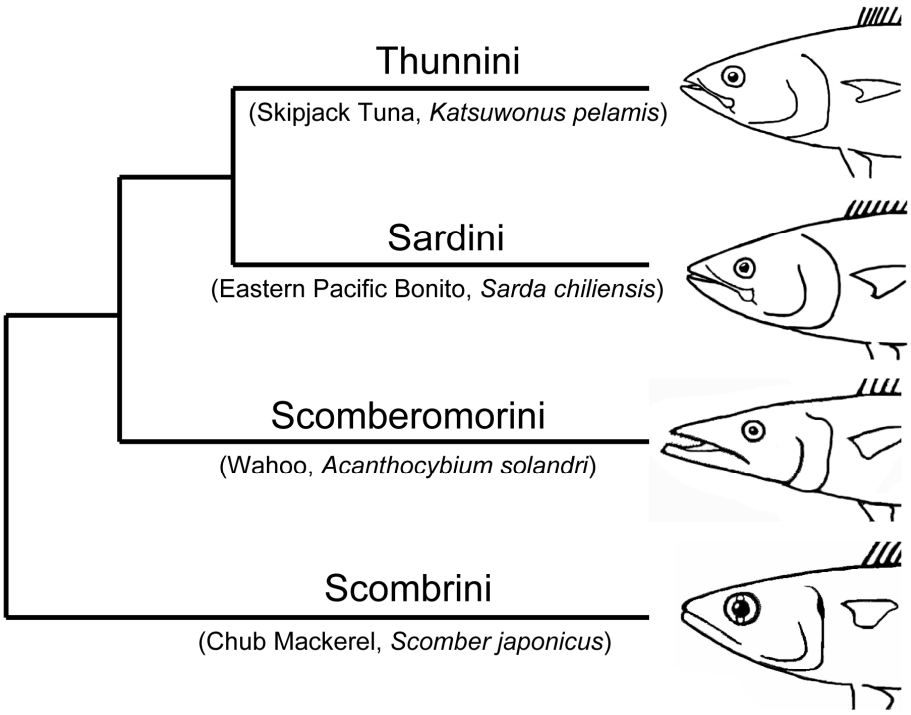

Figure 1.7: Scombrid phylogeny showing the four tribes of the subfamily Scombrinae and a species from each tribe examined in this study.

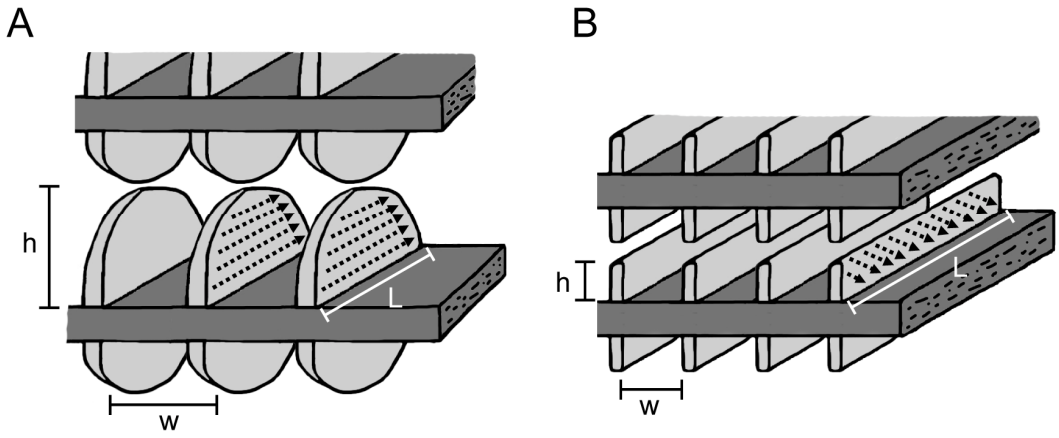

Figure 1.8: Generalized comparison of the gill filaments (dark grey) and lamellae (light grey) for **A:** most teleosts and **B:** most scombrids and billfishes. Lamellar blood-flow direction is indicated by dotted arrows; water flow between the lamellae is out of the page. Abbreviations: h, lamellar height; L, lamellar length; w, interlamellar channel width. Note: for simplicity, fusions of the gill filaments and lamellae are not shown for **B**.

LITERATURE CITED

Altringham JD, Block BA. 1997. Why do tuna maintain elevated slow muscle temperatures? Power output of muscle isolated from endothermic and ectothermic fish. J Exp Biol 200:2617-2627.

Altringham JD, Shadwick RE. 2001. Swimming and muscle function. In: Block BA, Stevens ED, editors. Tuna: Physiology, ecology and evolution. San Diego: Academic Press. p 313-344.

Beerkircher LR. 2005. Length to weight conversions for wahoo, *Acanthocybium solandri*, in the Northwest Atlantic. Col Vol Sci Papers ICCAT 58:1616-1619.

Block BA, Booth DT, Carey FG. 1992. Depth and temperature of the blue marlin, *Makaira nigricans*, observed by acoustic telemetry. Mar Bio 114:175-183.

Bograd SJ, Castro CG, Di Lorenzo E, Palacios DM, Bailey H, Gilly W, Chavez FP. 2008. Oxygen declines and the shoaling of the hypoxic boundary in the California Current. Geophys Res Lett 35:L12607.

Brill RW. 1979. Effect of body size on the standard metabolic rate of skipjack tuna, *Katsuwonus pelamis*. Fish Bull 77:494-498.

Brill RW. 1987. On the standard metabolic rates of tropical tunas, including the effect of body size and acute temperature change. Fish Bull 85:25-36.

Brill RW, Bushnell PG. 1991. Metabolic and cardiac scope of high-energy demand teleosts, the tunas. Can J Zool 69:2002-2009.

Brill RW, Dizon AE. 1979. Effect of temperature on isotonic twitch of white muscle and predicted maximum swimming speeds of skipjack tuna, *Katsuwonus pelamis*. Env Biol Fish 4:199-205.

Brill RW, Holts DB, Chang RKC, Sullivan S, Dewar H, Carey FG. 1993. Vertical and horizontal movements of striped marlin (*Tetrapturus audax*) near the Hawaiian Islands, determined by ultrasonic telemetry, with simultaneous measurement of oceanic currents. Mar Bio 117:567-574.

Brown CE, Muir BS. 1970. Analysis of ram ventilation of fish gills with application to skipjack tuna (*Katsuwonus pelamis*). J Fish Res Bd Canada 27:1637-1652.

Carey FG. 1990. Further acoustic telemetry observations of swordfish. In: Stroud RH, editor. Planning the future of billfishes. Atlanta, Georgia: National Coalition for Maine Conservation. p 103-122.

Carey FG, Teal JM. 1966. Heat conservation in tuna fish muscle. Proc Natl Acad Sci USA 56:1461-1469.

Chapman LJ. 2007. Morpho-physiological divergence across aquatic oxygen gradients in fishes. In: Fernandes MN, Rantin FT, Glass ML, Kapoor BG, editors. Fish respiration and environment. Enfield: Science Publishers. p 13-39.

Chatwin BM. 1959. The relationships between length and weight of yellowfin tuna (*Neothunnus macropterus*) and skipjack tuna (*Katsuwonus pelamis*) from the Eastern Tropical Pacific Ocean. Inter-Amer Trop Tuna Comm Bull 3:305-352.

Collette BB, Reeb C, Block BA. 2001. Systematics of the tunas and mackerels (Scombridae). In: Block BA, Stevens ED, editors. Tuna: Physiology, ecology and evolution. San Diego: Academic Press. p 5-30.

Conkright M, Levitus S, O'Brien T, Boyer T, Antonov J. 1998. World ocean atlas 1998. CD-ROM data set documentation. Technical report 15, NODC internal report. Silver Spring, MD.

Davie PS. 1990. Pacific marlins: Anatomy and physiology. Palmerston North, New Zealand: Simon Print. 88 p.

De Jager S, Dekkers WJ. 1975. Relation between gill structure and activity in fish. Neth J Zool 25:276-308.

DeMartini EE, Uchiyama JH, Williams HA. 2000. Sexual maturity, sex ratio, and size composition of swordfish, *Xiphias gladius*, caught by the Hawaii-based pelagic longline fishery. Fish Bull 98:489-506.

Dewar H, Graham JB. 1994. Studies of tropical tuna swimming performance in a large water tunnel. 1. Energetics. J Exp Biol 192:13-31.

Dickson KA. 1995. Unique adaptations of the metabolic biochemistry of tunas and billfishes for life in the pelagic environment. Environ Biol Fishes 42:65-97.

Dobson GP, Wood SC, Daxboeck C, Perry SF. 1986. Intracellular buffering and oxygen transport in the Pacific blue marlin (*Makaira nigricans*): Adaptations to high-speed swimming. Physiol Zool 59:150-156.

Donley JM, Dickson KA. 2000. Swimming kinematics of juvenile kawakawa tuna (*Euthynnus affinis*) and chub mackerel (*Scomber japonicus*). J Exp Biol 203:3103-3116.

Dowis HJ, Sepulveda CA, Graham JB, Dickson KA. 2003. Swimming performance studies on the eastern Pacific bonito *Sarda chiliensis*, a close relative of the tunas (family Scombridae) II. Kinematics. J Exp Biol 206:2749-2758.

Freadman MA. 1981. Swimming energetics of striped bass (*Morone saxatilis*) and bluefish (*Pomatomus saltatrix*): Hydrodynamic correlates of locomotion and gill ventilation. J Exp Biol 90:253-265.

Graham JB. 2006. Aquatic and aerial respiration. In: Evans DH, Claiborne JB, editors. The physiology of fishes. Third ed. Boca Raton: CRC Press. p 85-117.

Graham JB, Dickson KA. 2000. The evolution of thunniform locomotion and heat conservation in scombrid fishes: New insights based on the morphology of *Allothunnus fallai*. Zool J Linn Soc 129:419-466.

Graham JB, Dickson KA. 2001. Anatomical and physiological specializations for endothermy. In: Block BA, Stevens ED, editors. Tuna: Physiology, ecology and evolution. San Diego: Academic Press. p 121-165.

Gray IE. 1954. Comparative study of the gill area of marine fishes. Biol Bull Mar Biol Lab, Woods Hole 107:219-225.

Hughes GM. 1966. The dimensions of fish gills in relation to their function. J Exp Biol 45:177-195.

Hughes GM. 1970. Morphological measurements on the gills of fishes in relation to their respiratory function. Folia Morph 18:78-95.

Hughes GM. 1972. Morphometrics of fish gills. Respir Physiol 14:1-25.

Hughes GM. 1984a. General anatomy of the gills. In: Hoar WS, Randall DJ, editors. Fish physiology, vol 10A. Orlando: Academic. p 1-72.

Hughes GM. 1984b. Measurement of gill area in fishes: Practices and problems. J Mar Biol Ass UK 64:637-655.

Hughes GM, Morgan M. 1973. The structure of fish gills in relation to their respiratory function. Biol Rev 48:419-475.

Johnson GD. 1986. Scombroid phylogeny: An alternative hypothesis. Bull Mar Sci 39:1-41.

Korsmeyer KE, Dewar H. 2001. Tuna metabolism and energetics. In: Block BA, Stevens ED, editors. Tuna: Physiology, ecology and evolution. San Diego: Academic Press. p 35-78.

Lauder GV. 1984. Pressure and water flow patterns in the respiratory tract of the bass (*Micropterus salmoides*). J Exp Biol 113:151-164.

Magnuson JJ. 1978. Locomotion by scombrid fishes: hydromechanics, morphology, and behavior. In: Hoar WS, Randall DJ, editors. Fish physiology, vol 7. New York: Academic Press. p 239-313.

Mandic M, Todgham AE, Richards JG. 2009. Mechanisms and evolution of hypoxia tolerance in fish. Proc R Soc B 276:735-744.

Muir BS. 1970. Contribution to the study of blood pathways in teleost gills. Copeia 1970:19-28.

Muir BS, Brown CE. 1971. Effects of blood pathway on the blood-pressure drop in fish gills, with special reference to tunas. J Fish Res Bd Can 28:947-955.

Muir BS, Hughes GM. 1969. Gill dimensions for three species of tunny. J Exp Biol 51:271-285.

Muir BS, Kendall JI. 1968. Structural modifications in the gills of tunas and some other oceanic fishes. Copeia 1968:388-398.

Olson KR, Dewar H, Graham JB, Brill RW. 2003. Vascular anatomy of the gills in a high energy demand teleost, the skipjack tuna (*Katsuwonus pelamis*). J Exp Zool 297A:17-31.

Palzenberger M, Pohla H. 1992. Gill surface area of water-breathing freshwater fish. Rev Fish Biol Fisheries 2:187-196.

Piiper J. 1971. Gill surface area: Fishes. In: Altman PL, Dittmer DS, editors. Respiration and circulation. Bethesda, Maryland: Federation of American Societies for Experimental Biology. p 119-121.

Ponce-Díaz G, Ortega-García S, González-Ramírez PG. 1991. Analysis of sizes and weight-length relation of the striped marlin, *Tetrapturus audax* (Philippi, 1887) in Baja California Sur, Mexico. Cien Mar 17:69-82.

Prince ED, Goodyear CP. 2006. Hypoxia-based habitat compression of tropical pelagic fishes. Fish Oceanogr 15:451-464.

Roberts JL. 1975. Active branchial and ram gill ventilation in fishes. Biol Bull Mar Biol Lab, Woods Hole 148:85-105.

Roberts JL, Rowell DM. 1988. Periodic respiration of gill-breathing fishes. Can J Zool 66:182-190.

Sepulveda C, Dickson KA. 2000. Maximum sustainable speeds and cost of swimming in juvenile kawakawa tuna (*Euthynnus affinis*) and chub mackerel (*Scomber japonicus*). J Exp Biol 203:3089-3101.

Sepulveda CA, Dickson KA, Graham JB. 2003. Swimming performance studies on the eastern Pacific bonito *Sarda chiliensis*, a close relative of the tunas (family Scombridae) I. Energetics. J Exp Biol 206:2739-2748.

Sepulveda CA, Knight A, Nasby-Lucas N, Domeier ML. in review. Fine-scale movements of the swordfish (*Xiphias gladius*) in the Southern California Bight. Fish Oceanogr.

Steen JB, Berg T. 1966. The gills of two species of haemoglobin-free fishes compared to those of other teleosts, with a note on severe anaemia in an eel. Comp Biochem Physiol 18:517-526.

Stevens ED, Lightfoot EN. 1986. Hydrodynamics of water flow in front of and through the gills of skipjack tuna. Comp Biochem Physiol 83A:255-259.

Wegner NC, Sepulveda CA, Graham JB. 2006. Gill specializations in high-performance pelagic teleosts, with reference to striped marlin (*Tetrapturus audax*) and wahoo (*Acanthocybium solandri*). Bull Mar Sci 79:747-759.

Westneat MW, Wainwright SA. 2001. Mechanical design for swimming: muscle, tendon, and bone. In: Block BA, Stevens ED, editors. Tuna: Physiology, ecology and evolution. San Diego: Academic Press. p 271-311.

ACKNOWLEDGEMENTS

This research was supported by the National Science Foundation Grant #IOS-0817774, the Tuna Industry Endowment Fund at Scripps Institution of Oceanography,

the William H. and Mattie Wattis Harris Foundation, the Pfleger Institute of Environmental Research, the George T. Pfleger Foundation, and the Moore Family Foundation. N.C. Wegner was supported by the Nadine A. and Edward M. Carson Scholarship awarded by the Achievement Rewards for College Scientists (ARCS), Los Angeles Chapter, the Edna Bailey Sussman Foundation, and the National Science Foundation. We thank S. Aalbers, N. Ben-Aderet, D. Bernal, R. Brill, D. Cartamil, M. Domeier, T. Fullam, D. Fuller, M. Musyl, A. Nosal, N. Sepulveda, L. Williams, and the crews of the *Polaris Supreme* and *Oscar Elton Sette* who helped in specimen acquisition and vascular-casting perfusions, E. York of the SIO Analytical Facility for technical assistance with microscopy work, and C. Anderson for help with statistical analyses. We additionally thank P. Hastings, M. McHenry, F. Powell, and R. Rosenblatt for reviewing versions of this manuscript.

This chapter, in full, was submitted for publication as:

Wegner NC, Sepulveda CA, Bull KB, Graham JB. In press. Gill morphometrics in relation to gas transfer and ram ventilation in high-energy demand teleosts: Scombrids and billfishes. J Morph. The dissertation author is the primary investigator and author of this paper.

CHAPTER 2: STRUCTURAL ADAPTATIONS FOR RAM VENTILATION: GILL FUSIONS IN SCOMBRIDS AND BILLFISHES

ABSTRACT

Gill fusions provide structural support for ram ventilation in scombrids (tunas, bonitos, Spanish mackerels, mackerels) and billfishes (marlins, swordfish). For scombrids, a progressive increase within the family for reliance upon ram ventilation correlates with the elaboration of gill fusions. Mackerels (tribe Scombrini) only utilize ram ventilation at fast cruising speeds and lack gill fusions. In Spanish mackerels (tribe Scomberomorini), some species have interlamellar fusions which bind adjacent lamellae on each filament and maintain the spatial dimensions of the interlamellar channels. The wahoo, *Acanthocybium solandri*, a highly specialized member of this tribe, also possesses filament fusions, which are formed by cartilaginous extensions of the filament rods covered by bony epithelial toothplates. Both bonitos (tribe Sardini) and tunas (tribe Thunnini) are obligate ram ventilators and have complete lamellar fusions that connect the lamellae of one filament to the closely positioned lamellae of the adjacent filament. In addition, the gills of the most derived tuna genus, *Thunnus*, have filament fusions formed by extensions of the filament mucosal epithelium. Billfishes, also obligate ram ventilators, have cartilaginous filament fusions similar to those found in the wahoo; however, some billfishes differ with respect to lamellar fusions: striped marlin, *Kajikia audax*, and sailfish, *Istiophorus platypterus*, have lamellar and interlamellar fusions, while the swordfish, *Xiphias gladius*, lacks both. Examination of a large body-size range of some scombrids and billfishes shows that

gill fusions begin to develop as small as 2.0 cm fork length (FL), perhaps indicating the use of ram ventilation at the small juvenile stage. Filament fusions also appear to develop early, however, usually following the formation of lamellar fusions. In addition to augmenting gill rigidity, filament fusions also appear to increase branchial resistance in order to slow and streamline the high-speed branchial flow produced by ram ventilation.

INTRODUCTION

Tunas, bonitos, and mackerels (family Scombridae) and the billfishes (families Istiophoridae, Xiphiidae) are continuous swimmers and breathe using ram ventilation, a mechanism in which the forward momentum of the fish forces water flow into the mouth and through the branchial chamber (Brown and Muir, 1970; Stevens, 1972; Roberts, 1975; Graham, 2006). Ram ventilation transfers the energetic cost of active gill ventilation to the swimming musculature and because mouth and opercular motions are minimized, both respiratory and swimming efficiency are increased (Freadman, 1979; 1981; Steffensen, 1985). However, at the relatively high swimming speeds of scombrids and billfishes, ram ventilation poses two challenges. First, the ram ventilatory stream must be slowed and streamlined to create optimal flow conditions for gas exchange at the respiratory lamellae. Second, the gill epithelium must be reinforced in order to maintain normal orientation with respect to the forceful branchial flow. Recent work by Wegner et al. (in press) has shown that changes in scombrid and billfish gill morphometrics increase gill resistance and help in slowing

the ram ventilatory stream. In addition, some scombrids and billfishes have structural supports in the form of gill fusions which bind the filaments and lamellae and increase overall rigidity of the branchial sieve (Muir and Kendall, 1968; Muir, 1969; Johnson, 1986; Wegner et al., 2006).

Gill fusions can be divided into two groups: filament and lamellar. Filament fusions bind adjacent filaments within a gill hemibranch and have been documented in tunas of the genus *Thunnus*, the billfishes (*Istiophorus*, *Kajikia*, and *Xiphias)*, and one non-tuna scombrid, the wahoo, *Acanthocybium solandri* (Muir and Kendall, 1968; Johnson, 1986). In *Thunnus*, filament fusions are formed by the expansion of the mucosal filament epithelium to bridge the interfilament space (Muir and Kendall, 1968). In contrast, billfish and wahoo filament fusions are formed by cartilaginous extensions of the filament rods covered by bony epithelial toothplates (Johnson, 1986).

Lamellar fusions, which bind the gill lamellae and thus secure the spatial integrity of the lamellar pores (= interlamellar channels), take two forms. Complete lamellar fusions, which are found in tunas, connect the lamellae on one filament to the closely positioned and opposing lamellae of the adjacent filament, thus providing support to both the gill filaments and lamellae (Muir and Kendall, 1968; Muir, 1969; Wegner et al., 2006). Interlamellar fusions bind adjacent lamellae on the same filament, but do not extend to connect with the lamellae on the neighboring filament. These fusions have been documented for wahoo and striped marlin, *Kajikia audax* (Wegner et al., 2006); however, in the striped marlin, interlamellar fusions on adjacent

filaments grow together in some areas of the gills, thus forming complete lamellar fusions (Wegner et al., 2006).

The diversity of gill fusion type and structure can be expected to reflect interspecific differences in reliance upon, or specialization for, ram ventilation. Although all scombrids and billfishes use ram ventilation, basic information about the occurrence of fusions and their structure is not available for many species, and there are few data addressing how fusion structure may change with body size or the range of swimming speeds employed by these fishes. This comparative study thus examines the gills from 26 scombrid species and six species of billfishes in order to determine how factors such as body size, swimming speed, and the degree of dependence upon ram ventilation have all influenced the site of occurrence and elaboration of fusions. Because the family Scombridae demonstrates a progression in adaptations for fast, continuous swimming (from least derived mackerels to most derived tunas) and an associated graded increase in reliance on ram ventilation, determination of gill fusion type and pattern along this gradient can provide insight into the structural requirements of ram ventilation.

METHODS

Gill tissue collection

Gills were collected from 18 scombrid and three billfish species: albacore (*Thunnus alalunga*, n=2), yellowfin tuna (*Thunnus albacares*, n=19), bigeye tuna (*Thunnus obesus*, n=1), Pacific bluefin tuna (*Thunnus orientalis*, n=5), longtail tuna

(*Thunnus tonggol*, n=2), skipjack tuna (*Katsuwonus pelamis*, n=4), kawakawa (*Euthynnus affinis*, n=4), black skipjack (*Euthynnus lineatus*, n=9), frigate tuna (*Auxis thazard*, n=2), eastern Pacific bonito (*Sarda chiliensis*, n=20), leaping bonito (*Cybiosarda elegans*, n=7), wahoo *Acanthocybium solandri*, n=9), narrow-barred Spanish mackerel (*Scomberomorus commerson* n=5), Queensland school mackerel (*Scomberomorus queenlandicus*, n=5), Pacific sierra (*Scomberomorus sierra*, n=5), shark mackerel (*Grammatorcynus bicarinatus*, n=2), Indian mackerel (*Rastrelliger kanagurta*, n=2), Pacific chub mackerel *Scomber japonicus*, n=20), sailfish (*Istiophorus platypterus*, n=2), striped marlin (*Kajikia audax* n=7), and swordfish (*Xiphias gladius*, n=5).

Scombrid and billfish species were collected off the coasts of: 1. Southern California, USA and Baja California and Baja California Sur, Mexico (yellowfin tuna, albacore, black skipjack, frigate tuna, eastern Pacific bonito, wahoo, chub mackerel, striped marlin, and swordfish), 2. Hawaii, USA (yellowfin tuna, skipjack tuna, wahoo, striped marlin, and swordfish), 3. Costa Rica (black skipjack, Pacific sierra, and sailfish), and 4. Queensland, Australia (longtail tuna, kawakawa, leaping bonito, narrow-barred Spanish mackerel, Queensland school mackerel, and shark mackerel). Gills from Pacific bluefin tuna were collected during their harvest from holding pens offshore of Ensenada, Baja California, Mexico.

Captured specimens were euthanized by severing the spinal cord in accordance with protocol S00080 of the University of California, San Diego Institutional Animal Care and Use Committee. The gills from one or both sides of each specimen were

immediately excised and fixed in 10% formalin buffered in sea water. A low-pressure seawater hose was used to keep the gills wet during excision, which, depending on the size of the fish, required up to 10 min.

Preserved specimens

Preserved specimens housed in scientific collections at Scripps Institution of Oceanography, the National Museum of Natural History, the Australia Museum, and the Australia National Fish Collection were also examined. Most of the hundreds of specimens examined had undergone substantial degradation of the gill tissue, usually caused by prolonged air exposure or freezing prior to fixation, which precluded accurate determination of fusion status. The few scombrids for which gill data could be obtained are as follows: yellowfin tuna (n=6), blackfin tuna (*Thunnus atlanticus*, n=6), longtail tuna (n=6), skipjack tuna (n=4), kawakawa (n=8), bullet tuna (*Auxis rochei*, n=2), frigate tuna (n=5), Australian bonito (*Sarda australis*, n=1), striped bonito (*Sarda orientalis*, n=2), Atlantic bonito (*Sarda sarda*, n=1), narrow-barred Spanish mackerel (n=1), Monterey Spanish mackerel (*Scomberomorus concolor*, n=1), and double-lined mackerel (*Grammatorcynus bilineatus*, n=4). Although all preserved billfish gill tissue had undergone substantial degradation precluding the determination of lamellar fusion status, billfish filament fusions have a cartilaginous base and are covered by epithelial toothplates, which made it possible to record their presence in some specimens. Included are: blue marlin (*Makaira nigricans*, n=1),

shortbill spearfish (*Tetrapturus angustirostris*, n=2), roundscale spearfish (*Tetrapturus georgii*, n=1), and swordfish (n=5).

Other preserved material included a size series of small yellowfin tuna (1.5 – 5.5 cm, n=6) and sailfish (12.5 – 32.0 cm, n=12) and small specimens of little tunny (*Euthynnus allateratus*, n=1), black skipjack (n=1), Atlantic bonito (n=1), and Queensland school mackerel (n=1). These specimens were used to examine the development of gill fusions.

Body size

Fish length measurements were taken, and when possible, each specimen was weighed using an electric scale. In cases where body mass was not directly measured, estimates were made using length-weight regressions published for the different species (Chatwin, 1959; Faruk Kara, 1979; Muthiah, 1985; Ramos et al., 1986; McPherson, 1992; Hsu et al., 2000; Chiang et al., 2004; Beerkircher, 2005; de la Serna et al., 2005; Moazzam et al., 2005; Vieira et al., 2005).

Gill fusion assessment

Fixed gill tissue from each specimen was examined to determine the presence or absence of the different fusion types: filament fusions (either composed of a mucosal epithelium, or having a cartilaginous base and covered in bony epithelial toothplates), lamellar fusions, and interlamellar fusions. For most larger specimens (>1 kg), filament fusion type and the presence of complete lamellar fusions could be

determined by direct observation with the naked eye or aided by a dissection microscope. In smaller specimens (< 1 kg), and those for which complete lamellar fusions were not obvious (e.g., species with interlamellar fusions or lacking lamellar fusions), scanning electron microscopy (SEM) was used to assess lamellar fusion status. For SEM analysis, small sections of gill tissue (usually 1 cm^2 or less) were removed from each specimen, rinsed in deionized water, and either dehydrated in 100% ethanol (20-25% increments over 24 h) and critical-point dried, or dehydrated in 100% tert-butyl alcohol (25% increments over 24 h, and rinsed twice at 100%), frozen in the alcohol at 4 °C, and freeze dried. Dried material was then sputter-coated in gold-palladium and viewed using an FEI Quanta 600 SEM under high-vacuum mode.

RESULTS

Table 1 shows the presence and type of gill fusions for the 26 scombrid and six billfish species examined in this study. Fusion status for each genus is mapped onto the scombrid and billfish phylogenies in Figure 1.

Filament fusions

This study confirms previous descriptions that filament fusions in tunas of the genus *Thunnus* are composed of a mucosal epithelium, while those of wahoo and billfishes are formed by cartilaginous extensions of the filament rods and covered by bony epithelial toothplates (Johnson, 1986). This work also documents the occurrence of epithelial filament fusions in three additional *Thunnus* species, Pacific bluefin,

albacore and longtail tuna, and the presence of cartilaginous-based filament fusions in three additional billfish species in two genera (*Makaira*, *Tetrapturus*): blue marlin, shortbill spearfish, and roundscale spearfish.

The pattern of filament fusions in each species is fairly consistent and does not show large changes with body size once developed (these structures are not present in the very small yellowfin tuna and sailfish examined). In the *Thunnus* and billfish species examined and the wahoo, filament fusions on the trailing (water-exit) edges of the gill filaments occur along nearly their entire length (i.e., from the base to the tip). However, on the leading (water-entry) edge of the filaments there are differences between species in the prevalence of filament fusions (Fig. 2A-G). These different patterns range from three *Thunnus* species which lack filament fusions entirely on the leading edge (albacore, blackfin tuna, longtail tuna) (not shown in Fig. 2), to the swordfish in which the filaments are bound by fusions along nearly their entire length (Fig. 2G).

Lamellar and interlamellar fusions

Structural details for lamellar and interlamellar fusions are shown in Figure 3. Lamellar fusions (Fig. 3A) connect lamellae on one filament to opposing lamellae on the adjacent filament. This study reports lamellar fusions in all of the tuna species examined (6 out of the 8 species of *Thunnus*, and all species from the genera *Katsuwonus*, *Euthynnus*, and *Auxis*) (Table 1, Fig. 1) and documents for the first time, lamellar fusions in all species of the bonito genera *Sarda* and *Cybiosarda* (Table 1,

Fig. 1). Figure 3A shows lamellar fusions in the eastern Pacific bonito. Interlamellar fusions (Fig. 3B) connect adjacent lamellae on the same filament but do not extend to the lamellae of the adjacent filament. This study verifies a previous report (Wegner et al., 2006) of interlamellar fusions in the striped marlin and wahoo, and further documents these fusions in the sailfish and one species of *Scomberomorus*, the Queensland school mackerel (Fig. 3C,D). The interlamellar fusions of Queensland school mackerel and wahoo are thinner and less complete (i.e., fusions do not bind all of the lamellae along the length of the filament) than those of striped marlin and sailfish (cf. Fig. 3C,D with 3B), which are well developed and in many cases grow together to form complete lamellar fusions (Fig. 3E). Although nearly all the lamellae in tunas and bonitos are bound by complete lamellar fusions, remnants of interlamellar fusions from development (see below) are often found at the filament tips (Fig. 3F).

Fusion development

Figures 4-6 show the progressive development of lamellar fusions in a size series of juvenile yellowfin tuna. At 1.5 cm (103 mg) the gill filaments and lamellae are fully developed but lack fusions (Fig. 4). A 2.0 cm (154 mg) specimen, however, has some interlamellar fusions near the filaments tips (Fig. 5A-E). Fusion formation appears to involve the curving of the leading lamellar lateral edge toward the tip of the filament until it contacts the neighboring lamella (Fig. 5C-E). This is consistent with histological reports (Wegner et al., 2006) which show the lamellar lateral edges embedded in complete lamellar fusions curved toward the tip of the filament in a 49.2

kg yellowfin tuna. By 3.0 - 3.2 cm (453 - 915 mg) interlamellar fusions start to grow together to form complete lamellar fusions (Fig. 6). However, interlamellar fusions persist near the filament tip, which appear to continue into the adult stage (see Fig. 3F for a 1.45 kg eastern Pacific bonito), and lamellae near the base of the filaments remain free of fusions. By 5.5 cm (2.22 g) most of the interlamellar fusions have grown together to form complete lamellar fusions, which have progressed further towards the base of the filaments leaving fewer non-fused lamellae. In the 8.0 cm little tunny, the 10.9 cm black skipjack, and the 11.5 cm Atlantic bonito, all lamellae are completely bound by lamellar fusions. A size series of 13 sailfish (12.5 – 33.0 cm, 4.5 - 95.5 g) show that as in the yellowfin tuna, interlamellar fusions first form near the filament tip and extend toward the filament base as body size increases (shown for 28.5 cm sailfish in Fig. 7). No complete lamellar fusions were observed in any of the small sailfish examined.

DISCUSSION

Many species utilize ram ventilation in order to increase respiratory efficiency at fast swimming speeds (Roberts, 1975; Freadman, 1979; 1981; Graham, 2006). This transfers the energetic cost of active ventilation associated with cyclic mouth and opercular movements to the swimming musculature and reduces branchial resistance (Brown and Muir, 1970; Freadman, 1979; 1981; Steffensen, 1985). Likely associated with their epipelagic habitat and need for continuous swimming to maintain hydrostatic equilibrium, scombrids and billfishes show an increased reliance upon ram

ventilation in comparison to most other fishes (Brown and Muir, 1970; Roberts, 1978; Stevens and Lightfoot, 1986; Davie, 1990; Graham and Dickson, 2004). Higher scombrids (i.e., tunas and bonitos) and billfishes have lost the branchial musculature required for active ventilation and therefore are obligate ram ventilators. This study of 26 scombrids and six billfishes provides data demonstrating the correlation between branchial fusions and reliance upon ram ventilation. Although many fish groups utilize ram ventilation while swimming at fast velocities, gill fusions only appear present in species highly dependent upon this form of respiration, where the continuous high-pressure ventilatory stream requires fusions to maintain the spatial and structural integrity of the gills and, in some cases, slow branchial flow in order to optimize gas transfer efficiency.

Ram ventilation and gill fusion

Scombrids. This study comparing the gill-fusion status of species distributed among the four tribes of the Scombridae demonstrates a correlation between the progressive development of graded adaptations related for high-performance swimming, including a dependence on ram ventilation, and the occurrence of branchial fusions.

The mackerels (*Scomber* and *Rastrelliger* = Tribe Scombrini) are the most primitive members of the scombrid subfamily Scombrinae (Fig. 1). There are no studies of the respiratory biomechanics of *Rastrelliger*, however Roberts (1975) showed that the Atlantic chub mackerel, *Scomber scombrus*, is not an obligatory ram

ventilator; it uses active gill ventilation during slow swimming and transitions to ram ventilation at speeds between 53 - 75 cm s^{-1} (2.7 - 4.7 body lengths s^{-1}). Neither *Scomber* nor *Rastrelliger* have gill fusions (Fig. 1, Table 1), but studies with *S. japonicus* (Wegner et al., in press) demonstrated two lamellar features, a long filament-attachment surface and high frequency (i.e., the number of lamellae per length of filament), that parallel the lamellar structure in bonitos and tunas and may thus contribute to ram ventilation. Specifically, long lamellae reinforce the gill by providing an extended surface for attachment to the filament and, in addition to enhancing total gill area, a greater lamellar frequency contributes to gas-transfer efficiency by slowing the water-flow velocity and minimizing physiological dead space.

The Spanish mackerels (*Grammatorcynus*, *Scomberomorus*, and *Acanthocybium* = Tribe Scomberomorini, Fig. 1) are intermediate to the mackerels and the more derived tunas and bonitos. Morphological features such as a well-developed lateral keel on the caudal peduncle distinguish this group from the mackerels and suggest an increased capacity for fast, sustainable swimming. While virtually nothing is known about this group's range of swimming speeds or its dependence upon ram ventilation, the finding (Table 1, Fig. 1) of interlamellar fusions in Queensland school mackerel, *Scomberomorus queenslandicus*, but not in other species of this genus or in *Grammatorcynus* suggests varying levels of dependence on, and specialization for, ram ventilation. The wahoo, considered a specialized offshoot of *Scomberomorus* (Collette et al., 2001), has interlamellar fusions similar to those of

the Queensland school mackerel as well as cartilaginous filament fusions. A more rigid wahoo gill sieve suggests a greater dependence on ram ventilation than that of other members in the tribe.

The bonitos (Tribe Sardini) and tunas (Tribe Thunnini) are the most derived scombrids. Regarded as sister groups, tunas and bonitos share several morphological features related to high-performance swimming and, although tunas have a greater degree of physiological and biochemical specialization [e.g., regional endothermy, greater enzymic activities, higher metabolic rate, and a larger gill surface area (Sepulveda et al., 2003; Graham and Dickson, 2004; Wegner et al., in press)], both tunas and bonitos are obligate ram ventilators (Brown and Muir, 1970; Sepulveda et al., 2003). All of the bonitos and tunas examined in this study possess complete lamellar fusions. By binding lamellae on adjacent filaments (Fig. 3A), these fusions add to the gill's structural integrity and maintain constant lamellar pore dimensions, which increases gas-transfer efficiency. In addition, mucosal epithelial filament fusions (Table 1, Figs. 1,2) contribute to the gill rigidity of *Thunnus*, the most derived tuna genus. These fusions appear to correlate with a generally larger body size and hence the faster cruising speed. In the smaller species of *Thunnus* (i.e., albacore, blackfin tuna, longtail tuna), filament fusions are only found on the trailing edges of the gill hemibranchs. However, in the larger body-sized species (i.e., bigeye, yellowfin, and bluefin tunas) filament fusions are also present on the leading edge (Fig. 2A-C).

Billfishes. All billfishes are thought to be obligate ram ventilators and there is not a trend toward progressive gill-fusion complexity within this group. All of the 6 species examined have cartilaginous-based filament fusions covered in epithelial toothplates which are present on both the leading and trailing edges of the filaments. However, some differences occur in lamellar fusion status; sailfish and striped marlin gills are similar in the presence of lamellar and interlamellar fusions, while the swordfish lacks both. Lamellar fusion status remains unresolved in *Makaira*, *Istiompax*, and *Tetrapturus* due to the poor quality of the lamellar structure of the preserved specimens examined. However, based on the billfish phylogeny shown in Figure 1 and the presence of interlamellar and lamellar fusions in both the striped marlin and sailfish, these two types of lamellar fusion are also likely present in these three genera.

Gill fusion development and correlations with body size

The finding of interlamellar fusions in a 2.0 cm FL yellowfin tuna (Fig. 5) and complete lamellar fusions in a 3.2 cm specimen (Fig. 6) is consistent with the observation (Muir and Kendall, 1968) of complete lamellar fusions in a 3 cm skipjack tuna and indicates that tunas and bonitos make an early transition to the use of, and possible reliance upon, ram ventilation. Also supporting this contention are the findings of complete lamellar fusions in small (< 12 cm) little tunny, black skipjack, and Atlantic bonito (Table 1). In contrast, the occurrence of interlamellar rather than complete lamellar fusions in 12.5 - 33.0 cm sailfish suggests a slower transition to a

complete reliance upon ram ventilation. The lack of interlamellar fusions in a small (22.7 cm) Queensland school mackerel, but their presence in larger individuals (46.9 – 58.5) suggests a similar trend (Table 1).

The development of filament fusions at relatively small body sizes appears to be a consistent feature in all species examined. Although not appearing in a 95.5 g (33.0 cm) sailfish, filament fusions completely cover the trailing edges of the gill filaments and approximately one-third to one-half the leading edges in a 1.3 kg (56.5 cm) swordfish. In a 6.9 kg (88.5 cm) swordfish, filament fusions are fully formed and cover both the leading and trailing edges as shown in Figure 2. In tunas, filament fusions are completely formed on the trailing edges and partially formed in on the leading edge in a 1.6 kg (43.5 cm) yellowfin, a 0.83 kg (38.5 cm) longtail tuna, a 1.6 kg (46.0 cm) blackfin tuna, and a 2.1 kg (75.0 cm) wahoo.

Gill fusions and water flow

The complete development of filament fusions at a small body size suggests their role in more than gill support. Muir and Kendell (1968) proposed that filament fusions may also aid respiration by restricting both the speed and volume of water entering the lamellar channels. In this way, filament fusions would act in concert with modifications in lamellar shape and number which, while of major importance for gas exchange, also increase branchial resistance and both slow and streamline ram ventilatory flow (Wegner et al., in press). Moreover, the finding of a negative correlation between lamellar frequency and the prevalence of filament fusions in some

species suggests that the added resistance of filament fusions may have relaxed selection for a high lamellar frequency (Wegner et al., in press). For example, lamellar frequency is higher in scombrids lacking filament fusions (e.g., Pacific chub mackerel, eastern Pacific Bonito, and skipjack tuna) and lowest in the swordfish in which filament fusions cover both the entire leading and trailing edges of the gill filaments (Fig. 2G). Other scombrids and billfishes are intermediate in this respect. Bluefin and yellowfin tunas and the wahoo, which have filament fusions along 30-40% of their leading filament edges (Fig. 2A,B,D) have higher lamellar frequencies than the striped marlin, which has fusions covering 70-80% of its leading filament edges (Fig. 2F).

The role of filament fusions in slowing and streamlining the ram-ventilatory stream may help to explain their distribution on the leading edge of the gill filaments. With the exception of the swordfish, in which filament fusions cover the entire leading edge (Fig. 2G), fusions in other species are most abundant near the gill arch (Fig. 2A-F). This appears to correlate with the area of highest water inertia, and filament fusions at this location may help to disperse the flow of water evenly along the length of the filaments (i.e., fusions would limit the volume of water entering the interlamellar channels near the gill arch). The distinctions in filament fusion patterns between species may therefore reflect interspecific differences in the branchial stream. For example, in the smaller bodied *Thunnus* species (i.e., albacore, blackfin tuna, longtail tuna) water inertia in the branchial chamber may be lower than that of the

larger members of this genus swimming at faster speeds, and thus filament fusions may not be required on the leading edge to help evenly disperse water flow.

Evolution of gill fusions

Figure 1 suggests that filament fusions have independently evolved three times for use in ram ventilation: once in the billfishes, and twice in scombrids (in the wahoo, and again in the genus *Thunnus*). The similarity of the cartilaginous and epithelial toothplate-covered filament fusions of the wahoo and billfishes, along with a number of other shared characters, led Johnson (1986) to propose that the billfishes are sister group to the wahoo and should be included within the family Scombridae. This would indicate the independent evolution of filament fusions had happened only twice. However, recent molecular work (Orrell et al., 2006) suggests separate billfish and scombrid suborders, and thus supports the independent evolution of these structures three times.

The number of appearances of lamellar fusions for ram ventilation remains less clear. One possibility is that lamellar fusions have independently evolved twice, once in scombrids and once in billfishes. Under this scenario, the interlamellar fusions of *Scomberomorus* and the wahoo would be the primitive character state that led to the lamellar fusions of bonitos and tunas. This hypothesis is supported by the ontogeny of yellowfin lamellar fusion development in that lamellae are first bound by interlamellar fusions which subsequently grow together to form complete lamellar fusions.

However, this theory implies the loss of interlamellar fusions in *Grammatorcynus* and some members of *Scomberomorus*.

Conclusions for scombrid and billfish specializations for ram ventilation

Gill adaptation for ram ventilation must slow and streamline the high-pressure ventilatory stream to create optimal flow conditions in the interlamellar channels for gas exchange, and increase gill rigidity to maintain gill configuration in face of the forceful ventilatory stream. The results of this study combined with gill morphometric data (Wegner et al., in press) show that the progressive changes in the gill structure of both scombrids and billfishes for ram ventilation include: 1. Lamellae that are long and low in profile (height) which creates an extended axis for attachment to the gill filament and increases lamellar stability. 2. A high lamellar frequency which works in conjunction with long lamellae to increase branchial resistance and slow the ram ventilatory stream. 3. Binding of adjacent lamellae on the same filament (interlamellar fusions) to secure lamellar pore dimensions. 4. Binding of interlamellar fusions to form complete lamellar fusions which further strengthens lamellar pore integrity and increases filament rigidity. 5. Formation of filament fusions which provide additional support to the gills and increase branchial resistance to slow and streamline ram ventilatory flow.

Table 2.1: Gill fusions in scombrids and billfishes

Species Name	Common Name	n Collected	n Museum	FL (cm)	Mass (kg)	Lamellar Fussion	Filament Fusion
Thunnus alalunga	Albacore	2	-	82.0	11.3	LF	Epith
Thunnus albacares	Yellowfin tuna	19	6	43.5 - 182.0	1.6 - 94.0	LF	Epith
Thunnus atlanticus	Blackfin tuna	-	6	46.0 - 52.0	1.6 - 2.4	LF	Epith
Thunnus obesus	Bigeye tuna	1	-	136.0	46.0	LF	Epith
Thunnus orientalis	Pacific bluefin tuna	5	-	86.0 - 120.0	12.2 - 32.3	LF	Epith
Thunnus tonggol	Longtail tuna	2	6	38.5 - 85.5	0.83 - 9.6	LF	Epith
Katsuwonus pelamis	Skipjack tuna	4	4	36.0 - 77.0	1.8 - 9.6	LF	None
Euthynnus affinis	Kawakawa	4	8	32.0 - 78.0	0.48 - 6.0	LF	None
Euthynnus lineatus	Black skipjack	11	-	19.3 - 42.0	0.10 - 1.31	LF	None
Auxis rochei	Bullet tuna	-	2	21.8 - 36.0	0.11 - 0.76	LF	None
Auxis thazard	Frigate tuna	2	5	33.0 - 44.5	0.56 - 1.48	LF	None
Sarda australis	Australian bonito	-	1	33.0	0.52	LF	None
Sarda chiliensis	Eastern Pacific bonito	20	-	27.5 - 82.0	0.15 - 6.4	LF	None
Sarda orientalis	Striped bonito	-	2	48.0 - 50.5	1.45 - 1.56	LF	None
Sarda sarda	Atlantic bonito	-	1	48.0	1.58	LF	None
Cybiosarda elegans	Leaping bonito	7	-	30.6 - 35.5	0.44 - 0.67	LF	None
Acanthocybium solandri	Wahoo	9	-	75.0 - 152.0	2.1 - 24.2	IF	Cart
Scomberomorus commerson	Narrow-barred Spanish mackerel	5	-	43.5 - 96.0	0.59 - 7.0	None	None
Scomberomorus concolor	Monterey Spanish mackerel	-	1	55.0	1.29	None	None
Scomberomorus queenslandicus	Queensland school mackerel	5	1	46.9 - 58.5	0.87 - 1.65	IF	None
Scomberomorus sierra	Pacific sierra	5		47.0 - 50.0	0.75 - 0.90	None	None
Grammatorcynus bicarinatus[1,2]	Shark mackerel	2	-	-	3.5 - 4.5	None	None
Grammatorcynus bilineatus	Double-lined mackerel	-	4	41.5 - 51.0	0.59 - 0.95	None	None
Rastrelliger kanagurta	Indian mackerel	2	-	31.5	0.43	None	None
Scomber japonicus	Chub mackerel	20		21.0 - 40.0	0.10 - 0.74	None	None
Istiophorus platypterus[3]	Sailfish	2		200.0 - 207.0	31.0 - 34.4	IF, LF	Cart
Kajikia audax[3]	Striped marlin	7	-	95.0 - 188.5	8.0 - 70.0	IF, LF	Cart
Xiphias gladius[3]	Swordfish	5	-	103.0 - 187.0	20.0 - 125.1	None	Cart

Table 2.1: Gill fusions in scombrids and billfishes, Continued

Species Name	Common Name	n Collected	n Museum	FL (cm)	Mass (kg)	Lamellar Fussion	Filament Fusion
Billfishes (poor condition)							
Mikaira nigricans[4]	Blue marlin		1	-	-	-	Cart
Tetrapturus angustirostris[1,3]	Shortbill spearfish		2	132.0 - 143.0	-	-	Cart
Tetrapturus georgii[1,3]	Roundscale spearfish		1	173.0	-	-	Cart
Xiphias gladius[3]	Swordfish		5	56.5 - 88.5	1.3 - 6.4	-	Cart
Juveniles[5]							
Thunnus albacares	Yellowfin tuna		6	1.5 - 5.2	0.10 - 2.22 g	IF, LF	None
Euthynnus alleteratus	Little tunny		1	8.0	4.6 g	LF	None
Euthynnus lineatus	Black skipjack		1	10.9	16.4 g	LF	None
Sarda Sarda	Atlantic bonito		1	11.5	10.0 g	LF	None
Scomberomorus queenlandicus	Queensland school mackerel		1	22.7	65.0 g	None	None
Istiophorus platypterus	Sailfish		13	12.4 - 33.0	4.5 - 95.5 g	IF	None

Notes:
[1]Length-weight regressions not available
[2]Weights were measured, but lengths were not determined
[3]Length is given as lower jaw fork length
[4]Length and weight unknown; based on gill size likely > 40 kg
[5]Juvenile scombrid and billfish mass is reported in grams.

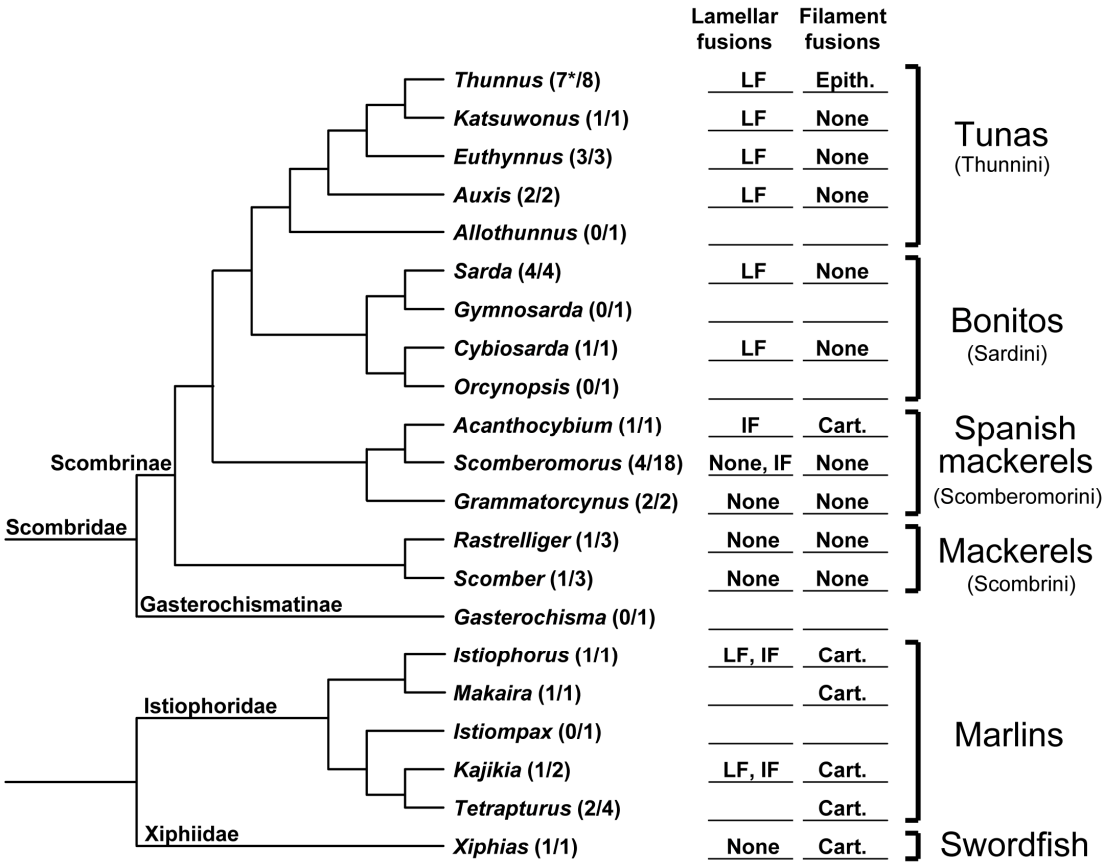

Figure 2.1: Scombrid and billfish cladograms showing the presence of the different gill fusion types for each genus. The number of species examined as a ratio of the total number in the genus is given in parentheses. Abbreviations: Cart., cartilaginous filament fusions; Epith., epithelial filament fusions; IF, interlamellar fusions; LF, lamellar fusions. Blank spaces indicate that fusion status remains undetermined. Scombrid cladogram based on Collette et al. 2001; billfish cladogram based on Collette et al. 2006. *Included in the number of *Thunnus* species examined is the bluefin tuna, *T. thynnus*, for which fusion data were reported by Muir and Kendall (1968).

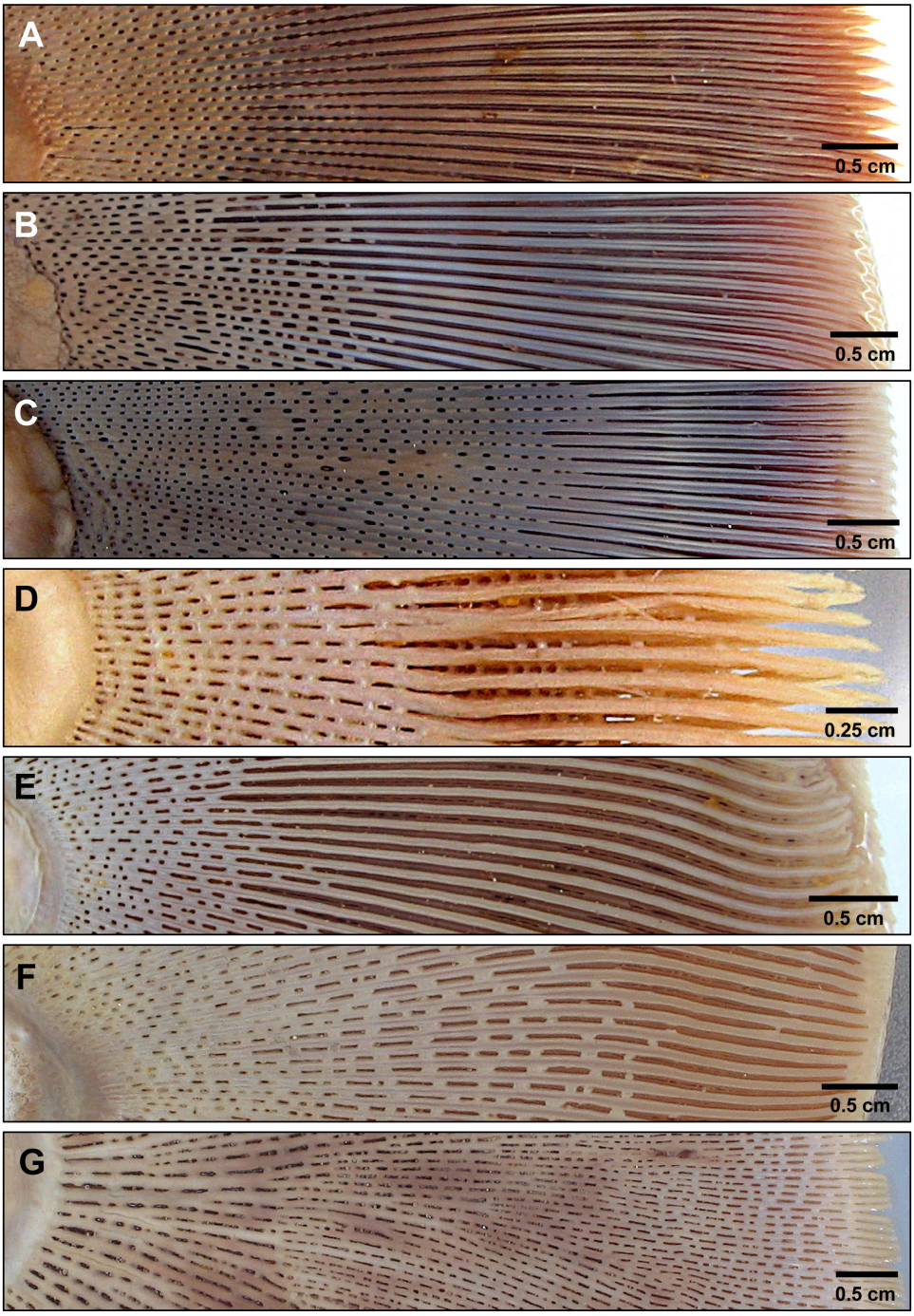

Figure 2.2: Filament fusions on the leading edge of the anterior hemibranch of the third gill arch near the cerato-epibranchial joint for: **A:** a 32.3 kg Pacific bluefin tuna, **B:** a 72.0 kg yellowfin tuna, **C:** a 46.0 kg bigeye tuna, **D:** a 24.2 kg wahoo, **E:** a 34.4 kg sailfish, **F:** a 67.8 kg striped marlin, and **G:** a 64.9 kg swordfish. **F** and **G** are from Wegner et al. (in press). The three *Thunnus* species lacking filament fusions on the leading edge and billfishes for which only preserved, museum specimens were available are not pictured.

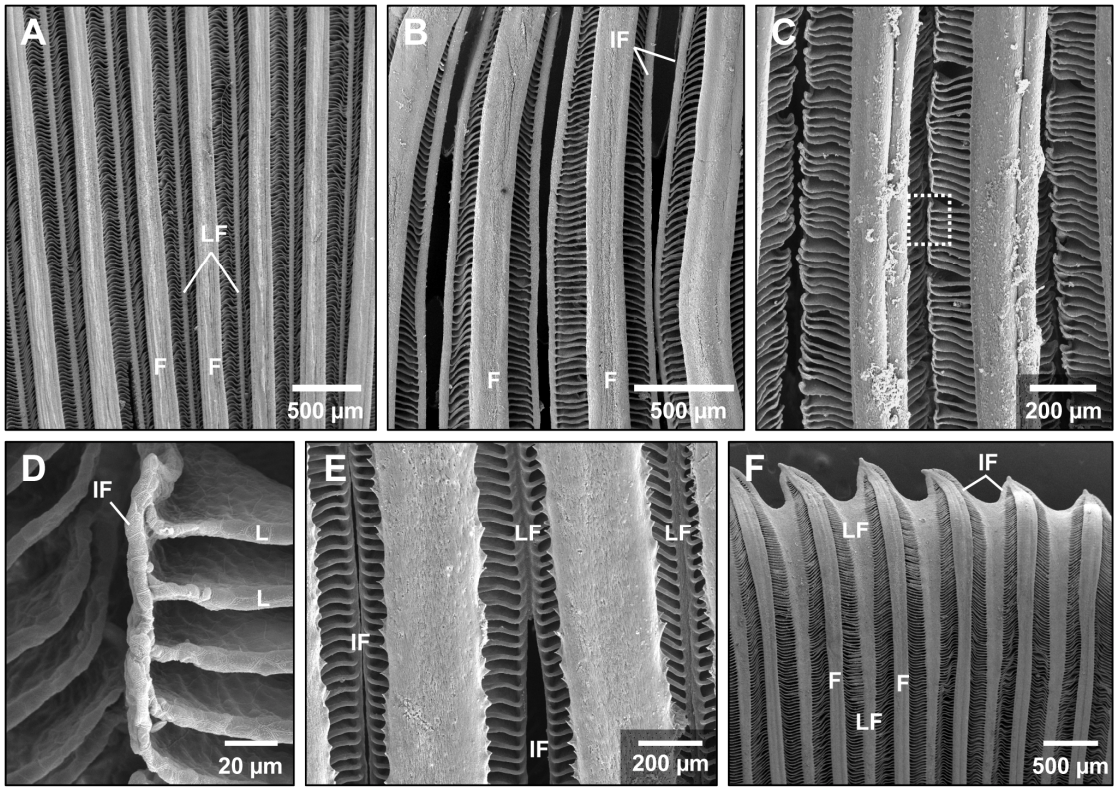

Figure 2.3: SEM images of lamellar and interlamellar fusions from **A:** a 1.45 kg eastern Pacific bonito, **B:** a 45.0 kg striped marlin, **C:** a 1.07 kg Queensland school mackerel, **D:** a 1.07 kg Queensland school mackerel (magnified image of box in C), **E:** a 25.0 kg striped marlin, and **F:** a 1.45 kg eastern Pacific bonito. B and E are from Wegner et al. (2006). Abbreviations: F, filament; IF, interlamellar fusion; L, lamellae; LF, lamellar fusion. Water flow is into the page.

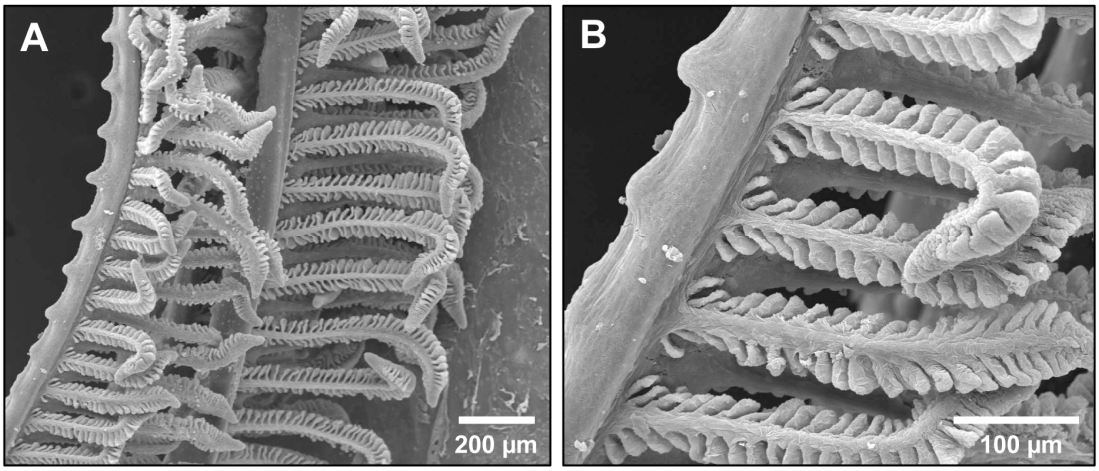

Figure 2.4: Gill arches and filaments from a 1.5 cm (103 mg) yellowfin tuna.

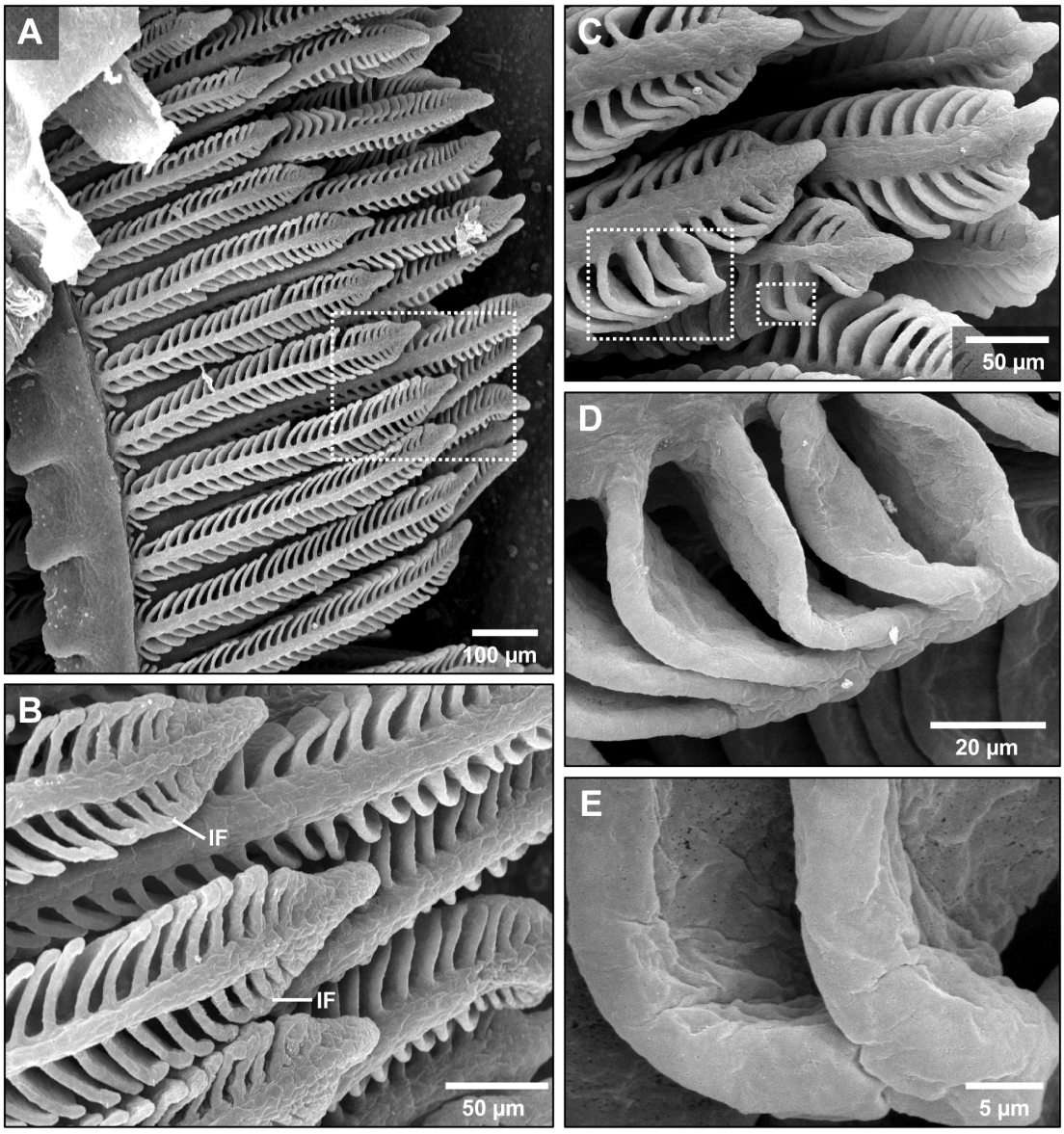

Figure 2.5: SEM images of the gill filaments and lamellae of a 2.0 cm (154 mg) yellowfin tuna. **A:** Filaments from the first gill arch. **B:** Enlarged image of dotted box in A showing interlamellar fusions forming near some filament tips. **C:** Filament tips with interlamellar fusions. **D:** Magnification of dotted box in **C** (left). **E:** Enlarged image of dotted box in **C** (right) showing the curving of a lamella toward the filament tip to fuse with the adjacent lamella. Abbreviations: IF, interlamellar fusion.

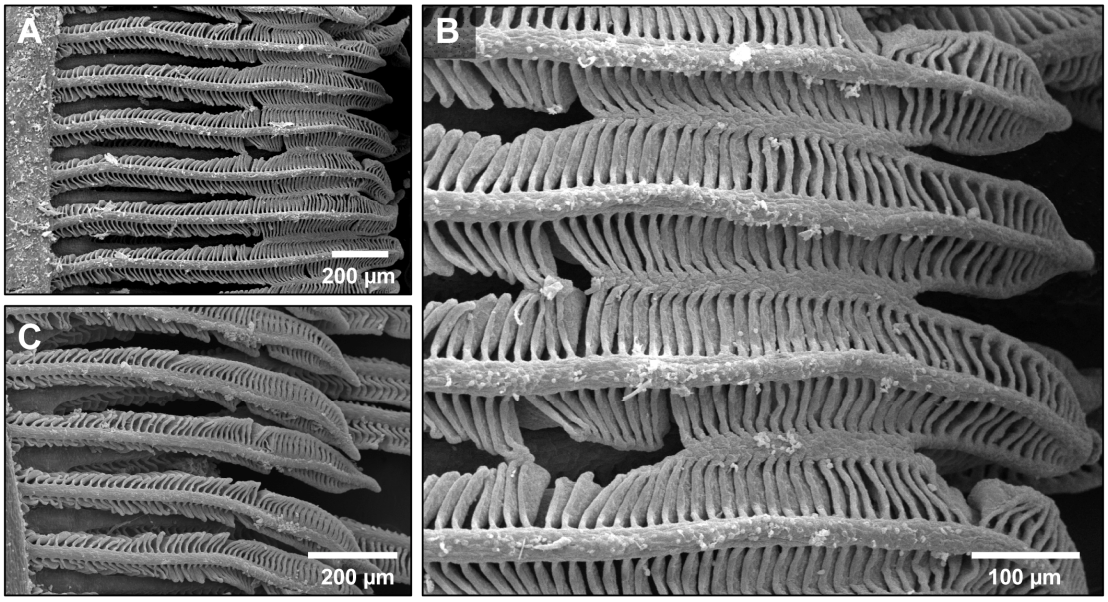

Figure 2.6: SEM images of the gill filaments in a 3.2 cm (915 mg) yellowfin tuna. **A:** Gill filaments showing interlamellar fusions near the tips that grow together to form complete lamellar fusions, while no fusions are present near the base of the filaments. **B:** Magnified image of dashed box in **A**. **C:** Gill filaments showing interlamellar fusions near the tips but no lamellar fusions.

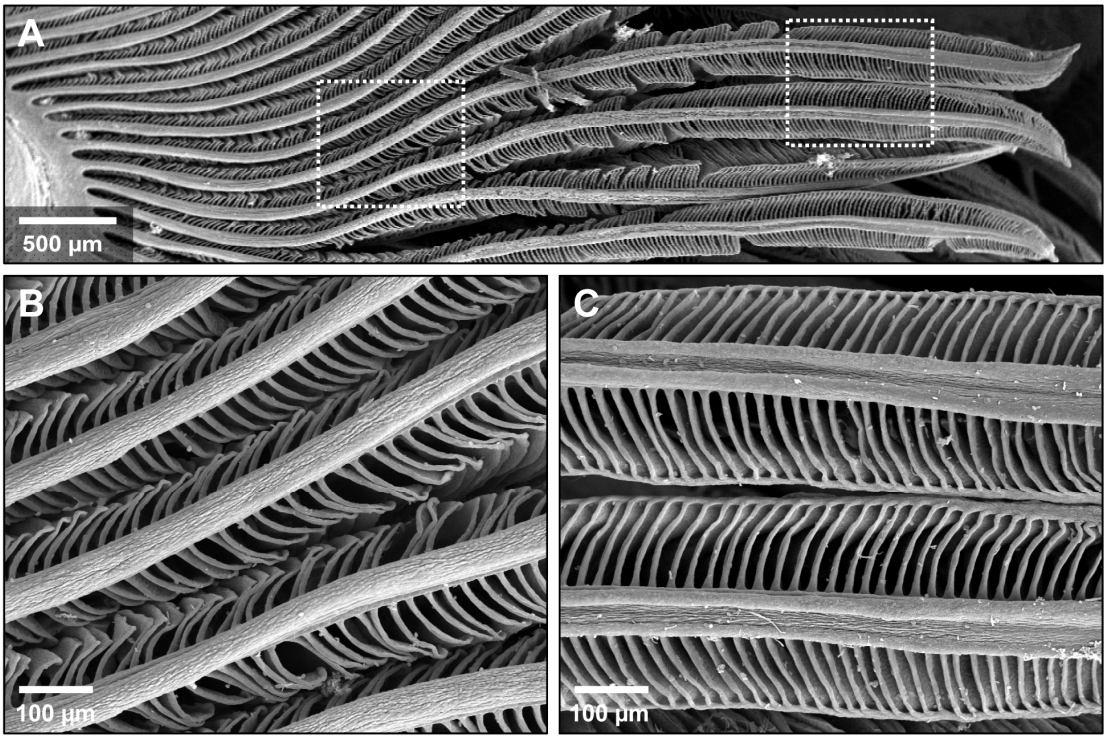

Figure 2.7: Gills filaments from a 28.5 cm (68.0 g) sailfish. **A:** Synoptic view of the entire gill filament length leaving the gill arch on left. **B:** Enlarged image of dotted box in **A** (left) showing non-fused lamellae near the base of the filaments. **C:** Magnified box in **A** (right) showing interlamellar fusions near the filament tips.

LITERATURE CITED

Beerkircher LR. 2005. Length to weight conversions for wahoo, *Acanthocybium solandri*, in the Northwest Atlantic. Col Vol Sci Papers ICCAT 58:1616-1619.

Brown CE, Muir BS. 1970. Analysis of ram ventilation of fish gills with application to skipjack tuna (*Katsuwonus pelamis*). J Fish Res Bd Canada 27:1637-1652.

Chatwin BM. 1959. The relationships between length and weight of yellowfin tuna (*Neothunnus macropterus*) and skipjack tuna (*Katsuwonus pelamis*) from the Eastern Tropical Pacific Ocean. Inter-Amer Trop Tuna Comm Bull 3:305-352.

Chiang W-C, Sun C-L, Yeh S-Z, Su W-C. 2004. Age growth of sailfish (*Istiophorus platypterus*) in waters off eastern Taiwan. Fish Bull 102:251-263.

Collette BB, McDowell JR, Graves JE. 2006. Phylogeny of recent billfishes (Xiphioidei). Bull Mar Sci 79:455-468.

Collette BB, Reeb C, Block BA. 2001. Systematics of the tunas and mackerels (Scombridae). In: Block BA, Stevens ED, editors. Tuna: Physiology, ecology and evolution. San Diego: Academic Press. p 5-30.

Davie PS. 1990. Pacific marlins: Anatomy and physiology. Palmerston North, New Zealand: Simon Print. 88 p.

de la Serna JM, Ortiz de Urbina JM, Alot E, García S, Rioja P. 2005. Biological parameters of bullet tuna (*Auxis rochei*) observed in the Spanish Mediterranean fisheries. Col Vol Sci Pap ICCAT 58:517-526.

Faruk Kara O. 1979. Observations on growth and relationship between length and weight of *Sarda sarda* (Bloch). Inv Pesq 43:95-105.

Freadman MA. 1979. Swimming energetics of striped bass (*Morone saxatilis*) and bluefish (*Pomatomus saltatrix*): Gill ventilation and swimming metabolism. J Exp Biol 83:217-230.

Freadman MA. 1981. Swimming energetics of striped bass (*Morone saxatilis*) and bluefish (*Pomatomus saltatrix*): Hydrodynamic correlates of locomotion and gill ventilation. J Exp Biol 90:253-265.

Graham JB. 2006. Aquatic and aerial respiration. In: Evans DH, Claiborne JB, editors. The physiology of fishes. Third ed. Boca Raton: CRC Press. p 85-117.

Graham JB, Dickson KA. 2004. Tuna comparative physiology. J Exp Biol 207:4015-4024.

Hsu CC, Liu HC, Wu CL, Huang ST, Liao HK. 2000. New information on age composition and length-weight relationship of bluefin tuna, *Thunnus thynnus*, in the southwestern North Pacific. Fish Sci 66:485-493.

Johnson GD. 1986. Scombroid phylogeny: An alternative hypothesis. Bull Mar Sci 39:1-41.

McPherson GR. 1992. Age and growth of the narrow-barred Spanish mackerel (*Scomberomorus commerson* Lacepede, 1800) in north-eastern Queensland waters. Aust J Mar Freshwater Res 43:1269-1282.

Moazzam M, Osmany HB, Zohra K. 2005. Indian mackerel (*Rastrelliger kanagurta*) from Pakistan-I. Some aspects of biology and fisheries. Rec Zool Surv Pakistan 16:58-75.

Muir BS. 1969. Further observations on gill modifications of oceanic fishes. Copeia 1969:629.

Muir BS, Kendall JI. 1968. Structural modifications in the gills of tunas and some other oceanic fishes. Copeia 1968:388-398.

Muthiah C. 1985. Fishery and bionomics of tunas at Mangalore. CMFRI Bull 36:51-70.

Orrell TM, Collette BB, Johnson GD. 2006. Molecular data support separate scombroid and xiphioid clades. Bull Mar Sci 79:505-519.

Ramos A, Alot E, Camiñas JA. 1986. Relacion talla/peso de la melva, *Auxis thazard*, para el Atlantico y Mediterraneo. Col Vol Sci Pap ICCAT 25:265-268.

Roberts JL. 1975. Active branchial and ram gill ventilation in fishes. Biol Bull Mar Biol Lab, Woods Hole 148:85-105.

Roberts JL. 1978. Ram gill ventilation in fish. In: Sharp GD, Dizon AE, editors. The physiological ecology of tunas. San Francisco: Academic Press. p 83-88.

Sepulveda CA, Dickson KA, Graham JB. 2003. Swimming performance studies on the eastern Pacific bonito *Sarda chiliensis*, a close relative of the tunas (family Scombridae) I. Energetics. J Exp Biol 206:2739-2748.

Steffensen JF. 1985. The transition between branchial pumping and ram ventilation in fishes: Energetic consequences and dependence on water oxygen tension J Exp Biol 114:141-150.

Stevens ED. 1972. Some aspects of gas exchange in tuna. J Exp Biol 56:809-823.

Stevens ED, Lightfoot EN. 1986. Hydrodynamics of water flow in front of and through the gills of skipjack tuna. Comp Biochem Physiol 83A:255-259.

Vieira KR, Lins Oliveira JE, Barbalho MC, Aldatz JP. 2005. Aspects of the dynamic population of blackfin tuna (*Thunnus atlanticus* - Lesson, 1831) caught in the northeast Brazil. Col Vol Sci Pap ICCAT 58:1623-1628.

Wegner NC, Sepulveda CA, Bull KB, Graham JB. in press. Gill morphometrics in relation to gas transfer and ram ventilation in high-energy demand teleosts: scombrids and billfishes. J Morph.

Wegner NC, Sepulveda CA, Graham JB. 2006. Gill specializations in high-performance pelagic teleosts, with reference to striped marlin (*Tetrapturus audax*) and wahoo (*Acanthocybium solandri*). Bull Mar Sci 79:747-759.

ACKNOWLEDGEMENTS

This research was supported by the National Science Foundation Grant #IOS-0817774, the Tuna Industry Endowment Fund at Scripps Institution of Oceanography, the Pfleger Institute of Environmental Research, the George T. Pfleger Foundation, and the Moore Family Foundation. N.C. Wegner was supported by the Nadine A. and Edward M. Carson Scholarship awarded by the Achievement Rewards for College Scientists (ARCS), Los Angeles Chapter, and the National Science Foundation. Wegner's travel to Australia was funded by the Kennel-Haymet Student Lecture Award. This work would not have been possible without the many scientists and fishermen that helped in the acquisition of gill samples; we thank N. Ben-Aderet, D. Bernal, R. Brill, D. Cartamil, K. Dickson, J. Finan, D. Fuller, A. Graham, S. Griffiths,

D. McCarthy, M. McGrouther, M. Musyl, J. Pepperell, K. Schaefer, H. Walker, L. Williams, and the crews of the *Polaris Supreme* and *Oscar Elton Sette*. Juvenile yellowfin tuna samples were donated by the Jeanne Wexler from the Inter-American Tropical Tuna Commission's Achotines Laboratory. Pacific bluefin tuna gills were provided compliments of Eric Pedersen. We additionally thank E. York of the SIO Analytical Facility for technical assistance with microscopy work and P. Hastings, M. McHenry, F. Powell, and R. Rosenblatt for reviewing versions of this manuscript.

Chapter 2, in full, is currently being prepared for submission for publication as: Wegner NC, Sepulveda CA, Aalbers SA, Graham JB. Structural adaptations for ram ventilation: Gill fusions in scombrids and billfishes. Journal to be determined. The dissertation author is the primary investigator and author of this paper.

CHAPTER 3: FUNCTIONAL MORPHOLOGY OF THE GILLS OF THE SHORTFIN MAKO, *ISURUS OXYRINCHUS*, A LAMNID SHARK

ABSTRACT

This study examines the gill structure of a lamnid shark, the shortfin mako (*Isurus oxyrinchus*) in order to determine the extent to which its gill structure is convergent with that of tunas for specializations required to increase gas exchange and withstand the forceful branchial flow induced by ram ventilation. Mako gill structure is also compared to that of the blue shark (*Prionace glauca*), an epipelagic species with lower metabolic requirements and not dependent on ram ventilation. The mako has about one-half the total gill area of a comparably sized tuna, but more than twice the proportionate gill area of the blue shark and other non-lamnid shark species. Also distinguishing mako gill structure from that of other sharks are shorter diffusion distances at the gill lamellae and a more fully developed diagonal lamellar blood-flow pattern similar to that found in tunas and other high-energy demand teleosts. Mako gills lack the filament and lamellar fusions of tunas and other ram-ventilating teleosts. However, one to two vascular sacs, located near the leading edge (water-entry side) of each mako lamella, appear to have a supporting function in that they protrude from the lamellar surface and abut sacs of the adjacent lamella. These in-series abutments stabilize the water-entry region of each lamella and maintain the width of the interlamellar channels. Moreover, because blood flow through the sacs is continuous with gill circulation, changes in vascular pressure could potentially influence water volume and speed past the lamellae. However, vascular sacs also occur in the blue

shark and no other structural elements of the mako gill appear specialized for ram ventilation. Rather, the basic elasmobranch gill design and the pattern of branchial circulation are all conserved in mako gills. Despite specializations that increase gill area and efficacy relative to other sharks, the retention of basic features of the elasmobranch gill design appears to have limited selection for the higher total gill areas, greater metabolic capacity, and adaptations for effective ram ventilation achieved by tunas.

INTRODUCTION

Sharks of the family Lamnidae have a suite of adaptations for fast, continuous swimming and show a remarkable evolutionary convergence with tunas. Both lamnids and tunas are streamlined and have undergone comparable changes in myotomal structure in which the red (aerobic) muscle occurs in a more central and anterior position within the body and contributes to the common occurrence of the thunniform swimming mode in both groups (Bernal et al., 2003a; Donley et al., 2004; Shadwick, 2005; Gemballa et al., 2006; Perry et al., 2007). In addition, the blood supply to the red muscle passes through counter-current heat exchangers (*retia mirabilia*), which conserve aerobic heat produced during continuous swimming (Carey and Teal, 1966; Carey et al., 1971; Bernal et al., 2001). The advantages of red-muscle endothermy are increased muscle power output and the acceleration of metabolically mediated processes (Altringham and Block, 1997; Graham and Dickson, 2001; Dickson and Graham, 2004; Bernal et al., 2005). Correspondingly, lamnids and

tunas have higher oxygen demands than most other fishes (Brill, 1979; 1987; Dewar and Graham, 1994; Korsmeyer and Dewar, 2001; Sepulveda et al., 2007), as well as larger hearts with higher cardiac outputs and pressures, higher blood hemoglobin concentrations and hematocrits, and higher muscle myoglobin concentrations to facilitate oxygen supply to the aerobic musculature (Emery, 1986; Brill and Bushnell, 1991; Lai et al., 1997; Bernal et al., 2001; Brill and Bushnell, 2001; Bernal et al., 2003a; Bernal et al., 2003b). However, despite this array of convergent properties, the overall metabolic capacity of lamnids, while exceeding that of other sharks, does not match that of tunas (Bernal et al., 2003a; Bernal et al., 2003b; Dickson and Graham, 2004).

Relatively little is known about comparative aspects of lamnid-tuna convergence of gill structure, which requires modifications for increased gas transfer and resistance to deformation in the face of the steady, high pressure branchial flow induced by ram ventilation. For tunas, gas exchange is enhanced by gill surface areas that are as much an order of magnitude greater than those of most other teleosts (Muir and Hughes, 1969; Wegner et al., in press) and by short diffusion distances resulting from slender lamellae with a thin respiratory epithelium (water-blood barrier distance) (Hughes, 1970; Hughes and Morgan, 1973; Hughes, 1984a; Wegner et al., 2006). In addition, a diagonal blood flow pattern in tuna lamellae minimizes vascular resistance and contributes to gill efficacy by allowing a closer match between the residence time of blood at the exchange surface and the time required for gas transfer (Muir and Brown, 1971; Olson et al., 2003; Wegner et al., in press). Tuna adaptations for

managing the force and streamlining of ram-ventilatory flow include lamellar and, in some species, filament fusions, which stiffen the gills (Muir and Kendall, 1968; Johnson, 1986; Wegner et al., 2006), and the flow resistance imposed by long and closely spaced lamellae (Wegner et al., in press).

Data on lamnid gill structure are limited to two papers that reporting opposite findings. Emery and Szczepanski (1986) found that the gill surface area of two lamnids (the shortfin mako, *Isurus oxyrinchus*, and white shark, *Carcharodon carcharias*) are 2-3 times greater than those of other pelagic shark species. In contrast, Oikawa and Kanda (1997), who examined only one shortfin mako specimen, reported that its gill surface area was similar to that of other sharks. Other factors associated with oxygen uptake in the lamnid gill (e.g., lamellar diffusion distances and blood-flow patterns) have gone unstudied, and there are no reports dealing with the relationship of ram ventilation to lamnid gill design. Relative to teleosts, the path of water flow through shark gills is more tortuous and involves much greater contact with surfaces that potentially impede flow. Sharks have interbranchial septa, which originate at the gill arches, bind adjacent hemibranchs, and extend out to the lateral edge of the body to form the gill flaps. While this configuration likely stiffens the gills for ram ventilation by binding the trailing edges of the filaments, it necessarily imposes greater flow resistance because water passing between the lamellae must subsequently flow through septal channels to exit the gill.

This study compares the gill structure of the shortfin mako to that of tunas and the blue shark (*Prionace glauca*), a non-lamnid, which has lower metabolic

requirements and is not dependent on ram ventilation. The objective is to determine the extent to which mako gill structure differs from that of other sharks and is convergent with tunas in specializations for increased gas exchange required by heightened aerobic demands and for the continuous force imposed on the gills by ram ventilation.

METHODS

Gill collection

Gills were acquired opportunistically from 20 makos (4.6 – 71.0 kg, 77.0 – 187.5 cm FL) and 8 blue sharks (2.4 – 47.8 kg, 72.0 – 197.0 cm FL) collected for other studies or taken in scientific long-line cruises conducted by the National Marine Fisheries Service in waters off of Southern California and the Hawaiian Islands. Captured sharks were euthanized by severing the spinal cord at the base of the chondrocranium in accordance with protocol S00080 of the University of California, San Diego Institutional Animal Care and Use Committee. The mass of each specimen was determined with an electronic scale or, when direct measurement was not possible, by length-weight regression equations (Kohler et al., 1995).

Three procedures were used to prepare the gills for examination:

1. For the majority of sharks collected, all five gill arches from one or both sides of the branchial chamber were excised and fixed in 10% formalin buffered in seawater. This tissue was used to determine gill area dimensions, measure lamellar thickness and

the water-blood barrier distance, and examine general morphology using scanning electron and light microscopy.

2. Small sections of the first gill hemibranch were excised from four makos (9.0 – 33.0 kg, 90.0 – 132.0 cm FL) and one blue shark (44.0 kg, 197.0 cm FL) and placed in 4% paraformaldehyde in 10 mM phosphate buffered saline (PBS) for 24 h. Fixed tissue was then removed from the paraformaldhyde solution, rinsed in 10mM PBS followed by two changes of 75% ethanol to remove the fixative. These samples were used in immunochemical treatments to determine the position of mitochondria-rich cells (MRC) and also to prepare microscope slides for morphological analysis. It is important to note that gill samples prepared in treatments 1 and 2 were excised immediately following euthanasia and that a low-pressure salt water hose was used to keep the tissues moist during the dissection in order to prevent the degradation of fine gill structure that occurs with prolonged air exposure following capture (< 20 min, Wegner pers. obs.).

3. Five makos (5.0 – 21. 2 kg, 76.0 – 127.0 cm FL) and two blue sharks (3.4, 17.1 kg, 84, 141 cm FL) were perfused with microvascular casting solution (either Batson's #17 Anatomical Corrosion Kit, Polysciences Inc., Warrington, PA or Mercox, Ladd Research, Williston, VT). Euthanized sharks were placed ventral side up in a V-shaped cradle and the gills were irrigated with aerated sea water. The heart was exposed by mid-line incision, a catheter inserted, and the specimen was perfused with heparinized shark saline for 2-3 min followed by microvascular casting solution. Perfusions were conducted at 70-95 mmHg which is consistent with ventral-aortic

systolic pressures observed in swimming makos (Lai et al., 1997). After complete polymerization (< 15 min), the gills were excised; one side was placed in 10% formalin buffered in seawater, and the second was macerated in washes of 10-20% KOH until all of the tissue was removed. The resulting plastic replica casts were then rinsed, air dried, and used for examination of the gill vasculature and for mako gill-area measurements.

Gill surface area

Total gill surface area was estimated for five makos (two that had been injected with microvascular casting solution and three that had gill tissue fixed in 10% formalin) following the methods of Muir and Hughes (1969) and Hughes (1984b) and using the equation:

$$A = L_{fil} \cdot 2n_{lam} \cdot A_{lam} \quad (1)$$

where A is the total gill area, L_{fil} is the total length of all of the gill filaments (i.e., total filament length), n_{lam} is the mean number of lamellae per length of filament (i.e., lamellar frequency; this is multiplied by two to account for the two rows of lamellae, one on each side of the filament), and A_{lam} is the mean bilateral surface area of a lamella.

Total filament length was determined by counting all of the gill filaments on the five gill arches from one side of the branchial chamber. Filaments were divided into bins of 20 and the length of the medial filament (i.e., number 10, 30, 50, etc.) was determined and assumed to represent the average length of individual filaments in that

bin. The total length of all the filaments in each bin was calculated and the bins from all five gill arches were added to determine the total filament length for one side of the branchial chamber. This value was then multiplied by two to account for the gill filaments from the other side of the body.

Filaments from the third gill arch were determined to be representative of average lamellar frequency and lamellar bilateral surface area. Therefore, the medial filament of each bin on the anterior and posterior hemibranchs of the third arch was sampled. To determine lamellar frequency, digital images were acquired of the base, middle, and tip of each filament using a camera mounted on a dissection microscope. For lamellar bilateral area, individual lamellae were dissected from the base, middle, and tip of the sampled filaments, mounted on slides, and photographed. Filament and lamellar images were analyzed using NIH Image J computer software.

Gill microstructure

Gill tissue fixed in 10% formalin was examined using both light and scanning electron microscopy (SEM). For light microscope preparation, fixed tissue was embedded in paraffin, and semi-thin sections (5 μm) were mounted on slides and stained with hematoxylin and eosin. For SEM, fixed tissue was rinsed with deionized water, slowly dehydrated to 100% ethanol (20-25% increments over 24 hours), and critical-point dried. Other sections of fixed gill tissue were rinsed in deionized water, dehydrated with tert-butyl alcohol (25% increments over 24 hours and rinsed twice at 100%), and frozen in the alcohol at 4 °C. Frozen samples were then placed into a

freeze dryer until all of the alcohol was extracted from the tissue. Both critically-point-dried and freeze-dried tissue was sputter coated with gold-palladium, and viewed using a FEI Quanta 600 SEM under high-vacuum mode. Because critical-point drying can cause a slight shrinkage in gill tissue, cross-sections through freeze-dried lamellae were used to estimate lamellar thickness and the water-blood barrier distance. These measurements were made for eight makos and four blue sharks by randomly sampling filaments from the 2nd, 3rd, and 4th gill arches. Longitudinal cross sections of the freeze-dried filaments were then mounted perpendicular to the SEM field of view and 15 measurements of the two different dimensions were made for each shark.

Gill tissue fixed in paraformaldehyde was used to determine the distribution of mitochondria-rich cells using immunohistochemical methods of Piermarini et al. (2002) and Hyndman and Evans (2007). Gill tissue was dehydrated in ethanol, embedded in paraffin and sliced into 7 μm sections mounted on slides and heated at 37 °C overnight. Slides were analyzed with monoclonal, anti-chicken Na^+-K^+-ATPase (α5, 1/100), developed by Dr. Douglas Fambrough and obtained from the Developmental Studies Hybridoma Bank under the auspices of the National Institute of Child Health and Human Development of the University of Iowa (Department of Biological Sciences, Iowa City, IA). Immunoreactivity was visualized with 3,3'-diaminobenzidine tetrahydrochloride (Biogenex, San Roman, CA). Other sections of paraformaldhyde-fixed tissue were mounted on slides and histologically stained with Masson Trichrome (Humason, 1997).

Details of general gill circulation were obtained by viewing macerated vascular casts using the SEM under low-vacuum mode. Mako and blue shark lamellar blood flow patterns were examined by randomly sampling 15 lamellae from each shark cast. SEM-acquired digital images were analyzed with Image J by measuring the angle of blood flow relative to the lamellar long axis midway along the length of each lamella.

Statistical analysis

Mass-regression equations for gill area and dimensions were determined using least-squares analysis. Significant differences in lamellar thickness, the water blood barrier distance, and the angle of lamellar blood flow between species were determined by the t-test ($P < 0.05$).

RESULTS

Gill surface areas and dimensions

Table 1 shows good general agreement in the mass-regression equations for total gill surface area and its constituent dimensions (L_{fil}, n_{lam}, A_{lam}) determined for five makos in this study and the data of Emery and Szczepanski (1986). Also shown in Table 1 is a comparison of values derived from these equations for a 4.48 kg mako, which is the size of the single specimen examined by Oikawa and Kanda (1997). The smaller gill area reported by these authors results from an underestimation of lamellar bilateral area which they calculated by measuring lamellar length and height and

assuming a triangular lamellar shape. Because most mako lamellae are generally rectangular, this underestimates lamellar size by a factor of two.

Lamellar dimensions and structure

Table 2 shows lamellar measurements for 8 makos and 4 blue sharks. Mako lamellar thickness (mean = 11.38 μm) is significantly less than that of the blue shark (15.24 μm), as is the water-blood barrier distance (mako, 1.15 μm; blue shark, 1.65 μm). Immunochemical-treated cross sections of mako and blue shark lamellae (Fig. 1) show that mitochondria-rich cells, which are involved in ion and acid-base balance, are present in both the lamellar and interlamellar filamental epithelium of the blue shark, but occur primarily only in the interlamellar epithelium of the gill filaments in the mako. The absence of MRCs in the lamellar epithelium of the mako contributes to a thinner water-blood barrier distance and lamellar thickness. Table 2 also shows little change in mako lamellar thickness with body size, while the larger blue sharks examined have thicker lamellae.

Figure 2 compares the patterns of lamellar blood flow in the shortfin mako (A), the blue shark (B), and two-high energy demand teleosts, the yellowfin tuna, *Thunnus albacares* (C), and the eastern Pacific bonito, *Sarda chiliensis* (D). Common to all four species is the presence of a diagonal flow pattern which differs from that observed for most fishes where blood flows parallel to and along the length of the lamellar long axis. However, the degree to which these species are specialized for this pattern varies in terms of blood delivery and collection, the angle of diagonal flow,

and the extent to which the diagonal pattern proceeds across the lamellar height. In yellowfin tuna (Fig. 4C), blood leaving the afferent lamellar arteriole enters several outer marginal channels that distribute flow along the lateral lamellar edge from which blood proceeds diagonally at an angle of 48.5 ± 10.3° relative to the long axis of the lamella; efferent blood is collected in an inner marginal channel (Wegner et al., in press). In the mako (Fig. 4A), two outer marginal channels typically distribute flow to the lamellar lateral edge, and the angle of diagonal flow (38.4 ± 6.7°) is significantly less. In addition, diagonal flow only extends across two-thirds to three-fourths of the lamellar height and then turns parallel to the long axis of the lamella; blood, therefore, is not collected by a single inner marginal channel. Both the blue shark (Fig. 4B) and eastern Pacific bonito (Fig. 4D) show patterns similar to that of the mako; however, the angles of diagonal flow in both species (blue shark = 28.1 ± 7.2°, bonito = 31.9 ± 6.7°) are significantly less. In the blue shark, a second outer marginal channel is often absent, and when present, is poorly developed.

Examination of mako and blue shark lamellae also reveals the presence of previously undescribed vascular "sacs" near the leading (efferent) lamellar edges (Fig. 3A). For both species, 1-2 vascular sacs are present on each lamella and their number generally correlates with lamellar size; lamellae near the filament base or associated with shorter filaments have a smaller bilateral surface area and tend to possess only a single vascular sac. On larger lamellae, near the middle or tip of the filaments, two vascular sacs are often present. The location of the vascular sacs on each lamella is consistent in that sacs from adjacent lamellae abut one another (Fig. 3B-D) suggesting

a function in lamellar stability and spacing. In addition, the efferent lateral edges of mako and blue shark lamellae are covered by a thicker epithelium than that of the lamellar respiratory surface (Fig. 3C). No quantifiable differences in these features were found between the mako and blue shark.

Gill vasculature

The general architecture of the mako gill vasculature is consistent with that of other elasmobranchs. Figure 4 shows the basic features of the gill filament circulation in the mako, which consists of three distinct vascular pathways: respiratory, nutrient, and interlamellar (Fig. 4). Blood enters the respiratory vasculature via the afferent filamental artery (AFA), which distributes blood along the length of the filament to the corpus cavernosum (CC) (Fig 4A-D). Afferent lamellar arterioles (ALA) rise from the corpus cavernosum to supply blood to the gill lamellae (Fig 4E); post-lamellar blood flow is collected in efferent lamellar arterioles (ELA), which feed into an efferent filamental artery (EFA) (Fig. 4F). Gill nutrient vessels (Fig. 4G,H) originate from EFAs and efferent branchial arteries (not shown) and extend throughout the filaments and interbranchial septum. The interlamellar vessels (Fig 4A, D-H) usually lay perpendicular to the long axis of the filament and extend underneath the interlamellar epithelium, over the corpus cavernosum, and beneath the epithelium lining the septal channel where they connect with the interlamellar vessels of the adjacent filament. The interlamellar vasculature appears to be connected to the main blood supply through anastomoses with small nutrient vessels.

DISCUSSION

Gill structure and gas exchange

Gill structure and function strongly correlate with activity and metabolic demand; active fishes typically have larger gill surface areas and shorter diffusion distances than species with lower aerobic requirements (Gray, 1954; Hughes, 1966; 1970; Hughes and Morgan, 1973; De Jager and Dekkers, 1975; Wegner et al., in press). This study of the gill structure of the shortfin mako further confirms this correlation and supports the conclusions of Emery and Szczepanski (1986) that lamnid gill surface areas are 2-3 times larger than those of other sharks (Table 3). Also correlating with activity is the mako's lamellar thickness (11.38 μm) and its water-blood barrier distance (1.15 μm), both of which are significantly less than those of the blue shark (15.24 μm, 1.65 μm) (Table 2). Water-blood barrier distances measured for both the mako and the blue shark are far less than the mean distances (4.85 - 11.27 μm) reported for four less-active, benthic elasmobranch genera (*Scyliorhinus*, *Squalus*, *Galeorhinus*, *Raja*) (Hughes and Wright, 1970).

The mako and blue shark also have a diagonal blood flow pattern through the gill lamellae which previously had only been documented for a few high-energy demand teleosts (Fig. 2). This pattern differs from that of most fishes in which the course of the blood flow through a lamella extends along its entire length, parallel to the lamellar long axis. Although it somewhat compromises the counter-current exchange mechanism, diagonal lamellar blood flow is considered to be an adaptation

that optimizes the relationship between the distance (= residence time) red blood cells spend in lamellar vessels and the time required for oxygen diffusion and loading by hemoglobin (Muir and Brown, 1971; Olson et al., 2003; Wegner et al., 2006; Wegner et al., in press). Because gas transfer in these fishes is augmented by shorter diffusion distances, the residence time needed for oxygenation becomes less than the time required for blood to move through a vessel parallel to and the length of the lamellar long axis. Diagonal flow through more numerous shorter channels should contribute to exchange efficacy by closely matching blood residence time to the time constants for the movement and binding of enough oxygen to saturate hemoglobin. An additional advantage imparted by diagonal flow is a reduction in vascular resistance (Muir and Brown, 1971). This effect is illustrated by using the Hagen-Poiseuille equation to describe the effects of lamellar-vessel length and diameter on the pressure change (Δp) occurring across a lamella:

$$\Delta p=(32\mu V l)/d^2 \ \text{(dynes/cm}^2\text{)} \qquad (2)$$

where μ is viscosity, V is the mean velocity of blood flow, l is vessel length, and d vessel diameter. Under conditions of laminar flow, vascular resistance is minimized by either increasing vessel diameter or decreasing its length. Because vessel diameter in active fishes is constrained by requirements to minimize diffusion distances, a decrease in vessel length, achieved by diagonal flow, is used to minimize the trans-lamellar vascular pressure gradient.

The diagonal blood-flow pattern seen in mako lamellae (Fig. 2A) suggests selection for the optimization of gas transfer efficacy and the conservation of vascular

pressure. However, because the mako diagonal flow angle is 38.4 ± 6.7°, the relative advantages would be less than those realized by the higher angles of tunas at 50-60°, (Muir and Brown, 1971; Wegner et al., in press) which, with a high blood hemoglobin concentration and a thinner water-blood barrier [0.5 – 0.6 μm in tunas (Hughes, 1970; Wegner et al., 2006), 1.15 μm for the mako (Table 2)] can potentially optimize gas transfer in shorter vessels. General support for the idea of a graded capacity to optimize oxygenation and vascular resistance is further suggested by the blue shark, which has a diagonal flow angle of 28.1 ± 7.2° and a correspondingly thicker water-blood barrier (1.65 μm) than the mako. The reduced angle of blue shark lamellar blood flow also correlates with longer, wider blood vessels resulting in thicker lamellae (Table 2). Finally, data in Table 2 show very little change in mako lamellar thickness with body size, but an increased lamellar thickness in larger blue sharks. This suggests that a greater angle of mako diagonal flow conserves lamellar thickness with growth, which has implications for both gas exchange and blood-flow resistance.

Gill structure and ram ventilation

In ram ventilating fishes the gills must be sufficiently rigid to maintain structural integrity and orientation in order to continue efficient gas exchange while utilizing the forceful branchial stream produced by fast, continuous swimming. Figure 5 compares the basic gill design features of the mako shark and tunas. The elasmobranch interbranchial septum, an extension of the gill arch that attaches to and supports the trailing edges of the gill filaments as it extends laterally outward to form

the gill flap, has been suggested as an important structural feature contributing to gill reinforcement for ram ventilation (Benz, 1984). Teleosts lack this septum and, because the greater part of each gill filament extends without support into the downstream flow, tunas and other rapidly swimming ram-ventilating teleosts have developed wide, cartilaginous (or in some cases ossified) filament rods (Iwai and Nakamura, 1964) and fusions which bind the gill filaments and lamellae (Muir and Kendall, 1968; Johnson, 1986; Wegner et al., 2006) (Fig. 5). Because the full length of each elasmobranch filament is connected to the interbranchial septum, this structure lessens the requirement for additional support for ram ventilation and, even-though the septal structure likely adds considerably resistance to branchial flow, selection for this ventilation mode and for continuous swimming in the mako and other lamnids appears to have taken place within this morphological framework. Thus, with a few exceptions, the basic organization of the mako gill is similar to that of other elasmobranchs.

Other components important in elasmobranch gill support are closely linked to cardiovascular function. The corpus cavernosum, which is in-series with the respiratory circulation (Fig. 4), is thought to function as a hydrostatic skeleton for the gill filament. However, despite the shortfin mako's dependence on ram ventilation, the size and position of the corpus cavernosum does not appear to differ from that of less active elasmobranchs (Cooke, 1980; Olson and Kent, 1980). This study also documents a vascular feature that appears important for lamellar support, previously undescribed vascular "sacs" near the water entry edge of lamellae in both the shortfin

mako and blue shark (Fig. 3, Fig. 5). These sacs appear quite similar to the "button-like epithelial outgrowths" described for the spiny dogfish, *Squalus acanthias*, by De Vries and De Jager (1984), who suggested these structures function to keep the interlamellar spaces open. However, rather than epithelial, the spacers of the mako and blue shark are vascular and are thus likely subject to vasoactive agents and alterations in cardiac output and branchial perfusion. The connection of both the corpus cavernosa and lamellar sacs to the respiratory circulation thus suggests the operation of a vascular, pressure-based mechanism (subject to vasoactive control) for maintaining both filament and lamellar structural integrity. In addition, because vascular sacs are located near the water entry edge of each lamella, changes in their size could possibly affect both the volume and velocity of the ram-ventilatory flow stream through the interlamellar channels. Catecholamines, which are stored in, and readily released from, large central venous sinuses in sharks readily affect heart activity and gill perfusion (Opdyke et al., 1982; Randall and Perry, 1992; Olson and Farrell, 2006), could serve to modulate such a mechanism. Also, the recent finding of endothelin (ET_A and ET_B) receptors on the lamellar pillar cells of many fishes, including some elasmobranchs (Evans and Gunderson, 1999; Stensløkken et al., 2006; Hyndman and Evans, 2007) implicates their role in regulating branchial perfusion.

A structural feature that might function in conjunction with vascular regulation is suggested by Fig. 3C, which shows that the leading lateral edges of mako lamellae have a much thicker epithelium than occurs in the gas-exchanging region of the lamellae. This thickening resembles that described in the wahoo, *Acanthocybium*

solandri, a ram-ventilating teleost (Wegner et al., 2006). For the mako this thick region in conjunction with the lamellar sacs, could contribute to an overall bracing of the lamellae for ram ventilation.

Mako gills and upper limits for the lamnid-tuna convergence

Lamnid sharks and tunas show a remarkable evolutionary convergence in specializations for locomotion, kinematics, aerobic muscle position, regional endothermy, oxygen delivery to the musculature, and cardiac physiology (Bernal et al., 2001; Bernal et al., 2003a; Bernal et al., 2003b; Donley et al., 2004; Graham and Dickson, 2004; Shadwick, 2005). However, despite this suite of similarities, the aerobic capacity of the mako, while greater than that of other sharks, remains less than that of tunas (Graham et al., 1990; Sepulveda et al., 2007). Tuna standard metabolic rate is about twice that of the mako (Brill, 1979; 1987; Dewar and Graham, 1994; Sepulveda et al., 2007), and this is correlated with an approximately two-fold greater gill surface area (Table 3). The results of this study suggest that basic design features of the elasmobranch gill (Fig. 5), combined with other physiological characters, limit the maximum capacity of lamnid aerobic performance at a lower level than that of tunas.

Comparison of the gill morphometrics (Table 3) recruited by lamnids and tunas to increase gill surface area provides insight into the selective factors affecting and potentially limiting lamnid gill size. The mechanisms underlying the increase in lamnid gill surface area above that of other sharks include a large lamellar bilateral

surface area (mako) and a high total filament length (white shark). Dimensional changes of this nature are consistent with those leading to increased gill areas in many other fishes and with theoretical predictions for augmenting area without increasing gill resistance (Hughes, 1966). Although tunas also have a relatively high total filament length, their gill area is further increased by a high number of lamellae per length of filament (Table 3). This high lamellar frequency additionally serves to increase branchial resistance to water flow and likely helps to slow and streamline the ram-ventilatory flow (Wegner et al., in press). In contrast, resistance to water flow through lamnid gills is likely inherently high due to the forcing of water through the septal channels of the elasmobranch gill, and although this may help slow the ram-ventilatory stream, it likely precludes the recruitment of a high lamellar frequency to augment gill surface area (a high lamellar frequency would further increase resistance). Accordingly the lamellar frequencies in the mako and white shark are not significantly greater than in some non-lamnid sharks and are half those of tunas and other high-energy demand teleosts (Table 3).

In addition to having a smaller gill surface area than tunas, the mako has both a greater water-blood barrier distance and lamellar thickness. The greater thickness of the water-blood barrier is likely required to provide structural support to its larger lamellae. The greater thickness of mako lamellae [11.38 μm in comparison to 5.88 μm in yellowfin tuna (Wegner et al., 2006)] correlates with larger blood channel diameters that are required to accommodate the large red blood cells intrinsic to all elasmobranchs. Thus, although mako diffusion distances are shorter than those in the

blue shark and other elasmobranchs, they are much greater than those of tunas and this, in addition to a smaller gill area, may ultimately limit comparable gill function.

Summary

This study demonstrates three morphological features that distinguish mako gills from those of other sharks and that correlate with the mako's relatively higher metabolic demand: 1. a larger gill surface area, 2. shorter lamellar diffusion distances, and 3. a more fully developed diagonal blood-flow pattern through the lamellae. However, in comparison to tunas, the mako gill area is about half the size, the water-blood barrier is twice as thick, and the angle of lamellar diagonal blood flow is reduced. In addition, the findings of this study suggest that mako gill structure is not more specialized than that of the blue shark in features related to ram ventilation. However, in contrast, tunas and other active teleosts have gills that are highly modified for ramming through filament and lamellar fusions to increase gill rigidity (Muir and Kendall, 1968; Johnson, 1986; Wegner et al., 2006) and densely packed lamellae that play a role in slowing and streamlining branchial flow (Wegner et al., in press).

Differences in the degree of lamnid gill specialization appear related to the gill design. Although the elasmobranch interbranchial septum increases the structural integrity of the shark gill and may facilitate ram ventilation, it also presents a more tortuous water pathway that adds to branchial resistance and may limit gill area. Differences in the gill areas of lamnids and tunas parallel findings of previous lamnid-

tuna comparisons showing that, even though the two groups are convergent for adaptations that increase their rates of oxygen uptake and delivery, the relative metabolic capacity of lamnids, as determined by factors such as mitochondrial density, enzymatic activities, and oxygen consumption, remains less than that of tunas (Graham et al., 1990; Bernal et al., 2003a; Bernal et al., 2003b; Sepulveda et al., 2007).

Table 3.1: Regression equations for shortfin mako gill morphometrics

Source	Gill Surface Area (cm^2)	Total Filament Length (cm)	Lamellar Frequency (mm^{-1})	Lamellar Bilateral Surface Area (mm^2)
Regression equations				
Present Study	$y = 35.889x^{0.7834}$	$y = 612.310x^{0.2904}$	$y = 39.185x^{-0.1113}$	$y = 0.00748x^{0.6043}$
Emery and Szczepanski (1986)	$y = 57.544x^{0.7400}$	$y = 676.083x^{0.2800}$	$y = 100.00x^{-0.2000}$	$y = 0.00427x^{0.6600}$
Oikawa and Kanda (1997)	-	-	-	-
Mako at 4.48 kg				
Present Study	26023	7035.6	15.4	1.20
Emery and Szczepanski (1986)	28970	7118.0	18.6	1.10
Oikawa and Kanda (1997)	12040	5953.5	17.2	0.59

Table 3.2: Lamellar dimensions in the shortfin mako and blue shark.

Species	Weight (kg)	Fork Length (cm)	Lamellar Thickness (μm)	Water-Blood Barrier Distance (μm)
Shortfin Mako	4.6	77.0	11.26 ± 0.93	1.02 ± 0.13
Shortfin Mako	8.3	94.0	10.72 ± 1.33	1.03 ± 0.14
Shortfin Mako	10.5	101.5	10.34 ± 1.55	1.10 ± 0.20
Shortfin Mako	16.2	116.5	11.97 ± 1.86	1.16 ± 0.20
Shortfin Mako	34.0	134.0	11.39 ± 1.39	1.35 ± 0.31
Shortfin Mako	49.0	160.5	10.51 ± 0.88	1.23 ± 0.23
Shortfin Mako	55.5	167.0	12.27 ± 1.79	1.16 ± 0.16
Shortfin Mako	71.0	187.5	12.58 ± 1.57	1.14 ± 0.20
$\bar{\chi}$			**11.38 ± 1.61**	**1.15 ± 0.22**
Blue Shark	2.4	72.0	12.72 ± 1.90	1.44 ± 0.69
Blue Shark	3.4	84.0	13.39 ± 2.05	1.23 ± 0.23
Blue Shark	44.0	197.0	18.78 ± 3.20	2.07 ± 0.59
Blue Shark	47.9	196.0	16.06 ± 2.55	1.88 ± 0.35
$\bar{\chi}$			**15.24 ± 3.41**	**1.65 ± 0.59**

Table 3.3: Gill dimensions for the shortfin mako in comparison to other elasmobranchs and some high-energy demand teleosts determined by mass-regression equations at a body mass of 10 kg.

Species	Gill Surface Area (cm^2)	Total Filament Length (cm)	Lamellar Frequency (mm^{-1})	Lamellar Bilateral Surface Area (mm^2)	Mean Lamellar Thickness (μm)	Interlamellar spacing (μm)
Shortfin Mako[1]	48816	8883.2	14.06	1.95	11.38	59.75
Shortfin Mako[2]	52481	8912.5	15.85	1.86	-	-
White Shark[2]	51286	13803.8	13.80	1.35	-	-
Blue Shark[2]	18212	5370.3	11.22	1.51	15.24	73.88
Dusky Shark[2]	20418	7413.1	15.49	0.98	-	-
Skipjack Tuna[3]	130588	20027.2	29.34	1.11	-	-
Bluefin-Yellowfin Tuna[3]	99460	18850.5	26.74	0.98	5.88	31.51
Eastern Pacific Bonito[4]	64082	12741.5	31.11	0.81	-	-
Striped Marlin[4]	40778	20549.1	22.64	0.44	6.29	37.89

Note: [1]Present study, [2]Emery and Szczepanski (1986), [3]Muir and Hughes (1969), and [4]Wegner et al. (2009). Average lamellar thickness measurements were determined in this study for the mako and blue shark, and by Wegner et al. (2006) for yellowfin tuna and striped marlin. Interlamellar spacing is calculated from lamellar frequency and thickness data.

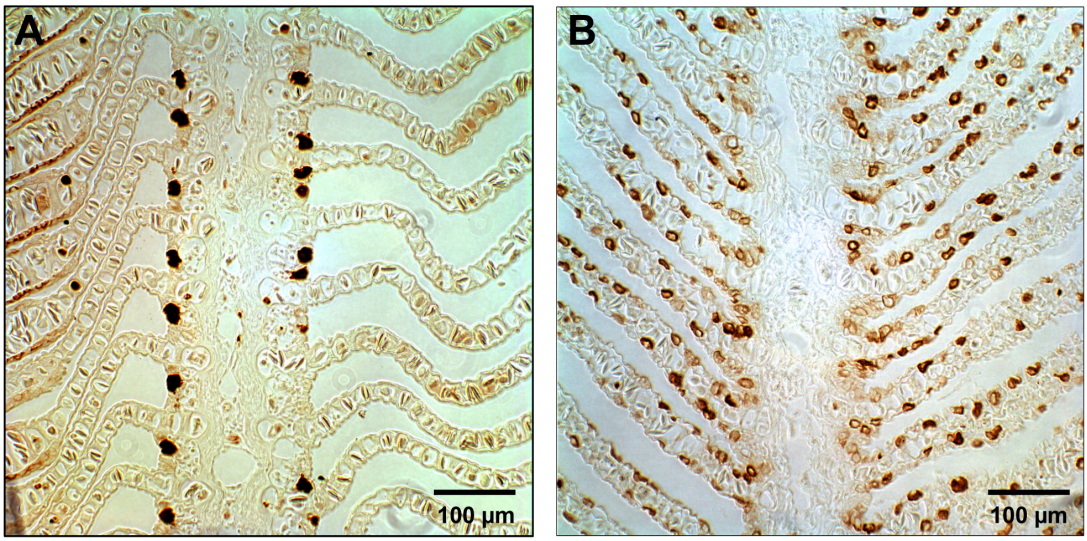

Figure 3.1: Longitudinal cross-sections through a gill filament of **A:** a 24.0 kg shortfin mako and **B:** a 44.0 kg blue shark showing the distribution of mitochondria rich cells (brown).

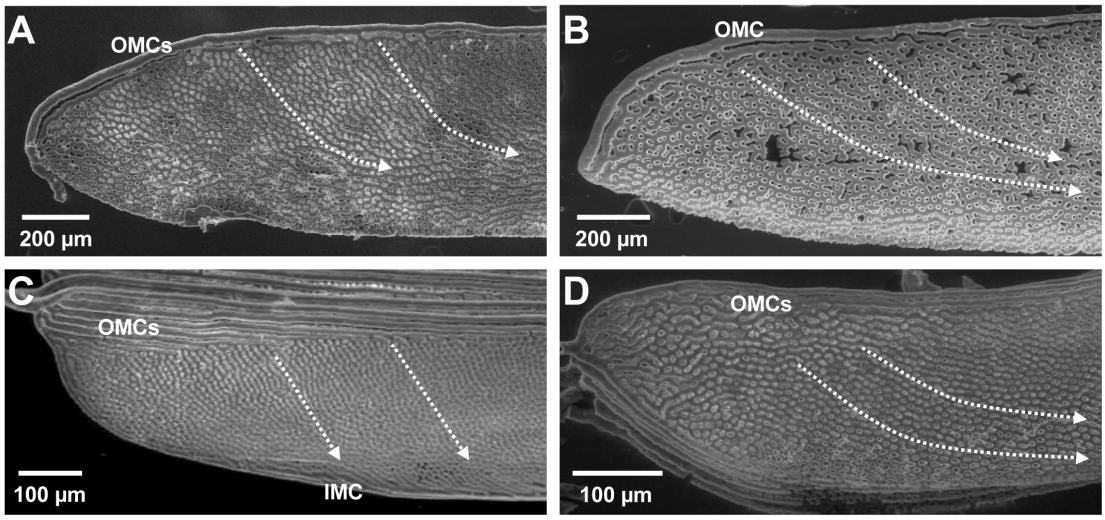

Figure 3.2: Scanning electron microscope images of lamellar casts in **A:** a 21.2 kg shortfin mako and **B**: a 17.1 kg blue shark showing the lamellar vascular channels and the depressions where pillar cells were located. Shown for comparison are cast lamellae from **C:** a 4.2 kg yellowfin tuna and **D:** a 1.87 kg eastern Pacific bonito (Wegner et al, in press). Blood flow is indicated by dotted arrows. Water flow is from right to left in all images. Abbreviations: IMC, inner marginal channel; OMC, outer marginal channel.

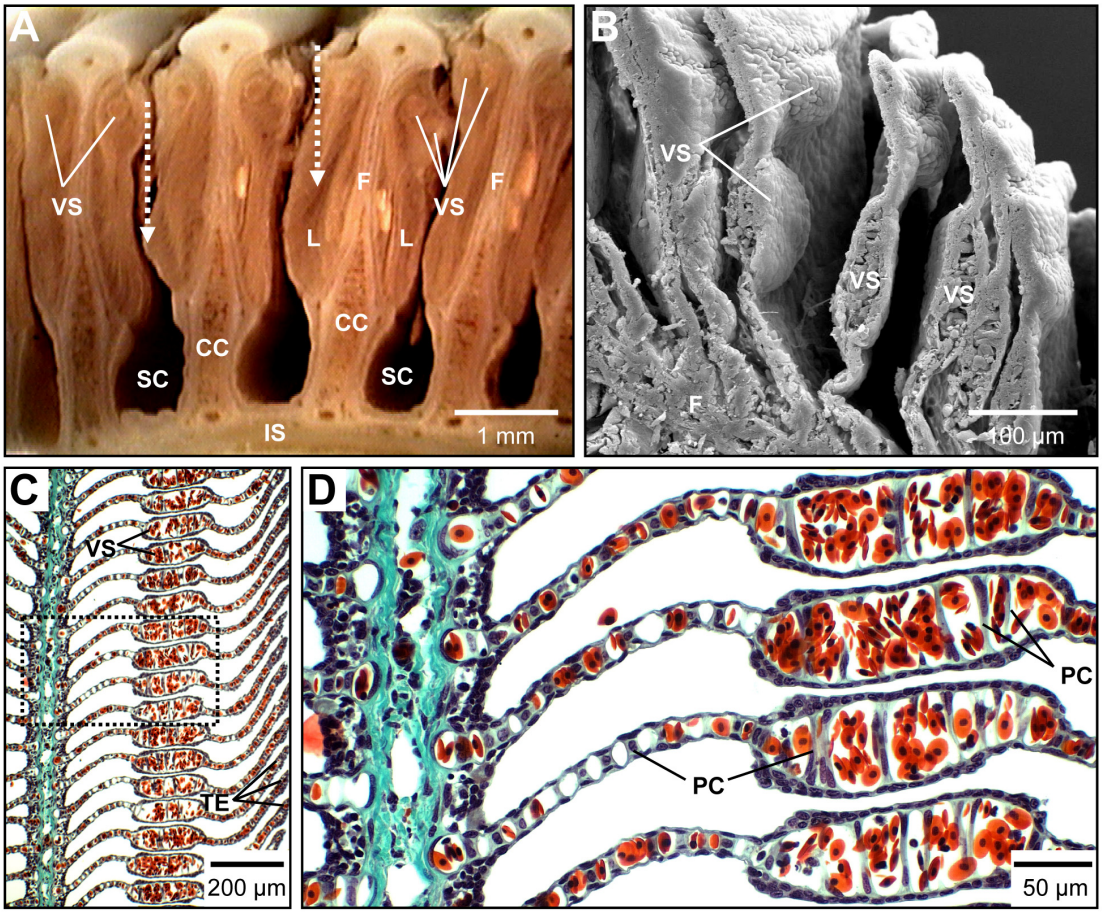

Fig. 3.3: Images of the lamellar vascular sacs in the shortfin mako. **A:** Four adjacent filaments from a 9.0 kg mako showing 1-2 vascular sacs on each lamella near the leading (water-entry) edge. Water flow is indicated by dotted arrows. **B:** Scanning electron microscope image of a longitudinal section through the gill filament of a 8.3 kg mako showing the lamellae and vascular sacs. **C:** Longitudinal section through a filament of a 9.0 kg mako showing the proximity of vascular sacs between adjacent lamellae and a thick epithelium near the outer marginal edge. **D:** Magnified image of dotted box in **C.** showing the details of the vascular sacs filled with red blood cells and supported by large pillar cells. Water flow is into the page in **B-D**. Abbreviations: CC, corpus cavernosum; F, filament; IS, interbranchial septum; L, lamella; PC, pillar cell; SC, septal channel; TE, thick epithelium; VS, vascular sac.

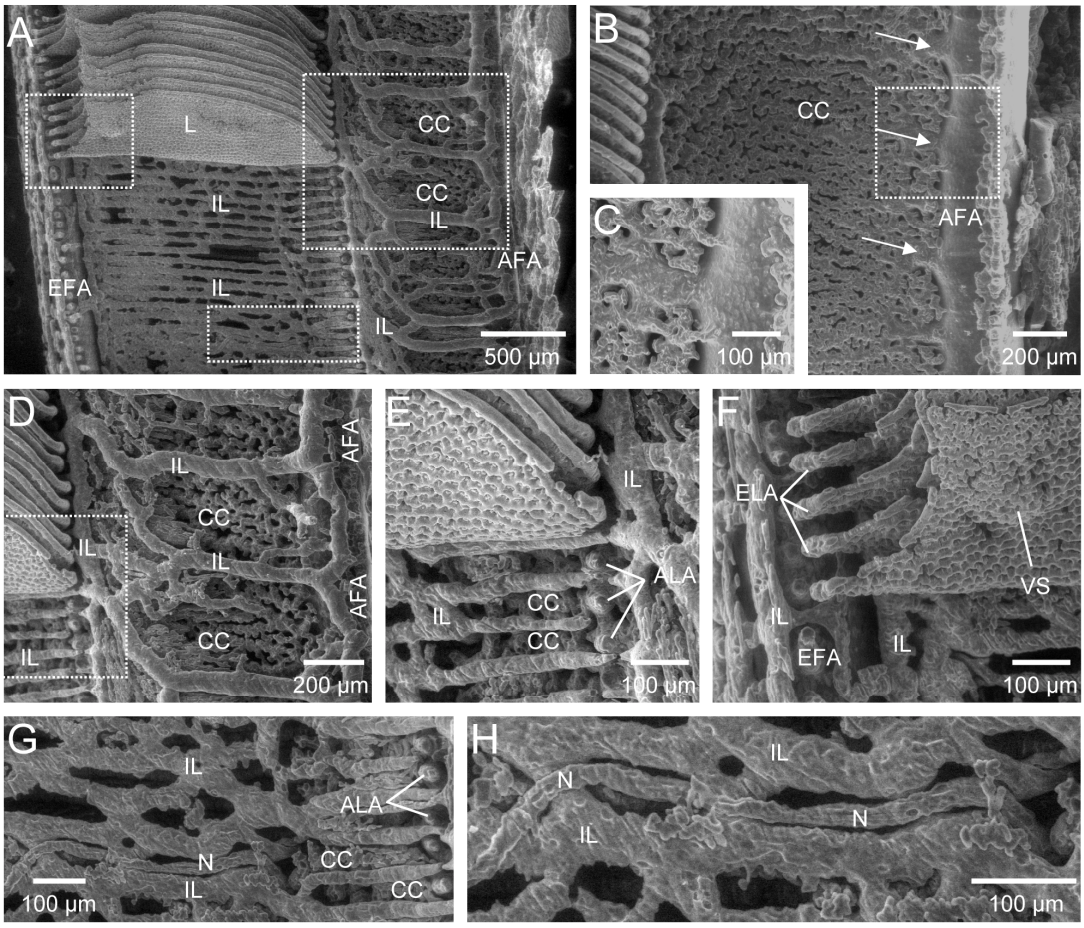

Figure 3.4: Scanning electron microscope images of the vascular casts from a 5.0 kg shortfin mako showing the general features of the gill filament circulation. **A:** Synoptic view of a gill filament. **B:** Magnified image of dashed box in **A** (upper right) with the interlamellar circulation removed to show the corpus cavernosum. Major connections of the corpus cavernosum to the afferent filamental artery to are shown by arrows. **C:** Enlarged image of box in **B** showing connections of the afferent filamental artery with the corpus cavernosum. **D:** Enlarged image of dashed box in **A** (upper right) with the interlamellar circulation still intact. **E:** Magnified image of dotted box in **D** showing the afferent lamellar arterioles leaving the corpus cavernosum and the interlamellar circulation running underneath the lamellae. **F:** Enlarged view of dotted box in **A** (upper left) showing the connection of the efferent lamellar arterioles to the efferent filament artery and the corrosion cast of a vascular sac on the efferent edge of a lamella. **G:** Magnified image of dashed box in **A** (bottom middle), showing a nutrient vessel intertwined with the interlamellar circulation. **H:** Enlarged view of **G**. Water flow is from left to right in all images. Abbreviations: AFA, afferent filamental artery; ALA, afferent lamellar arteriole; CC, corpus cavernosum; EFA, efferent filamental artery; ELA, efferent lamellar arteriole; L, lamella; IL, interlamellar vessel; N, nutrient vessel; VS, vascular sac.

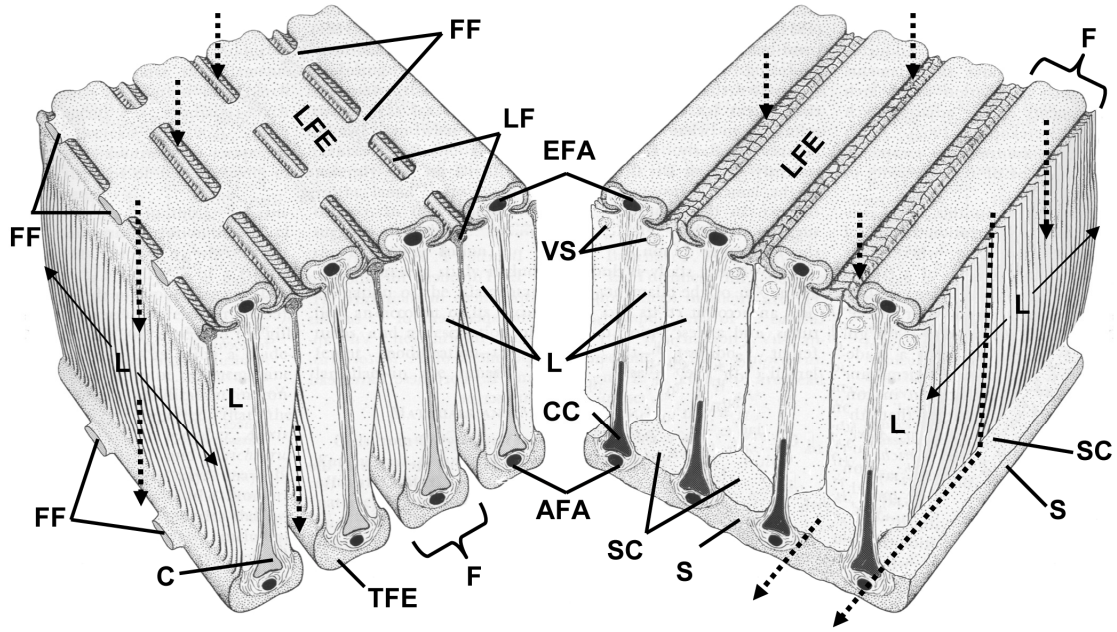

Figure 3.5: Comparison of the basic gill features in a tuna (left) and a shortfin mako (right). Dotted arrows indicate water flow direction. Abbreviations: AFA, afferent filamental artery; C, cartilaginous filament rod; CC, corpus cavernosum; EFA, efferent filamental artery; F, filament; FF, filament fusion; L, lamella; LF, lamellar fusion; LFE, leading filament edge; S, septum; SC, septal channel; TFE, trailing filament edge; VS, vascular sac. Tuna gill schematic modified from Muir and Kendall (1968) and Wegner et al. (2006).

LITERATURE CITED

Altringham JD, Block BA. 1997. Why do tuna maintain elevated slow muscle temperatures? Power output of muscle isolated from endothermic and ectothermic fish. J Exp Biol 200:2617-2627.

Bernal D, Dickson KA, Shadwick RE, Graham JB. 2001. Review: Analysis of the evolutionary convergence for high performance swimming in lamnid sharks and tunas. Comp Biochem Physiol 129:695-726.

Bernal D, Donley JM, Shadwick RE, Syme DA. 2005. Mammal-like muscles power swimming in a cold-water shark. Nature 437:1349-1352.

Bernal D, Sepulveda C, Mathieu-Costello O, Graham JB. 2003a. Comparative studies of high performance swimming in sharks I. Red muscle morphometrics, vascularization and ultrastructure. J Exp Biol 206:2831-2843.

Bernal D, Smith D, Lopez G, Weitz D, Grimminger T, Dickson K, Graham JB. 2003b. Comparative studies of high performance swimming in sharks II. Metabolic biochemistry of locomotor and myocardial muscle in endothermic and ectothermic sharks. J Exp Biol 206:2845-2857.

Brill RW. 1979. Effect of body size on the standard metabolic rate of skipjack tuna, *Katsuwonus pelamis*. Fish Bull 77:494-498.

Brill RW. 1987. On the standard metabolic rates of tropical tunas, including the effect of body size and acute temperature change. Fish Bull 85:25-36.

Brill RW, Bushnell PG. 1991. Metabolic and cardiac scope of high-energy demand teleosts, the tunas. Can J Zool 69:2002-2009.

Brill RW, Bushnell PG. 2001. The cardiovascular system of tunas. In: Block BA, Stevens ED, editors. Tuna: Physiology, ecology and evolution. San Diego: Academic Press. p 79-120.

Carey FG, Teal JM. 1966. Heat conservation in tuna fish muscle. Proc Natl Acad Sci USA 56:1461-1469.

Carey FG, Teal JM, Kanwisher JW, Lawson KD, Beckett JS. 1971. Warm-bodied fish. Amer Zool 11:137-145.

Cooke IRC. 1980. Functional aspects of the morphology and vascular anatomy of the gills of the endeavour dogfish, *Centrophorus scalpratus* (McCulloch) (Elasmobranchii: Squalidae). Zoomorphologie 94:167-183.

De Jager S, Dekkers WJ. 1975. Relation between gill structure and activity in fish. Neth J Zool 25:276-308.

Dewar H, Graham JB. 1994. Studies of tropical tuna swimming performance in a large water tunnel. 1. Energetics. J Exp Biol 192:13-31.

Dickson KA, Graham JB. 2004. Evolution and consequences of endothermy in fishes. Physiol Biochem Zool 77:998-1018.

Donley JM, Sepulveda CA, Konstantinidis P, Gemballa S, Shadwick RE. 2004. More than skin deep: Convergent evolution in mechanical design of lamnid sharks and tunas. Nature 429:61-65.

Emery SH. 1986. Hematological comparisons of endothermic vs. ectothermic elasmobranch fishes. Copeia 1986:700-705.

Emery SH, Szczepanski A. 1986. Gill dimensions in pelagic elasmobranch fishes. Biol Bull 171:441-449.

Evans DH, Gunderson MP. 1999. Characterization of an endothelin ETB receptor in the gill of the dogfish shark *Squalus acanthias*. J Exp Biol 202:3605–3610.

Gemballa S, Konstantinidis P, Donley JM, Sepulveda C, Shadwick RE. 2006. Evolution of high-performance swimming in sharks: Transformations of the musculotendinous system from subcarangiform to thunniform swimmers. J Morph 267:477-493.

Graham JB, Dewar H, Lai NC, Lowell WR, Arce SM. 1990. Aspects of shark swimming performance determined using a large water tunnel. J Exp Biol 151:175-192.

Graham JB, Dickson KA. 2001. Anatomical and physiological specializations for endothermy. In: Block BA, Stevens ED, editors. Tuna: Physiology, ecology and evolution. San Diego: Academic Press. p 121-165.

Graham JB, Dickson KA. 2004. Tuna comparative physiology. J Exp Biol 207:4015-4024.

Gray IE. 1954. Comparative study of the gill area of marine fishes. Biol Bull Mar Biol Lab, Woods Hole 107:219-225.

Hughes GM. 1966. The dimensions of fish gills in relation to their function. J Exp Biol 45:177-195.

Hughes GM. 1970. Morphological measurements on the gills of fishes in relation to their respiratory function. Folia Morph 18:78-95.

Hughes GM. 1984a. General anatomy of the gills. In: Hoar WS, Randall DJ, editors. Fish physiology, vol 10A. Orlando: Academic. p 1-72.

Hughes GM. 1984b. Measurement of gill area in fishes: Practices and problems. J Mar Biol Ass UK 64:637-655.

Hughes GM, Morgan M. 1973. The structure of fish gills in relation to their respiratory function. Biol Rev 48:419-475.

Hughes GM, Wright DE. 1970. A comparative study of the ultrastructure of the water-blood pathway in the secondary lamellae of teleost and elasmobranch fishes - benthic forms. Z Zellforsch 104:478-&.

Humason GL. 1997. Humason's animal and tissue techniques. Baltimore: The Johns Hopkins University Press. 597 p.

Hyndman KA, Evans DH. 2007. Endothelin and endothelin converting enzyme-1 in the fish gill: evolutionary and physiological perspectives. J Exp Biol 210:4286-4297.

Iwai T, Nakamura I. 1964. Branchial skeleton of the bluefin tuna with special reference to the gill rays. Bull Misaki Mar Biol Inst Kyoto Univ 6:21-25.

Johnson GD. 1986. Scombroid phylogeny: An alternative hypothesis. Bull Mar Sci 39:1-41.

Kohler NE, Casey JG, Turner PA. 1995. Length-weight relationships for 13 species of sharks from the western North Atlantic. Fish Bull 93:412-418.

Korsmeyer KE, Dewar H. 2001. Tuna metabolism and energetics. In: Block BA, Stevens ED, editors. Tuna: Physiology, ecology and evolution. San Diego: Academic Press. p 35-78.

Lai NC, Korsmeyer KE, Katz S, Holts DB, Laughlin LM, Graham JB. 1997. Hemodynamics and blood properties of the shortfin mako shark (*Isurus oxyrinchus*). Copeia 1997:424-428.

Muir BS, Brown CE. 1971. Effects of blood pathway on the blood-pressure drop in fish gills, with special reference to tunas. J Fish Res Bd Can 28:947-955.

Muir BS, Hughes GM. 1969. Gill dimensions for three species of tunny. J Exp Biol 51:271-285.

Muir BS, Kendall JI. 1968. Structural modifications in the gills of tunas and some other oceanic fishes. Copeia 1968:388-398.

Oikawa S, Kanda T. 1997. Some features of the gills of a megamouth shark and a shortfin mako, with reference to metabolic activity. In: Yano K, Morrisey JF, Yabumoto Y, Nakaya K, editors. Biology of the Megamouth Shark. Tokyo: Tokyo Univ. p 93-104.

Olson KR, Dewar H, Graham JB, Brill RW. 2003. Vascular anatomy of the gills in a high energy demand teleost, the skipjack tuna (*Katsuwonus pelamis*). J Exp Zool 297A:17-31.

Olson KR, Farrell AP. 2006. The cardiovascular system. In: Evans DH, Claiborne JB, editors. The physiology of fishes. Boca Raton: CRC Press. p 142–152.

Olson KR, Kent B. 1980. The microvasculature of the elasmobranch gill. Cell Tissue Res 209:49-63.

Opdyke DF, Carroll RG, Keller NE. 1982. Catecholamine release and blood pressure changes induced by exercise in dogfish. Amer J Physiol 242:R306-R310.

Perry CN, Cartamil DP, Bernal D, Sepulveda CA, Theilmann RJ, Graham JB, Frank LR. 2007. Quantification of red myotomal muscle volume and geometry in the shortfin mako shark (*Isurus oxyrinchus*) and the salmon shark (*Lamna ditropis*) using T-1-weighted magnetic resonance imaging. J Morph 268:284-292.

Piermarini PM, Verlander JW, Royaux IE, Evans DH. 2002. Pendrin immunoreactivity in the gill epithelium of a euryhaline elasmobranch. Am J Physiol Regul Integr Comp Physiol 283:R983-R992.

Randall DJ, Perry SF. 1992. Catecholamines. In: Hoar WS, Randall DJ, Farrell AP, editors. Fish physiology, vol 12B. San Diego: Academic Press. p 255–300.
Sepulveda CA, Graham JB, Bernal D. 2007. Aerobic metabolic rates of swimming juvenile mako sharks, *Isurus oxyrinchus*. Mar Biol 152:1087-1094.

Shadwick RE. 2005. How tunas and lamnid sharks swim: An evolutionary convergence. Am Sci 93:524-531.

Stensløkken KO, Sundin L, Nilsson GE. 2006. Endothelin receptors in teleost fishes: cardiovascular effects and branchial distribution. Am J Physiol 290:R852-R860.

Wegner NC, Sepulveda CA, Bull KB, Graham JB. in press. Gill morphometrics in relation to gas transfer and ram ventilation in high-energy demand teleosts: scombrids and billfishes. J Morph.

Wegner NC, Sepulveda CA, Graham JB. 2006. Gill specializations in high-performance pelagic teleosts, with reference to striped marlin (*Tetrapturus audax*) and wahoo (*Acanthocybium solandri*). Bull Mar Sci 79:747-759.

ACKNOWLEDGEMENTS

This research was supported by the National Science Foundation Grant #IOS-0817774, the Tuna Industry Endowment Fund at Scripps Institution of Oceanography, the William H. and Mattie Wattis Harris Foundation, the Moore Family Foundation, the Pfleger Institute of Environmental Research, and the George T. Pfleger Foundation. N.C. Wegner was supported by the Nadine A. and Edward M. Carson Scholarship awarded by the Achievement Rewards for College Scientists (ARCS), Los Angeles Chapter, the National Science Foundation, and the Edna Bailey Sussman Foundation. We thank S. Aalbers, N. Ben-Aderet, L. Field, D. Kacev, S. Kohin, H. Marshall, M. Musyl, R. Vetter, and the crews of the *David Star Jordan* and *Oscar Elton Sette* for their help in the collection and preparation of mako and blue shark gill tissue. We also thank K. Bull and L. Williams for helping with gill area measurements, and E. York and B. Neal for technical assistance with microscopy.

Chapter 3, in full, is currently being prepared for submission for publication as: Wegner NC, Sepulveda CA, Olson, KR, Hyndman KA, Graham JB. Functional morphology of the gills of the shortfin mako, *Isurus oxyrinchus*, a lamnid shark. J Morph. The dissertation author is the primary investigator and author of this paper.

CHAPTER 4: RAM VENTILATION IN THE SHORTFIN MAKO, *ISURUS OXYRINCHUS*: OXYGEN UTILIZATION AND THE BRANCHIAL PRESSURE GRADIENT

ABSTRACT

This report investigates aspects of ram ventilation in a lamnid shark, the shortfin mako, *Isurus oxyrinchus*, and examines the extent to which intrinsic structural differences in the gill design of elasmobranchs and teleosts may affect the lamnid-tuna convergence for high-performance swimming. The study of makos swimming in a water tunnel demonstrates that, despite differences in gill design, mouth gape, and basal swimming speeds, O_2 utilization at the gills (53.4 ± 4.2%) and the pressure gradient driving branchial flow (967.5 ± 261.1 dyn cm^{-2} at an average swimming speed of 38.8 ± 5.8 cm s^{-1}) for makos are similar to values reported for tunas. Also comparable to tunas are estimates of both the velocity (0.44 ± 0.06 cm s^{-1}) and the residence time (0.12 ± 0.02 s) of water in the interlamellar channels of the mako. However, mako and tuna gills differ in the sites of primary branchial resistance. In the mako, approximately 64% of the total branchial resistance resides with the septal channels, structures inherent to the elasmobranch gill and not present in tunas. The added resistance at this location is compensated by a correspondingly lower resistance at the gill lamellae, which is accomplished through wider interlamellar channels. Although greater interlamellar spacing minimizes branchial resistance, it also limits lamellar number and results in a lower total gill surface area for the mako relative to tunas. The elasmobranch gill design thus appears to constrain gill area and may potentially limit mako aerobic performance in comparison to tunas.

INTRODUCTION

The lamnid sharks (Family Lamnidae) and tunas (Family Scombridae) are convergent in a number of features related to fast, continuous swimming. Both groups have a streamlined, fusiform body and a unique position of the aerobic (red) musculature that enables both thunniform swimming and regional endothermy, the latter increasing muscle power and accelerating metabolic processes (Carey et al., 1971; Altringham and Block, 1997; Bernal et al., 2001a; Graham and Dickson, 2001). Relative to other fishes, both lamnids and tunas have high metabolic rates (Dewar and Graham, 1994; Dewar and Korsmeyer, 2001); however, it is now well established that lamnid aerobic capacity is less than that of tunas. Lamnids have lower mitochondrial densities and aerobic enzyme activities and smaller quantities of red muscle (Bernal et al., 2003a; Bernal et al., 2003b). The standard metabolic rate of one lamnid, the shortfin mako, *Isurus oxyrinchus*, is approximately one-half that of tunas (Brill, 1979; 1987; Dewar and Graham, 1994; Sepulveda et al., 2007) and this correlates with a proportionately smaller gill surface area (Muir and Hughes, 1969; Emery and Szczepanski, 1986). Data presented in Chapter 3 suggest that structural features inherent to the elasmobranch gill potentially limit lamnid gill surface area and may restrict the aerobic scope of this group.

The elasmobranch gill differs from that of teleosts in having interbranchial septa that bind together the anterior and posterior hemibranchs of each gill arch and extend out to the lateral edge of the body to form the gill flaps. Each interbranchial septum thus provides an extended base of attachment for all of the gill filaments, and

it is this characteristic that gave rise to the term elasmobranch (= strapped gill). Tunas and other bony fishes lack interbranchial septa; the filaments of each hemibranch are anchored to the gill arch but extend without septal support into the branchial cavity. This difference in gill design markedly affects the path of water flow. In tunas and other teleosts water that passes through the interlamellar channels freely exits the branchial chamber through the opercular opening. In contrast, water exiting the interlamellar channels of a lamnid impinges on the branchial septum where it is turned and forced through septal channels that open just inside the gill slits. Comparison of tuna and lamnid gill morphometrics (Chapter 3) suggests that the added resistance of the interbranchial septum may preclude the recruitment of a high lamellar frequency (i.e., the number of lamellae per length of filament) and may ultimately prevent lamnids from increasing gill surface area to the extent of tunas (the higher gill area of tunas results from a lamellar frequency that is twice that of lamnids). However, there have been no measurements or hydrodynamic estimates of the resistance to water flow incurred at the septal channels, and thus its effect on elasmobranch gill morphometrics and respiratory function has not been quantified.

Lamnids and tunas are both ram ventilators and thus depend on the forward momentum of continuous swimming to produce branchial flow. Although this aspect of respiration makes lamnid sharks and tunas difficult to maintain and study in controlled experiments, it facilitates hydrodynamic approximations of branchial flow in that the ventilatory volume and head pressure inducing flow through the gills can be estimated by measurements of swimming speed and mouth gape. Accordingly, ram

ventilation was first studied in tunas by tracing the path of water entering the mouth, through the gills, and out the opercular slits, and using corresponding morphological measurements to estimate the pressure gradient (from the mouth to opercula) required to drive branchial flow (Brown and Muir, 1970). *In vivo* studies of branchial resistance in anesthetized skipjack tuna, *Katsuwonus pelamis*, verified these initial pressure-gradient estimates and documented relatively high O_2 utilization in tuna gills (Stevens, 1972). Later morphological work further quantified water flow through the tuna gill sieve, providing estimates of the velocity, Reynold's number, and residence time of water flowing through the interlamellar channels (Stevens and Lightfoot, 1986).

In comparison to tunas, little is known about the lamnid ram-ventilatory stream. This study reports *in vivo* measurements made on small shortfin makos swimming in a water tunnel in which determinations of O_2 utilization and the branchial pressure gradient have been combined with morphometric data to model aspects of gill function related to ram ventilation.

METHODS

Mako shark collection, transport, and experimentation were conducted in accordance with protocol S00080 of the University of California, San Diego Institutional Animal Care and Use Committee.

Specimen collection

Six small shortfin makos (4.62 - 7.32 kg, 76.0 – 89.0 cm FL,) were individually collected 8-13 km offshore of Scripps Institution of Oceanography (SIO), La Jolla, CA. Five were captured by chumming, in which each shark attracted to the boat was fed a piece of bait on a barbless hook and pulled close enough (usually without setting the hook) to be dip-netted. One mako was caught by trolling with heavy fishing gear (fight time was less than 1 min).

Captured sharks were transported (30-50 min in duration) to the laboratory in a 90 l, rectangular (110 x 34 x 53 cm, length x width x height) tank used in previous studies (Donley et al., 2005; Sepulveda et al., 2007). This tank has a recirculating, aerated water system that pumps water through a funnel placed over the snout of the shark to induce branchial flow. Restraints on the anterior half of the body secured the head of the shark in the funnel while allowing it to make regular tail movements. At SIO, sharks were placed in a 5.4 m diameter, 24,500 l holding tank where they swam freely for 1-24 h.

Water tunnel experiments

Sharks were transferred from the holding tank into the working section (200 x 51 x 42 cm) of a 3000 l Brett-type water tunnel used in previous studies (Graham et al., 1990; Dewar and Graham, 1994; Bernal et al., 2001b; Dowis et al., 2003; Sepulveda et al., 2003; Sepulveda et al., 2007). Water flow through the tunnel was driven by a 45.7 cm (18 in) propeller connected to 40 hp variable-speed electric motor. An upstream diffuser-contraction section and honeycomb collimator streamlined water

entering the working section, and multiple airstones were used to maintain O_2 saturation. Water velocity in the working section was monitored by a FlowTracker Handheld Acoustic Doppler Velocimeter (SonTek, San Diego, CA). Continuous adjustment of water speed over a period of 1-2 h was required to condition the shark to swim steadily against the current with minimal change in positioning within the working section.

Once the shark was swimming regularly, a custom-made polarographic oxygen electrode (Warner Instruments, probe length = 70 mm, tip diameter = 2 mm, equilibration time ~ 15 s) connected to an oxygen meter (Strathkelvin Instruments Model 781) by a 3 m cable was used to regionally sample the PO_2 of post-branchial water in order to determine mako O_2 utilization. The swimming shark was gently guided to the top of the working section and the PO_2 in the exhalent flow from the top, middle, and bottom of each gill slit was sampled by advancing the O_2 probe approximately 5-10 mm into the slit. This distance was far enough to eliminate errors associated with the non-respiratory water flow along the body surface, but not too far inside the slit as to make contact with the gill filaments. Following the three regional measurements on a slit the O_2 sensor was withdrawn and the background O_2 of the swim tunnel water was resampled while the shark was allowed to continue swimming. Following regional measurements on all five gill slits, the O_2 sensor was mounted in a cowling device contoured to fit over all five gill slits and was used to determine an integrated estimate of O_2 utilization. The O_2 electrode was then recalibrated and regional slit and integrated O_2 measurements were then repeated for each shark. The

required time to make one series of measurements (15 gill slit + 2 cowling measurements) was approximately 30 min.

Following the O_2 utilization measurements, the pressure gradient between the mouth and the gill slits was determined by using two in-series Millar pressure transducers (SPR-1000 1 French, SPR-671 2 French) connected to an MPVS-300 amp interfaced with a Dataq acquisition system. Pressure transducers were threaded into position through guide catheters (5 mm diameter), one sutured to the tip of the tongue and entering the branchial cavity through the first gill slit, and a second sutured approximately 5mm inside the third gill slit along the same horizontal plane. To minimize pressure artifacts associated with the height of the water column (i.e., manometric height), sharks were placed in a harness that minimized changes in vertical position (depth) and pitch (relative vertical positioning of the in-series pressure transducers) but did not interfere with swimming motions. The sharks were then exposed to a series of water-flow velocities (0 - 73 cm/s) and the resulting pressures at the mouth and third gill slit were recorded.

Flow-field dimensions

Following the water tunnel experiments each shark was euthanized by severing the spinal cord immediately posterior to the chondocranium. The head of each specimen was fixed in 10% formalin buffered in sea water and used for morphological measurements needed to quantify water flow through the branchial chamber. These measurements and their application are as follows: 1. Mouth cross-sectional area to

determine ventilation volume, 2. Cross-sectional area between the gill arches (= gill bars) to calculate water velocity at this location, 3. Gill dimensions including total filament length, lamellar frequency, and lamellar length, height, and thickness to estimate water velocity and the pressure gradient associated with ventilatory flow through the interlamellar channels.

For each mako, mouth cross-sectional area was determined by comparing post-mortem head measurements to digital images of the shark's gape while it was swimming in the tunnel. The cross-sectional area between the gill arches was determined from a silicon cast made for each specimen of one side of the branchial chamber.

Gill measurements were determined as described in Chapter 3. Total filament length was calculated by counting all of the gill filaments from one side of the branchial apparatus. Filaments on each gill hemibranch were divided into bins of 20 and the medial filament from each bin (i.e., the 10^{th}, 30^{th}, 50^{th}, etc.) was assumed to represent the average filament length for that bin. The total length of the filaments in each bin was calculated, and all of the bins were added to determine the total filament length for one side of the branchial chamber; this quantity was then doubled to account for filaments on the opposite side.

To determine lamellar frequency and average lamellar length, the medial filament of each bin on the third gill arch was removed, and digital images of lamellae at the base, middle, and tip were acquired using a camera mounted on a light microscope. Lamellae from these sections were then dissected from each filament and

photographed to determine mean lamellar height. Finally, scanning electron microscopy (SEM) was used to determine lamellar thickness. Randomly selected sections of the filaments from the 3rd gill arch were rinsed in deionized water, slowly dehydrated in tert-butyl alcohol (25% increments over 24 h and rinsed twice at 100%), and frozen in the alcohol at 4 °C. Frozen sections were then placed in a freeze dryer until all of the alcohol was removed. Longitudinal cross-sections through the freeze-dried filaments were sputter coated with gold-palladium, mounted perpendicular to the SEM field-of-view, and photographed using an FEI Quanta 600 SEM under high-vacuum mode. Lamellar thickness was determined for 20 lamellae from each specimen. Digital images of each lamellar parameter were analyzed using NIH Image J computer software.

Statistics

Regional measurements of O_2 utilization were compared by the t-test using the significance criterion of $P < 0.05$. The relationship between the branchial pressure gradient and swimming speed was determined by least-squares analysis. Branchial dimensions and water-flow parameters combined for all six sharks are given as means ± standard deviation.

RESULTS

O_2 utilization

Regional measurements of O_2 utilization combined for all six makos are shown in Figure 1. The percentage of gill-O_2 utilization measured at the mid-region of each slit is significantly less than that at the dorsal and ventral slit positions (e.g., at the first gill slit, 20.1% utilization at the middle position is significantly less than 46.0% and 49.7% at the dorsal and ventral locations). O_2 utilizations measured at the dorsal and ventral positions do not differ significantly, with the exception of slit 5 where ventral utilization (75.5%) is significantly higher than that at the dorsal position (62.4%). The tabular data in Figure 1 show the mean O_2 utilization for each slit calculated by combining the three regional measurements (top, middle, and bottom) for all six makos. The mean O_2 utilization measured at the first gill slit (38.6 ± 17.1) is significantly less that that determined at slits 2-5. Utilization measured at gill slit 2 (47.6 ± 17.5) is significantly greater than that of slit 1, but is less than that of slits 3-5. O_2 utilizations determined at gill slits 3-5 do not differ significantly. The aggregate mean utilization of all slit measurements for all six sharks (53.2 ± 18.0%) is consistent with the integrated mean utilization determined for all slits using the cowling (53.4 ± 5.8%).

Pressure measurements

The total pressure differential (Δp_{tot}) measured between the front of the buccal cavity and the third gill slit is show in relation to swimming velocity (v_s) in Figure 2. The regression equation for this function is:

$$\Delta p_{tot} = 1.3473 \cdot v_s^{1.7938} \quad (1)$$

Much of the variation seen in Figure 2 is likely attributed to slight changes in the pitch of the shark. The harness used to stabilize mako position in the water tunnel during pressure measurements limited alterations in body angle to ± 2° relative to horizontal; this correlates to a 0.4 - 0.6 cm change in the relative height of the pressure transducers and a potential pressure change of 390 - 590 dyn cm^{-2}. However, it should be noted that some values of Δp_{tot} exceeded this expected range of variation. Pressure differentials that were less than zero (i.e. pressure at the third gill slit was higher than that at the mouth) or that were more than twice the dynamic pressure predicted for a given velocity (= $0.5\rho v^2$ where ρ is the density of seawater, and v is water velocity) were considered transducer errors and not included in the analysis.

Branchial water flow

The preferred mako swimming speeds in the water tunnel ranged from 32.7 - 45.5 cm s^{-1} (mean 38.8 ± 5.8 cm s^{-1}, 0.43 ± 0.06 body lengths per second) and are similar to cruising velocities observed in other sharks (Weihs et al., 1981). Table 1 integrates these basal swim speeds with measurements of branchial chamber and gill morphology, the pressure gradient, and O_2 utilization in order to examine the mako ram-ventilatory stream. Thus shown in Table 1 are estimates of branchial water-flow parameters at different locations along the respiratory tract, including details of water velocity, Reynold's number, and residence time in the interlamellar channels. Also estimated are the contributions of different sections of the respiratory-flow pathway to branchial resistance.

DISCUSSION

Branchial water flow

The mako ram-ventilatory stream begins with water entering the mouth, where the maximum ventilation volume (V_{gmax}) in $cm^3\ s^{-1}$ is determined by:

$$V_{gmax} = A_m \cdot v_s \quad (2)$$

where A_m is the cross-sectional area of the mouth (cm^2) and v_s is the swimming velocity ($cm\ s^{-1}$) (Table1). However, because of branchial resistance, the velocity of the ram-ventilatory flow is less than that of swimming speed (i.e., branchial resistance creates a slight water-displacing bow wave) (Brown and Muir, 1970); true ventilation volume (V_g) is calculated by:

$$V_g = (m \cdot MO_2) / (C_wO_2 \cdot U) \quad (3)$$

where m is fish mass (kg), MO_2 is oxygen consumption ($mgO_2\ kg^{-1}\ h^{-1}$), C_wO_2 is the concentration of oxygen in the water ($mgO_2\ l^{-1}$), and U is percent O_2 utilization (Brown and Muir, 1970). Values for these parameters in the mako are reported in Table 1 and estimates for V_g using this equation are 33% less than V_{gmax}. Water velocity entering the mako's mouth (v_m) is thus approximately one-third the swimming speed.

The velocity of water at subsequent locations along the ventilatory stream is determined by the law of continuity:

$$V_g = A_1v_1 = A_2v_2 \quad (4)$$

where the ventilation volume is the product of any cross-sectional area through which the flow is passing (A) and the velocity (*v*) at that point. At the gill arches water velocity is further reduced to approximately 40% of swimming speed (16.2 ± 4.1 cm s^{-1}, Table 1). Assuming the entire ventilatory stream subsequently enters the interlamellar channels, water velocity along the respiratory exchange surfaces is reduced by 2 orders of magnitude to approximately 1% of swimming velocity (0.44 ± .06 cm s^{-1} at an average swimming speed of 38.8 ± 5.8 cm s^{-1}).

Although this is likely a reasonable estimation for the average interlamellar water-flow velocity, regional differences in gill-O_2 utilizations suggest that flow may not be evenly distributed to the lamellae. The high inertia of water flow past the gill arches, indicated by its relatively fast velocity at this location (16.2 ± 4.1 cm s^{-1} at an average swim speed of 38.8 ± 5.8 cm s^{-1}, Table 1), may increase the volume of flow through the interlamellar channels near the gill arch and inline with the ventilatory stream entering the mouth. If branchial flow is sufficiently strong, the tips of the gill filaments from opposing hemibranchs can be forced apart thereby increasing anatomical dead space and allowing some flow to bypass the respiratory surfaces. One or both conditions may explain the significantly lower O_2 utilization measured at the middle of each gill slit (Fig. 1). Correspondingly, inertial water flow is likely greatest near the anterior gill arches, and this likely explains the significantly lower utilization measured at slits 1 (38.6 ± 17.1%) and 2 (47.6 ± 17.5%) in comparison to slits 3-5 (56.5 - 62.2%) (Fig. 1).

Despite these regional differences, it does not appear that a large amount of water bypasses the respiratory exchange surfaces, thereby reducing total O_2 utilization or significantly altering estimates of the mean interlamellar water-flow velocity determined by equation 4. Good agreement between the aggregate mean O_2 utilization for all the regional measurements (53.2 ± 18.0, Fig. 1) and the integrated utilization estimate made by placing a cowling over the gill slits (53.4 ± 4.2, Table 1) indicates the lower measurements at gill slits 1 and 2 do not disproportionately contribute to the aggregate mean utilization which would be expected by a high volume of water bypassing the gills. In addition, regional differences in O_2 utilization have been noted in a number of fishes and thus do not appear to be specific to the mako or to ram ventilation. For example, Piiper and Schumann (1967) reported a lower utilization at the first gill slit in the actively ventilating nursehound, *Scyliorhinus stellaris*. Differences in utilization at the dorsal, middle, and ventral positions of the opercular slits have been reported for teleosts, including ram-ventilating tunas (Jones et al., 1990) and actively ventilating rainbow trout, *Oncorhynchus mykiss* (Davis and Watters, 1970).

Pressure differential of the ventilatory stream

The total pressure differential of the ventilatory stream for each mako swimming at its mean velocity is determined by equation 1 and reported in Table 1. The components of this pressure differential can be further examined using Bernoulli's equation for fluid dynamics:

$$p + 0.5\rho v^2 + \rho gz = \text{constant} \quad (5)$$

where p is the hydrostatic pressure, $0.5\rho v^2$ is the hydrodynamic pressure (i.e., the pressure invested in the movement of the water), and ρgz is the manometric height (Vogel, 1994). For examination of flow in the horizontal plane manometric height can be ignored and the total head pressure (H) inducing flow through the branchial chamber is given by:

$$H_{tot} = p + 0.5\rho v^2 = \text{constant} \quad (6)$$

The total head pressure in front of the mouth is in the form of dynamic pressure (= $0.5\rho v^2$) and is thus dependent on swimming speed. However, as water enters the mouth, its velocity slows and dynamic pressure decreases while the static pressure rises proportionally. Engineering experience and analysis of tuna ram ventilation suggest that pressure drop in the buccal cavity (Δp_{bc}) is approximately 15% of the dynamic pressure (Brown and Muir, 1970). This loss in pressure is associated with the friction of water flow contacting the walls of the mouth and the gill arches. As water passes into the interlamellar spaces a further drop in pressure occurs and is estimated by Poiseuille's equation for laminar channel flow:

$$\Delta p_{lc} = (12 \cdot \mu \cdot v_{lc} \cdot l) / d^2 \quad (7)$$

where μ is the kinematic viscosity of seawater, v_{lc} is the velocity of water through the lamellar channels, l is lamellar channel length, and d is lamellar channel width (Brown and Muir, 1970). In the elasmobranch gill, water exits the interlamellar spaces into a septal channel, and because of its complex design (i.e., septal channel diameter increases as it extends towards the gill slits and post-lamellar water is entrained along

its entire length), the pressure differential associated with this flow cannot easily be accessed using the velocity-pressure relationships of hydrodynamics. However, knowing the total pressure differential and that of the buccal cavity and lamellar channels, pressure drop associated with septal channel flow (Δp_{sc}) is estimated by:

$$\Delta p_{sc} = \Delta p_{tot} - (\Delta p_{bc} + \Delta p_{lc}) \quad (8)$$

Estimated in this way, septal channel pressure drop accounts for approximately 64% of the total pressure differential.

Table 1 shows that the total pressure differential measured for ventilatory flow is greater than that of head pressure. This indicates a negative pressure at the gill slits (p_{gs}) which helps to pull water through the branchial apparatus and works in conjunction with head pressure to induce ventilatory water flow. The magnitude of this negative pressure, which is likely produced by the acceleration of water around the body of the swimming shark, is estimated by subtracting the total pressure differential from the pressure head; the mean for the six mako individuals is -180.7 ± 24.7 dyn cm^{-1} (Table 1). The ratio of p_{gs} to H_{tot} (i.e., the dimensionless pressure coefficient, C_p) is -0.23 ± 0.04, which is similar to the pressure coefficient measured at similar locations on swimming bluefish, *Pomatomus saltarix* (Dubois et al., 1974) and has been replicated using streamlined objects mounted in a water tunnel (Vogel, 1994).

Comparison of ventilatory flow and branchial resistance in lamnids and tunas

Because the volume of the ventilatory stream can be adjusted through changes in swimming speed, mouth gape, and presumably alterations to the size of the gill slits and opercular openings, it is not surprising that water flow parameters within the interlamellar channels of the mako are similar to those reported for skipjack tuna (Stevens and Lightfoot, 1986), despite differences in the body size of the specimens studied [4.62 – 7.34 kg, makos in this study; 1.67 kg, skipjack of Stevens and Lightfoot (1986)] and distinctions in gill morphology. Interlamellar water-flow velocity (0.44 ± 0.06 cm s^{-1}) and residence time (0.40 ± 0.07 s) in the mako (Table 1) are within the range of estimates for skipjack tuna (0.128 – 0.745 cm s^{-1}, 0.16 – 0.94 s) (Stevens and Lightfoot, 1986). The Reynold's number (R_e) associated with flow through mako interlamellar channels (0.12, Table 1) is larger than that of skipjack tuna [0.01 - 0.08, Stevens and Lightfoot (1986)] and reflects the mako's larger interlameller spacing (see R_e equation in Table 1); however, this still indicates that flow along the respiratory exchange surfaces is slow and dominated by viscous forces. Likely corresponding to similar interlamellar flow parameters, mako O_2 utilization (53.4 ±4.2%) is also comparable to that of tunas (range 44.3 – 56.0%) (Stevens, 1972; Bushnell and Brill, 1991; 1992).

The pressure gradients driving branchial flow in the mako and skipjack tuna are also fairly similar at basal (preferred) swimming speeds. For example, Muir and Brown (1970) estimated the total pressure drop through the branchial chamber of a 1.67 kg skipjack tuna swimming at 66 cm s^{-1} to be approximately 1100 dyns cm^{-2}. *In vivo* measurements made by Stevens (1972) and further analyzed by Stevens and

Lightfoot (1986) suggest this is a reasonable estimate. For makos a mean pressure gradient of 967.5 ± 261.1 dyn cm^{-2} was determined for a mean preferred swimming speed of 38.8 cm s^{-1} (Table 1). Although Δp_{tot} is thus comparable for tunas and the mako, the distribution of pressure drop within the branchial chamber varies. In skipjack, 800 dyn cm^{-2} (73% of the total resistance) is incurred as water passes through the interlamellar channels (Brown and Muir, 1970), as opposed to 289 dyn cm^{-2} (30% of total resistance) in the mako (Table 1). Given that interlamellar water-flow velocities are similar, equation 7 suggests the lower mako pressure gradient at this location is primarily attributed to its wider interlamellar spaces [55.8 μm for makos in this study (Table 1), 20 μm for skipjack tuna (Brown and Muir, 1970)], and this appears to be a needed compensation for the high resistance incurred at the septal channels (625 dyn cm^{-2}, 64% of mako total branchial resistance) a feature not present in the gills of tunas.

This study thus provides evidence that the septal channel of the elasmobranch gill significantly contributes to total gill resistance, and likely limits lamellar frequency and ultimately gill surface area in the mako and other lamnid sharks. Specifically, the interlamellar channel width in the mako is twice that of tunas resulting in one-half the lamellar frequency, and one-half the gill surface area. Correspondingly, mako standard metabolic rate (Sepulveda et al., 2007) is approximately one-half that of tunas (Brill, 1979; 1987; Dewar and Graham, 1994).

Table 4.1: Parameters of ram ventilation for six shortfin makos swimming in a water tunnel.

Symbol	Variable	Data Source	Mako 1	Mako 2	Mako 3	Mako 4	Mako 5	Mako 6	Mean ± SD
	Shark Measurements								
M	Mass (kg)	Direct measurement	4.62	4.71	5.01	6.77	6.95	7.34	-
FL	Fork length (cm)	Direct measurement	77.0	77.5	76.0	88.5	89.0	89.0	-
TL	Total length (cm)	Direct measurement	84.0	85.0	85.0	96.5	95.0	97.0	-
	Experimental Parameters								
T	Water Temperature (°C)	Direct measurement	17.9	19.4	19.3	17.0	18.2	17.7	-
$\mathbf{C_wO_2}$	Water O_2 concentration ($mgO_2\ l^{-1}$)	-	7.8	7.6	7.6	8.0	7.8	7.8	-
	Swimming and O_2 Consumption								
$\boldsymbol{v_s}$	Mean swimming velocity ($cm\ s^{-1}$)	Direct measurement	40.2	34.7	32.7	45.5	45.7	34.1	38.8 ± 5.8
$\boldsymbol{v_{s\text{-}TL}}$	Mean swimming velocity ($TL\ s^{-1}$)	v_s / TL	0.48	0.41	0.38	0.47	0.48	0.35	0.43 ± 0.06
$\mathbf{MO_2}$	O_2 consumption ($mgO_2\ kg^{-1}\ h^{-1}$)	$10^{(2.0937 + 0.97 v_{s\text{-}TL})}$	361.3	308.8	293.0	355.7	363.3	272.1	325.7 ± 39.5
U	O_2 Utilization (%)	Direct measurement	58.1	46.3	52.3	52.0	56.2	55.6	53.4 ± 4.2
	Oral Cavity Water Flow								
$\mathbf{A_m}$	Mouth cross-sectional area (cm^2)	Direct measurement	4.6	4.5	4.6	4.8	5.2	5.9	4.9 ± 0.5
$\mathbf{V_{gmax}}$	Max ventilation volume ($cm^3\ s^{-1}$)	$v_s \cdot A_m$	184.9	157.4	150.4	218.6	237.6	201.2	191.7 ± 34.2
$\mathbf{V_g}$	Ventilation volume ($cm^3\ s^{-1}$)	$(m \cdot MO_2) / (C_wO_2 \cdot U)$	102.3	114.8	102.6	160.8	160.0	127.9	128.1 ± 26.8
$\boldsymbol{v_m}$	Water velocity entering mouth ($cm\ s^{-1}$)	V_g / A_m	22.2	25.3	22.3	33.5	30.8	21.7	26.0 ± 5.0
$\mathbf{A_{ga}}$	Area between gill arches (cm^2)	Direct measurement	6.6	7.6	8.2	7.5	7.7	10.7	8.1 ± 1.4
$\boldsymbol{v_{ga}}$	Water velocity at gill arches ($cm\ s^{-1}$)	V_g / A_{ga}	15.5	15.1	12.4	21.4	20.7	11.9	16.2 ± 4.1
	Gill Dimensions								
$\mathbf{L_{fil}}$	Total filament length (cm)	Direct measurement	6986.4	7287.8	7580.8	8026.4	8186.8	8288.8	7726.2 ± 525.2
$\mathbf{f_{lam}}$	Lamellar frequency (mm^{-1})	Direct measurement	16.17	15.77	14.95	14.00	14.47	15.68	15.17 ± 0.84
$\mathbf{n_{lc}}$	Total number of lamellar channels	$L_{fil} \cdot f_{lam}$	1129504	1148922	1133512	1123320	1184434	1299528	1169870 ± 67202
$\boldsymbol{l}$	Lamellar channel length (mm)	Direct measurement	1.57	1.50	1.75	1.73	1.97	1.74	1.71 ± 0.16
$\boldsymbol{B}$	Lamellar channel height (mm)	Direct measurement	0.435	0.372	0.452	0.456	0.508	0.443	0.444 ± 0.044
$\boldsymbol{t}$	Lamellar thickness (μm)	Direct measurement	11.26	9.31	10.43	10.36	10.87	9.40	10.27 ± 0.78
$\boldsymbol{D}$	Lamellar channel width (μm)	$(1000 - (t \cdot f_{lam})) / f_{lam}$	50.60	54.12	56.45	61.10	58.25	54.38	55.82 ± 3.64
$\mathbf{A_{lc}}$	Lamellar channel cross-sect. area (cm^2)	$n_{lc} \cdot b \cdot d$	248.6	231.2	289.2	313.0	350.5	313.1	290.9 ± 44.5

Table 4.1: Parameters of ram ventilation for six shortfin makos swimming in a water tunnel, Continued

Symbol	Variable	Data Source	Mako 1	Mako 2	Mako 3	Mako 4	Mako 5	Mako 6	Mean ± SD
	Gill Water Flow								
v_{lc}	Interlamellar water velocity (cm s^{-1})	V_g / A_{lc}	0.41	0.50	0.35	0.51	0.46	0.41	0.44 ± 0.06
R_e	Interlamellar Reynold's number	$(0.5 \cdot \rho \cdot d \cdot v_{lc}) / \mu$	0.10	0.13	0.10	0.16	0.13	0.11	0.12 ± 0.02
R	Interlamellar water residence time (s)	l / v_{lc}	0.38	0.30	0.49	0.34	0.43	0.43	0.40 ± 0.07
	Water Pressure								
H_{tot}	Total head pressure (dyn cm^{-2})	$0.5 \cdot \rho \cdot v_s^2$	828.2	617.1	548.0	1061.0	1070.4	595.9	786.8 ± 236.5
H_d	Dynamic pressure at mouth (dyn cm^{-2})	$0.5 \cdot \rho \cdot v_m^2$	253.6	328.5	254.9	574.2	485.3	240.9	356.2 ± 140.8
Δp_{tot}	Total pressure drop (dyn cm^{-2})	$1.3473 \cdot v_s^{1.7938}$	1016.5	780.7	701.9	1269.4	1279.4	756.7	967.5 ± 261.1
Δp_{bc}	Buccal cavity pressure drop (dyn cm^{-2})	$0.15 \cdot H_m$	38.0	49.3	38.2	86.1	72.8	36.1	53.4 ± 21.1
Δp_{lc}	Interlamellar pressure drop (dyn cm^{-2})	$(12 \cdot \mu \cdot v_{lc} \cdot l) / d^2$	303.4	304.2	233.7	285.8	317.3	289.1	288.9 ± 29.3
Δp_{sc}	Septal channel pressure drop (dyn cm^{-2})	$\Delta p_{tot} - (\Delta p_{bc} + \Delta p_{lc})$	675.1	427.2	429.9	897.4	889.4	431.5	625.1 ± 228.6
p_{gs}	Negative pressure at gills slits (dyn cm^{-2})	$H_{tot} - \Delta p_{tot}$	-188.3	-163.6	-153.9	-208.4	-209.1	-160.8	-180.7 ± 24.7
C_p	Pressure coefficient at gills slits	p_{gs} / H_{tot}	-0.23	-0.27	-0.28	-0.20	-0.20	-0.27	-0.24 ± 0.04
	Constants								
μ	Kinematic viscosity of water (cm^2 s^{-1})	0.01							
ρ	Density of seawater (kg l^{-1})	1.025							

Note: Equation references: MO_2 (Sepulveda et al., 2007), R_e (Stevens and Lightfoot, 1986), V_g and Δp_{lc} (Brown and Muir, 1970).

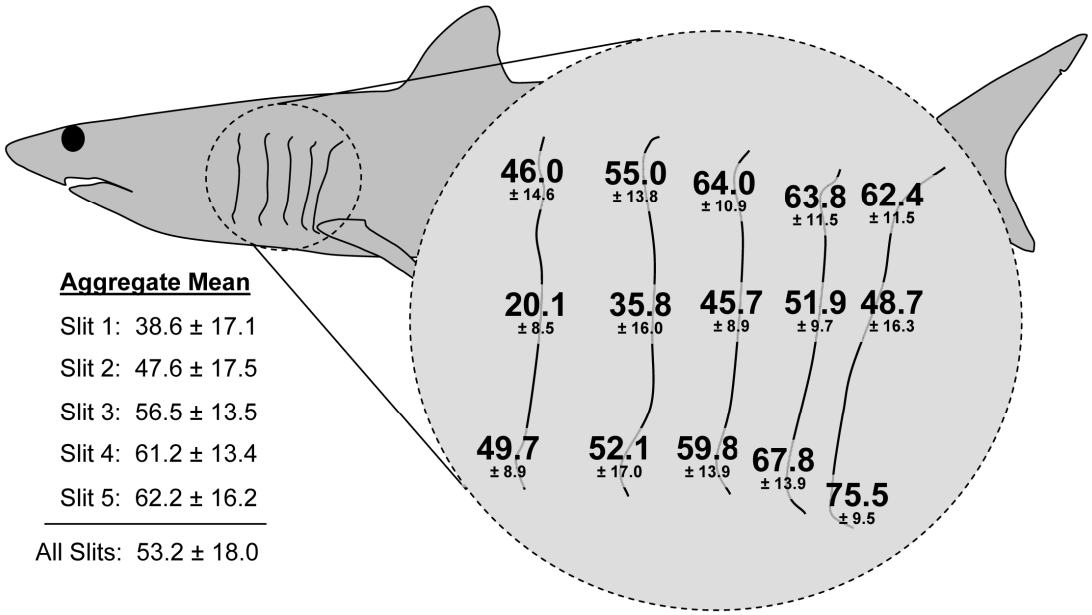

Figure 4.1: Regional measures of gill-O_2 utilization from six makos swimming at 38.8 ± 5.8 cm s^{-1}. Tabular data (left) show the aggregate mean for each gill slit. Means are ± standard deviation.

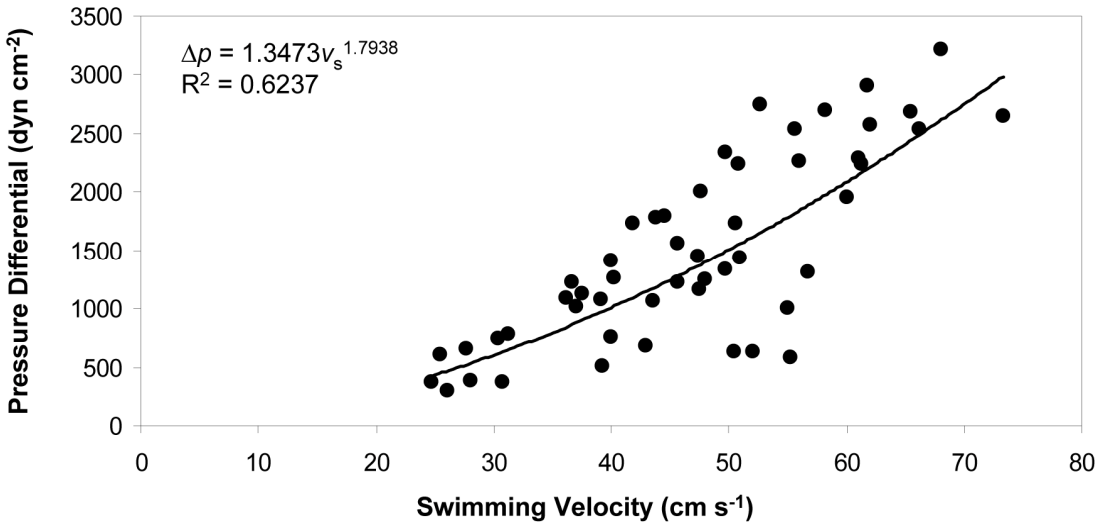

Figure 4.2: Pressure differential (Δp_{tot}) measured between the front of the buccal cavity and the third gill slit for six makos (4.6 - 7.3 kg) swimming at different velocities (v_S).

LITERATURE CITED

Altringham JD, Block BA. 1997. Why do tuna maintain elevated slow muscle temperatures? Power output of muscle isolated from endothermic and ectothermic fish. J Exp Biol 200:2617-2627.

Bernal D, Dickson KA, Shadwick RE, Graham JB. 2001a. Review: Analysis of the evolutionary convergence for high performance swimming in lamnid sharks and tunas. Comp Biochem Physiol 129:695-726.

Bernal D, Sepulveda C, Mathieu-Costello O, Graham JB. 2003a. Comparative studies of high performance swimming in sharks I. Red muscle morphometrics, vascularization and ultrastructure. J Exp Biol 206:2831-2843.

Bernal D, Sepulveda CA, Graham JB. 2001b. Water-tunnel studies of heat balance in swimming mako sharks. J Exp Biol 204:4043-4054.

Bernal D, Smith D, Lopez G, Weitz D, Grimminger T, Dickson K, Graham JB. 2003b. Comparative studies of high performance swimming in sharks II. Metabolic biochemistry of locomotor and myocardial muscle in endothermic and ectothermic sharks. J Exp Biol 206:2845-2857.

Brill RW. 1979. Effect of body size on the standard metabolic rate of skipjack tuna, *Katsuwonus pelamis*. Fish Bull 77:494-498.

Brill RW. 1987. On the standard metabolic rates of tropical tunas, including the effect of body size and acute temperature change. Fish Bull 85:25-36.

Brown CE, Muir BS. 1970. Analysis of ram ventilation of fish gills with application to skipjack tuna (*Katsuwonus pelamis*). J Fish Res Bd Canada 27:1637-1652.

Bushnell PG, Brill RW. 1991. Responses of swimming skipjack (*Katsuwonus pelamis*) and yellowfin (*Thunnus albacares*) tunas to acute hypoxia, and a model of their cardiorespiratory function. Physiol Zool 64:887-911.

Bushnell PG, Brill RW. 1992. Oxygen-transport and cardiovascular-responses in skipjack tuna (*Katsuwonus pelamis*) and yellowfin tuna (*Thunnus albacares*) exposed to acute-hypoxia. J Comp Physiol B 162:131-143.

Carey FG, Teal JM, Kanwisher JW, Lawson KD, Beckett JS. 1971. Warm-bodied fish. Amer Zool 11:137-145.

Davis JC, Watters K. 1970. Evaluation of opercular catheterization as a method for sampling water expired by fish. J Fish Res Bd Can 27:1627-1635.

Dewar H, Graham JB. 1994. Studies of tropical tuna swimming performance in a large water tunnel. 1. Energetics. J Exp Biol 192:13-31.

Donley JM, Sepulveda CA, Konstantinidis P, Gemballa S, Shadwick RE. 2005. Patterns of red muscle strain activation and body kinematics during steady swimming in a lamnid shark, the shortfin mako *Isurus oxyrinchus*. J Exp Biol 208:2377-2387.

Dowis HJ, Sepulveda CA, Graham JB, Dickson KA. 2003. Swimming performance studies on the eastern Pacific bonito *Sarda chiliensis*, a close relative of the tunas (family Scombridae) II. Kinematics. J Exp Biol 206:2749-2758.

Dubois AB, Cavagna GA, Fox RS. 1974. Pressure distribution on the body surface of swimming fish. J Exp Biol 60:581-591.

Emery SH, Szczepanski A. 1986. Gill dimensions in pelagic elasmobranch fishes. Biol Bull 171:441-449.

Graham JB, Dewar H, Lai NC, Lowell WR, Arce SM. 1990. Aspects of shark swimming performance determined using a large water tunnel. J Exp Biol 151:175-192.

Graham JB, Dickson KA. 2001. Anatomical and physiological specializations for endothermy. In: Block BA, Stevens ED, editors. Tuna: Physiology, ecology and evolution. San Diego: Academic Press. p 121-165.

Jones DR, Brill RW, Butler PJ, Bushnell PG, Heieis MRA. 1990. Measurement of ventilation volume in swimming tunas. J Exp Biol 149:491-498.

Muir BS, Hughes GM. 1969. Gill dimensions for three species of tunny. J Exp Biol 51:271-285.

Piiper J, Schumann D. 1967. Efficiency of O_2 exchange in the gills of the dogfish *Scyliorhinus stellaris*. Respir Physiol 2:135-148.

Sepulveda CA, Dickson KA, Graham JB. 2003. Swimming performance studies on the eastern Pacific bonito Sarda chiliensis, a close relative of the tunas (family Scombridae) I. Energetics. J Exp Biol 206:2739-2748.

Sepulveda CA, Graham JB, Bernal D. 2007. Aerobic metabolic rates of swimming juvenile mako sharks, Isurus oxyrinchus. Mar Biol 152:1087-1094.

Stevens ED. 1972. Some aspects of gas exchange in tuna. J Exp Biol 56:809-823.

Stevens ED, Lightfoot EN. 1986. Hydrodynamics of water flow in front of and through the gills of skipjack tuna. Comp Biochem Physiol 83A:255-259.

Vogel S. 1994. Life in moving fluids: The physical biology of flow. Princeton, New Jersey: Princeton University Press. 467 p.

Weihs D, Keyes RS, Stalls DM. 1981. Voluntary swimming speeds of two species of large carcharhinid sharks. Copeia 1981:219-222.

ACKNOWLEDGEMENTS

This research was supported by the National Science Foundation Grant #IOS-0817774, the Tuna Industry Endowment Fund at Scripps Institution of Oceanography, and the Moore Family Foundation. N.C. Wegner was supported by the Nadine A. and Edward M. Carson Scholarship awarded by the Achievement Rewards for College Scientists (ARCS), Los Angeles Chapter, and the National Science Foundation. We thank D. Cartamil, D. Head, C. Jew, D. Kacev, E. Kisfaludy, A. Nosal, C. Peters, C. Sepulveda, and K. Uyeji for help in various aspects of this project.

Chapter 4, in full, is currently being prepared for submission for publication as: Wegner NC, Lai NC, Bull KB, Graham JB. Ram ventilation in the shortfin mako, *Isurus oxyrinchus*: Oxygen utilization and the branchial pressure gradient. J Exp Biol. The dissertation author is the primary investigator and author of this paper.

APPENDIX CHAPTER: GILL SPECIALIZATIONS IN HIGH-PERFORMANCE PELAGIC TELEOSTS, WITH REFERENCE TO STRIPED MARLIN (*TETRAPTURUS AUDAX*) AND WAHOO (*ACANTHOCYBIUM SOLANDRI*)

BULLETIN OF MARINE SCIENCE, 79(3): 747–759, 2006

GILL SPECIALIZATIONS IN HIGH-PERFORMANCE PELAGIC TELEOSTS, WITH REFERENCE TO STRIPED MARLIN (*TETRAPTURUS AUDAX*) AND WAHOO (*ACANTHOCYBIUM SOLANDRI*)

Nicholas C. Wegner, Chugey A. Sepulveda, and Jeffrey B. Graham

ABSTRACT

Analysis of the gill structure of striped marlin, *Tetrapturus audax* (Philippi, 1887), and wahoo, *Acanthocybium solandri* (Cuvier, 1832), demonstrates similarities to tunas (family Scombridae) in the presence of gill specializations to maintain rigidity during fast, sustainable swimming and to permit the O_2 uptake required by high aerobic performance. For ram-gill ventilators such as tunas, wahoo, and striped marlin, a rigid gill structure prevents lamellar deformation during fast water flow. In tunas, lamellar fusions bind adjacent lamellae on the same filament to opposing lamellae of the neighboring filament. Examination of striped marlin and wahoo gill structure demonstrates a previously undescribed inter-lamellar fusion which binds juxtaposed lamellae on the same filament, but does not connect to opposing lamellae of the adjacent filament. Lamellar thicknesses and the water-blood barrier distances in striped marlin and wahoo are comparable to those of tunas and among the smallest recorded. Vascular replica casts reveal that striped marlin lamellar vascular channels are similar to tunas in having a diagonal progression that reduces lamellar vascular resistance. Wahoo lamellar channels, however, have a linear pattern similar to most other teleosts.

Tunas, bonitos, mackerels (family Scombridae), and billfishes (families Istiophoridae, Xiphiidae) are highly specialized for fast, continuous swimming. Both groups are ram ventilators [i.e., their nonstop movement forces water over the gills thus replacing active gill ventilation (Jones and Randall, 1978; Roberts and Rowell, 1988)] which, at faster swimming speeds, reduces drag associated with cyclic jaw movements for respiration (Brown and Muir, 1970; Freadman, 1981).

The gill design of tunas (tribe Thunnini) epitomizes specializations for ensuring rigidity required by ram ventilation and for meeting increased oxygen demands associated with high aerobic performance (Muir and Kendall, 1968; Hughes, 1970). Tunas possess lamellar fusions that bind the respiratory lamellae to create a rigid gill sieve (Fig. 1; Muir and Kendall, 1968). In addition, tunas of the genus *Thunnus* have filament fusions that support elongate gill filaments (Fig. 1A). Both fusion types prevent gill deformation during ram ventilation and thereby minimize anatomical dead space (i.e., the separation of filaments and lamellae due to the force of high-velocity water flow) (Muir and Kendall, 1968; Hughes, 1984). Tunas also have large gill areas that enhance gas exchange and microvascular specializations [slender lamellae and thin lamellar walls (the water-blood barrier distance)] that decrease diffusion distances (Muir and Hughes, 1969; Hughes, 1972; Hughes and Morgan, 1973; Hughes, 1984). In addition, the diagonal orientation of the vascular channels in tuna lamellae (Fig. 1B) increases the number of respiratory blood channels in parallel in the gills and conserves vascular pressure drop across the lamellae by minimizing blood-flow distance (Muir, 1970; Muir and Brown, 1971; Olson et al., 2003).

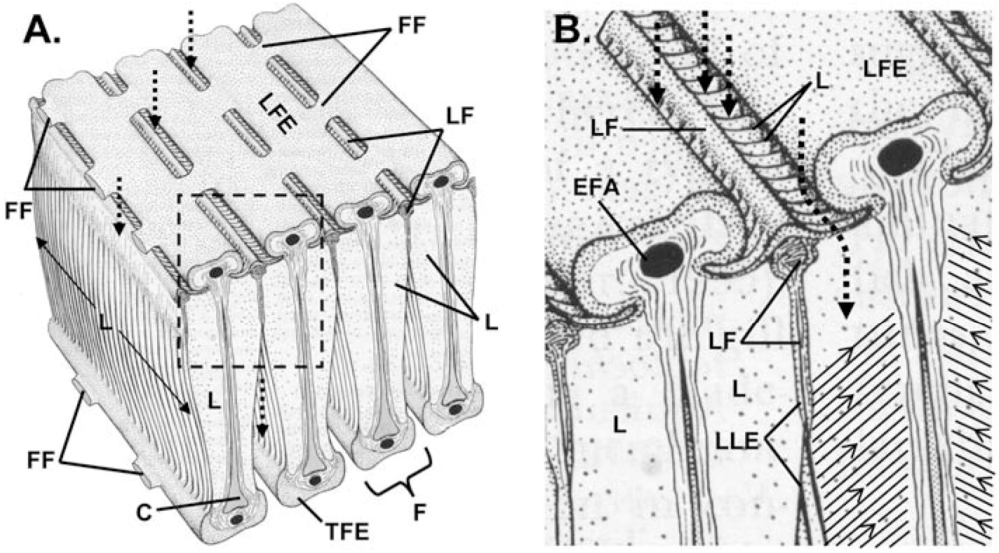

Figure 1. **A:** Cross-section through four adjacent gill filaments (F) depicting the filament and lamellar fusions of some ram-ventilating teleosts. Filament fusions (FF) connect adjacent filaments on the leading and trailing filament edges. **B:** Magnified view of the dashed box in A detailing the lamellar fusion and blood-flow pathways (as described for tunas) through the lamellae. Lamellar fusions (LF) connect the leading lateral (outer) edges of juxtaposed lamellae (L) on the same filament to the opposing lamellae of the adjacent filament. The lateral lamellar edges (LLE) are not usually bound along their entire length. Blood through tuna lamellae flows in a diagonal progression (solid arrows) from the lateral lamellar edge toward the filament base. Direction of water flow is indicated by dotted arrows. Other abbreviations: C: cartilaginous filament rod, EFA: efferent filament artery; LFE, leading filament edge; TFE, trailing filament edge. Figure modified from Muir and Kendall (1968).

While it is generally assumed that other high-performance fishes including billfishes and non-tuna members of the Scombridae have gill specializations similar to tunas, this has not been fully investigated. Filament fusions that connect adjacent gill filaments on the same hemibranch have been noted in gill descriptions of the istiophorids, swordfish, *Xiphias gladius* Linnaeus, 1758, and wahoo, *Acanthocybium solandri* (Cuvier, 1832) (Lütken, 1880; Trois, 1883; Kishinouye, 1923; Bevelander, 1934; Conrad, 1938; Muir and Kendall, 1968; Johnson, 1986). However, the status of lamellar fusions in these fishes is unclear. Muir and Kendall (1968) originally reported that billfishes and wahoo lack lamellar fusions, but Muir (1969) later affirmed their presence in the striped marlin, *Tetrapturus audax* (Philippi, 1887). Also lacking are details on gill microstructure and lamellar blood-flow pattern in billfishes and wahoo.

The objective of this study was to use scanning electron microscopy, light microscopy, and vascular replica casting to document structural and microvascular specializations in both striped marlin and wahoo. For comparison, we also examined the gills of yellowfin tuna, *Thunnus albacares* (Bonnaterre, 1788). This report reviews relevant literature on the gill structure of these fishes and documents several specializations related to ram ventilation, including the first description of a novel form of lamellar fusion.

Methods

Fish Collection.—Four striped marlin, seven wahoo, and seven yellowfin tuna were caught by hook and line off the coast of Baja California, Mexico, for the acquisition of gill tissue and preparation of gill vascular replica casts. All specimens were collected under the authorization of la Comisión Nacional de Acuacultura y Pesca, México, Permiso de Pesca de Fomento No. DGOPA/13308/210905/ and euthanized by surgically severing the spinal cord in accordance with Protocol S00080 of the Animal Care and Use Committee (University of California, San Diego). Striped marlin specimen weights were estimated at sea. For wahoo and yellowfin, fish fork lengths were measured, and specimen weights were subsequently calculated using length-weight regression equations (Chatwin, 1959; Beerkircher, 2005).

Tissue Fixation.—Following euthanization, gill tissue was removed from one striped marlin (25 kg), four wahoo (14.6, 18.5, 19.4, 24.2 kg), and six yellowfin tuna (11.0, 13.4, 15.3, 33.0, 39.9, 49.2 kg) and placed in 10% formalin buffered with seawater within 10 min of capture. The gills of a 70 kg striped marlin were extracted and placed in formalin approximately 3 hrs after capture. Gills from a 35 kg striped marlin were removed and placed on ice until immersed in formalin, also approximately 3 hrs post capture. Finally, gill tissue from a 45 kg marlin was excised and placed in formalin after the specimen had first been perfused with vascular casting solution.

Vascular Casting.—Vascular replica gill casts were made for one striped marlin (45 kg), three wahoo (12.8, 15.3, 19.4 kg), and one yellowfin tuna (4.3 kg). Specimens were euthanized and placed ventral side up in a V-shaped cradle, and the gills were ventilated with aerated seawater from a hose placed in the mouth. The heart was exposed by mid-line incision, a catheter inserted, and the specimen perfused with heparinized teleost saline (Brill and Dizon, 1979) followed by microvascular casting material (Mercox Resin, Ladd Research, Williston, Vermont). The casting solution was allowed to harden for several hours, after which the specimens were frozen until examination. In the laboratory, the specimens were thawed and the excised gill casts were macerated in washes of 20% KOH until all tissue was removed.

Gill Structure Analysis.—Striped marlin, wahoo, and yellowfin tuna gill tissue was examined using both light and scanning electron microscopy (SEM). For light microscope preparation, fixed tissue was embedded in paraffin, and semi-thin sections (5 μm) were mounted on slides and stained with hematoxylin and eosin. For SEM, fixed tissue was rinsed with deionized water and slowly dehydrated to 100% ethanol (20% increments over 24 hrs). The tissue was critically-point-dried, sputter coated with gold-palladium, and viewed under high-vacuum mode using a FEI Quanta 600 SEM. Cross-sections through critically-point-dried lamellae were used to estimate lamellar thickness and the water-blood barrier distance. Vascular replica casts were examined using low-vacuum mode SEM.

Results

Inter-lamellar Fusions.—Comparative SEM and light microscopy images of striped marlin, wahoo, and yellowfin tuna gills are shown in Figs. 2–5. A significant finding is that the majority of the gill lamellae in the striped marlin specimens examined are not bound by lamellar fusions. Rather, most lamellae are bound by a previously undescribed structure, which we have termed the inter-lamellar fusion. The inter-lamellar fusion connects the leading lateral edge of adjacent lamellae on the same filament (Fig. 2B–M). This differs from the lamellar fusion of tunas in that the inter-lamellar fusion does not extend to the opposing lamellae on the adjacent filament (compare Fig. 2D with Fig. 4A). The inter-lamellar fusion is thickest on the leading lamellar edge and quickly thins as it continues along the lateral edge of the

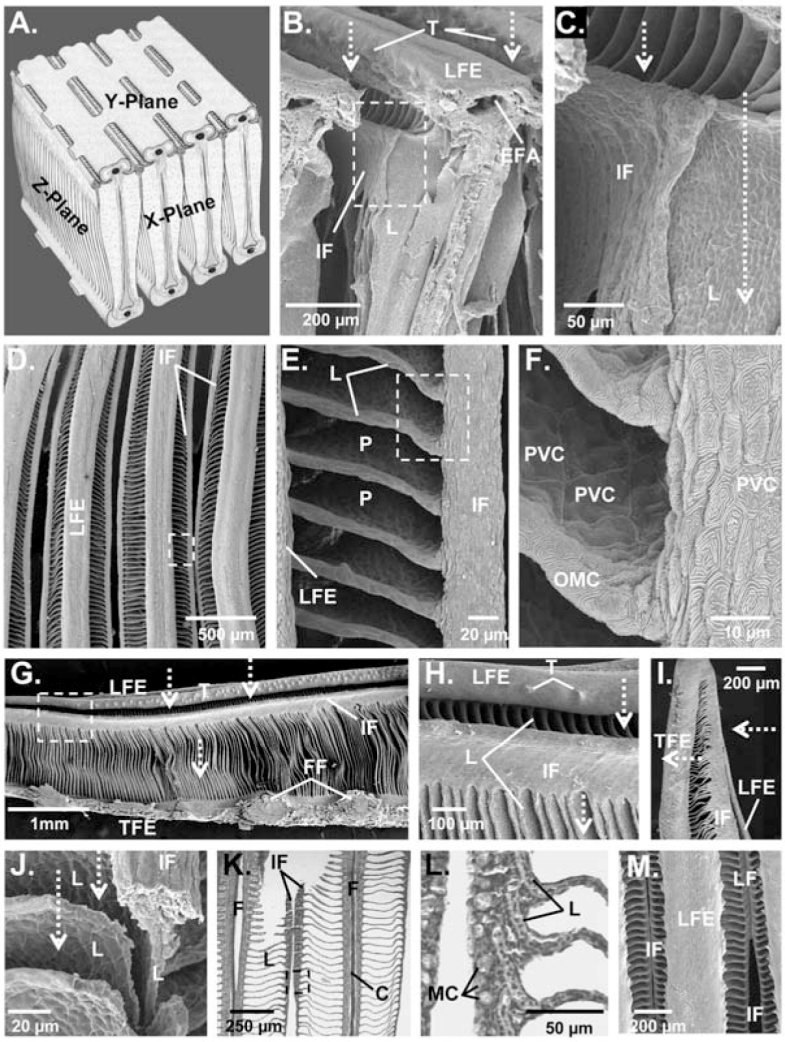

Figure 2. SEM and light microscope images of the inter-lamellar fusion in striped marlin (*Tetrapturus audax*). **A:** Reference diagram showing the three planes at which SEM and light microscope images were taken. See Figure 1 for additional diagram details. **B:** Cross-section through the leading (efferent) edge of adjacent gill filaments (x-plane). **C:** Enlarged area of the dashed box in B detailing the inter-lamellar fusion. **D:** View of the leading edge of adjacent gill filaments (y-plane). **E:** Magnified image of the dashed box of D showing the pores formed by the inter-lamellar fusion. **F:** Augmented view of E depicting the microridged pavement cells of the inter-lamellar epithelium and outer marginal channel, as well as the smooth pavement cells of the lamellar respiratory surface. **G:** Extension of the inter-lamellar fusion along the length of a filament (z-plane). **H:** Enlarged area of the dashed box in G. **I:** Inter-lamellar fusion along the filament tip (z-plane). **J:** Cross-section through the inter-lamellar fusion showing its thick leading edge and attachment to the background lamella (x-plane). **K:** Cross-section through the leading edge of two adjacent filaments (y-plane). **L:** Higher magnification of the dashed box in K showing the embedment of the lateral lamellar tips in the inter-lamellar fusion. **M:** Two inter-lamellar fusions from adjacent filaments growing together to form a complete lamellar fusion similar to that of tunas. Dotted arrows show the direction of water flow. Water flow is into the page in D–F, K–M. Images B–L are from a 45 kg striped marlin; M is from a 25 kg specimen. Abbreviations: C, cartilaginous filament rod; EFA, efferent filament artery; F, filament base; FF, filament fusion; IF, inter-lamellar fusion; L, lamellae; LF, lamellar fusion; LFE, leading filament edge; MC, mucous cell; P, lamellar pore; PVC, pavement cell; OMC, outer marginal channel; T, teeth of the epithelial toothplates; TFE, trailing filament edge.

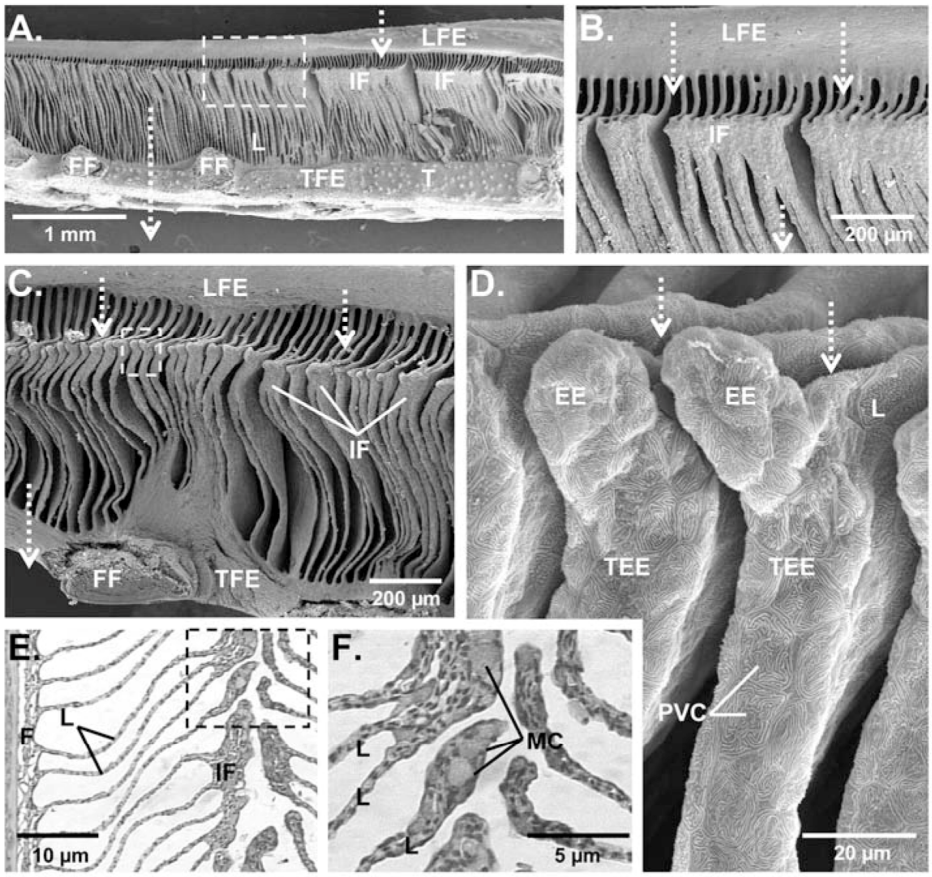

Figure 3. SEM and light microscope images depicting the positioning and structure of the inter-lamellar fusion in wahoo (*Acanthocybium solandri)*. **A:** View of the filament showing the irregularity of the inter-lamellar fusion (z-plane, refer to Fig. 2A). **B:** Magnified image of the inter-lamellar fusions in A. **C:** Image showing the thickened lateral lamellar edges of non-fused lamellae (z-plane). **D:** Magnified image of the lateral lamellar edges in C, detailing extensions of the lamellar epithelium which appear to be bridging the inter-lamellar spaces. **E:** Cross-section through fused and non-fused lamellae (y-plane). **F:** Magnified view of dashed box in E. Dotted arrows indicate the direction of water flow. Water flow is into the page in E and F. A–D are from a 19.4 kg wahoo, E,F are from a 14.4 kg specimen. Abbreviations: EE, epithelial extension; F, filament base; FF, filament fusion; IF, inter-lamellar fusion; L, lamellae; LFE, leading filament edge; MC, mucous cell; PVC, pavement cell; T, teeth of the epithelial toothplates; TFE, trailing filament edge; TEE, thickened epithelial edge.

lamellae (Fig. 2B,C,J). The fusion extends the full length of the filament (Fig. 2G) and at the filament tip it covers nearly the entire length of the lamellae (Fig. 2I).

SEM images of the fusion epithelial surface reveal the typical "fingerprinting" of pavement (squamous) cell microridges (Fig. 2F). These microridges [also observed on the striped marlin gill filament (not pictured) and lamellar outer marginal channel (Fig. 2F)] are characteristic of non-respiratory gill epithelia (Olson, 1996), while thin, non-ridged pavement cells comprise the lamellar respiratory surface (Fig. 2F). Stained cross-sections of the inter-lamellar fusion show that the lateral lamellar edges turn nearly 90° [toward the distal end of the filament (filament tip)] to approach neighboring lamellae, where they are connected by non-differentiated epithelial cells (Fig. 2L). These lateral lamellar edges therefore form the majority of the fusion's in-

ner wall (Fig. 2L). A thicker epithelium covers the outer edge of this lamellar bridging and forms the bulk of the fusion (Fig. 2L). The thick leading edge of the fusion is composed mainly of mucous (goblet) cells (Fig. 2L); as the fusion thins along the lateral lamellar edge it is composed solely of non-differentiated epithelial cells.

Inter-lamellar fusions are also present in wahoo (Fig. 3A–F), although they are somewhat irregular and less uniform than in striped marlin. Figure 3A–C shows both fused and non-fused lamellae along the length of a filament. No apparent pattern was noted for the presence or absence of inter-lamellar fusions in relation to gill arch number or position in the flow stream. Non-fused lamellae have a thick lateral lamellar edge, and in many cases, extensions of this thickened epithelium appear to reach toward adjacent lamellae (Fig. 3C,D). These epithelial extensions uniformly point toward the filament tip (Fig. 3C–F).

Like striped marlin, the wahoo inter-lamellar fusion is composed of stratified epithelium with a high concentration of mucous cells on its leading edge (Fig. 3E,F). Mucous cells are also present in the thickened epithelium of non-fused lamellae (Fig. 3F). The inter-lamellar fusion in wahoo is thinner than in striped marlin (compare Fig. 3E with 2L) and wahoo lateral lamellar edges (although turned toward the distal end of the filament) do not appear to form the inner wall of the fusion (Fig. 3F)

Lamellar Fusions.—The lamellar fusions of yellowfin tuna connect juxtaposed lamellae on the same filament to opposing lamellae on the adjacent filament (Fig. 4A,B). The fusion epithelial surface has microridged pavement cells surrounding mucous cell pores (Fig. 4C). Cross-sections through the fusion show that the leading edge is predominately composed of mucous cells, while the bulk of the fusion is composed of non-differentiated epithelial cells. The lamellar lateral edges are embedded in the fusion and curve toward the distal end of the filament, but not to the extent seen in striped marlin and wahoo (Fig. 4E).

In striped marlin, the majority of the lamellae are bound by inter-lamellar fusions; however, in some cases, inter-lamellar fusions from adjacent filaments appear to grow together to form complete lamellar fusions as described for tunas (Fig. 2M). Striped marlin sample size was not adequate to determine any significant patterns in the frequency of the completed lamellar fusions in relation to body size or position within the flow stream. In contrast, complete lamellar fusions were not observed in wahoo.

Microvascular Specializations.—Gill microvascular measurements for striped marlin, wahoo, and yellowfin tuna determined from critically point-dried gill tissue and vascular corrosion casts are shown in Table 1. The lamellar thickness (6.29 ± 1.36 μm) and water-blood barrier distance (0.531 ± 0.153 μm) of striped marlin are comparable to measurements determined for yellowfin tuna (5.88 ± 0.99, 0.537 ± 0.092 μm) in this study and previously reported values (Hughes, 1970; Muir and Brown, 1971). Wahoo lamellar thickness (5.16 ± 1.21 μm) is also similar, although the water-blood barrier thickness (0.860 ± 0.170 μm) is significantly greater ($P < 0.001$) than both striped marlin and yellowfin.

Yellowfin tuna vascular casts (Fig. 5B) confirm previous descriptions (Muir, 1970; Muir and Brown, 1971; Olson et al., 2003) of the blood-flow pattern through tuna lamellae. Blood leaving the afferent lamellar arteriole enters directly into outer marginal channels (OMC) extending along the lateral edge of the lamellae. From the OMCs, blood flows across the lamellae through diagonal channels (formed by pillar cells) that

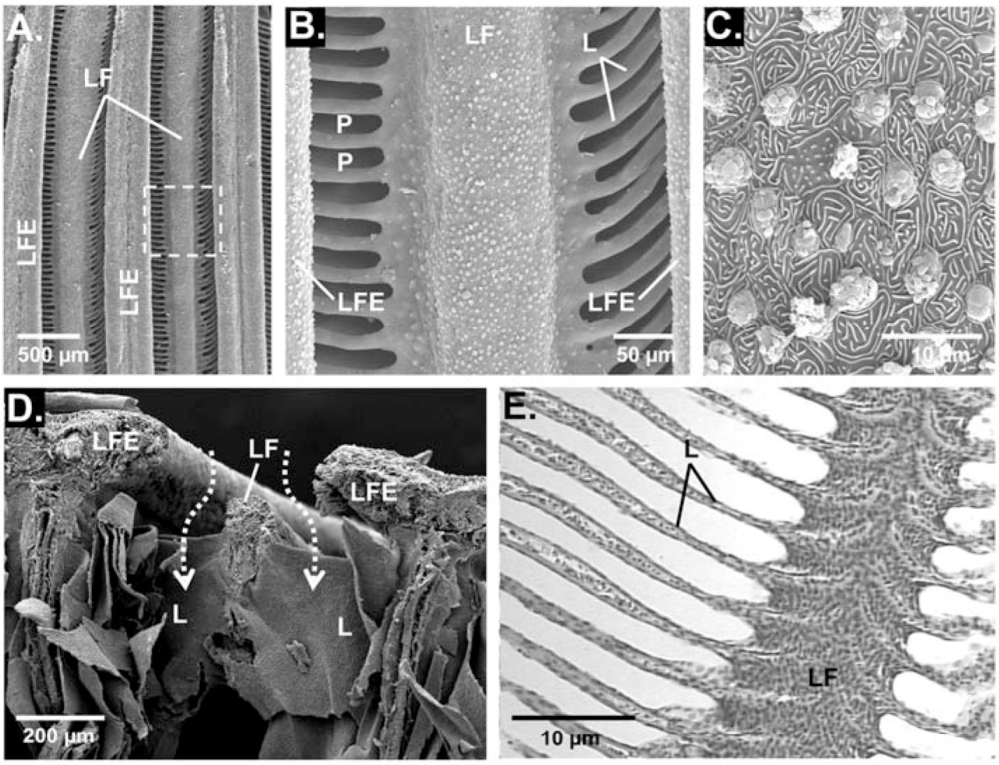

Figure 4. SEM and light microscope images of the lamellar fusion of yellowfin tuna (*Thunnus albacares*) **A:** View of the leading edge of adjacent filaments (y-plane, refer to Fig. 2A). **B:** Magnified view of the dashed box in A revealing the pores formed by the lamellar fusion. **C:** Further magnification of the lamellar fusion showing the high concentration of mucous cell pores on the leading epithelial surface. **D:** Cross-section through the leading edges of adjacent filaments showing the lamellar fusion (x-plane). **E:** Cross-section through the lamellar fusion revealing the lateral lamellar edges embedded in the fusion (y-plane). Dotted arrows show the direction of water flow. Water flow is into the page in A–C, E. A–C are from a 15.3 kg yellowfin, D,E are from a 49.2 kg specimen. Abbreviations: L, lamellae; LF, lamellar fusion; LFE, leading filament edge; P, lamellar pore.

have an angle of approximately 60° relative to the long-axis (Fig. 5B, Table 1). These diagonal channels empty into a single inner marginal channel (IMC) (Fig. 5B).

Striped marlin possess diagonal lamellar vascular channels similar to those of tunas; however, blood entry into the lamellae is unique (Fig. 5C). The afferent lamellar arteriole bifurcates and forms both the inner and outer marginal channels. Blood channels leaving the IMC flow toward the lateral edge, where some channels follow the OMC along the lateral edge, while others return inward and recombine with the IMC (Fig. 5C). For the majority of the lamellar length, blood leaves the OMC and flows medially inward at about 40° to the long-axis (Fig. 5C, Table 1); this angle is greater than that determined for a single specimen by Muir and Brown (1971). In contrast to yellowfin and striped marlin, wahoo have a more typical teleost design; blood flows through lamellar vascular channels that run parallel to the lamellar long-axis (Fig. 5D). Wahoo pillar cells are also spaced farther apart forming larger vascular channels (Fig. 5D).

Table 1. Comparison of microvascular characteristics in the gills of three high-performance teleosts and the rainbow trout, *Oncorhynchus mykiss* (Walbaum, 1792). Rainbow trout data are from Muir and Brown (1971)[a] and Hughes (1972)[b]. Measurements are ± standard deviation. *Measured from a 4.3 kg specimen.

Species	W (kg)	Lamellar thickness (μm)	Water-blood barrier distance (μm)	Average angle of lamellar blood flow	# of lamellae per mm filament
Tetrapturus audax	45	6.29 ± 1.36	0.531 ± 0.153	40°	25.47 ± 2.05
Acanthocybium solandri	19.4	5.16 ± 1.21	0.860 ± 0.170	0°	32.21 ± 2.14
Thunnus albacares	14.5	5.88 ± 0.99	0.537 ± 0.092	60°*	33.37 ± 1.15
Oncorhynchus mykiss	–	35[b]	6[b]	0°[a]	17[b]

Discussion

This study describes structural specializations in the gills of striped marlin and wahoo. While we note general similarities for these fishes and tunas in terms of adaptations for enhancing gas exchange across the lamellar surface and sustaining gill rigidity during ram ventilation, we document a fundamentally different inter-lamellar fusion in striped marlin and wahoo.

Filament Fusions.—Previous reports on gill structure noted fusions connecting adjacent filaments on the same hemibranch in billfishes, wahoo, and in the tuna genus *Thunnus* (Lütken, 1880; Trois, 1883; Kishinouye, 1923; Bevelander, 1934; Conrad, 1938; Muir and Kendall, 1968; Johnson, 1986). Muir and Kendall (1968) reported that these filament fusions, which usually occur on both the leading and trailing filament edges (Fig. 1A), are formed by extensions of the filament epithelium. However, Johnson (1986) subsequently showed that in billfishes and wahoo, filament fusions on the trailing edge are strengthened by cartilaginous extensions of the filament rods. Johnson (1986) further showed that billfish and wahoo filaments and filament fusions on both the leading and trailing edges are covered by bony epithelial toothplates (Fig. 2B,G,H), which may further stiffen the filaments and reinforce the fusions. In contrast, *Thunnus* filament fusions are solely composed of epithelial tissue and are not strengthened by cartilaginous fusions of the filament rods or by bony toothplates (Johnson, 1986).

Lamellar Fusions.—In tunas, lamellar fusions connect the leading edge of juxtaposed lamellae on the same filament to opposing lamellae on the adjacent filament (Figs. 1, 4; Muir and Kendall, 1968). Lamellar fusions thus maintain the distance between adjacent lamellae (pore width) which, as suggested by hydrodynamic models for skipjack tuna gills, is optimized for effective O_2 extraction while minimizing drag (Brown and Muir, 1970; Stevens and Lightfoot, 1986). Because lamellar fusions incorporate lamellae from adjacent filaments, they also prevent filaments from being separated during ram ventilation; this is particularly important for the smaller body-sized tuna genera (i.e., *Auxis*, *Euthynnus*, and *Katsuwonus*), which completely lack filament fusions (Muir and Kendall, 1968; Muir, 1969). Lamellar fusions may also play an important role in securing adjacent filaments in *Thunnus*, as the filament fusions on the leading edge generally do not extend to the filament tips, and appear absent on the leading edge in both blackfin, *Thunnus atlanticus* (Lesson, 1831) (Muir and Kendall, 1968) and albacore, *Thunnus alalunga* (Bonnaterre, 1788) (Wegner, unpubl. data).

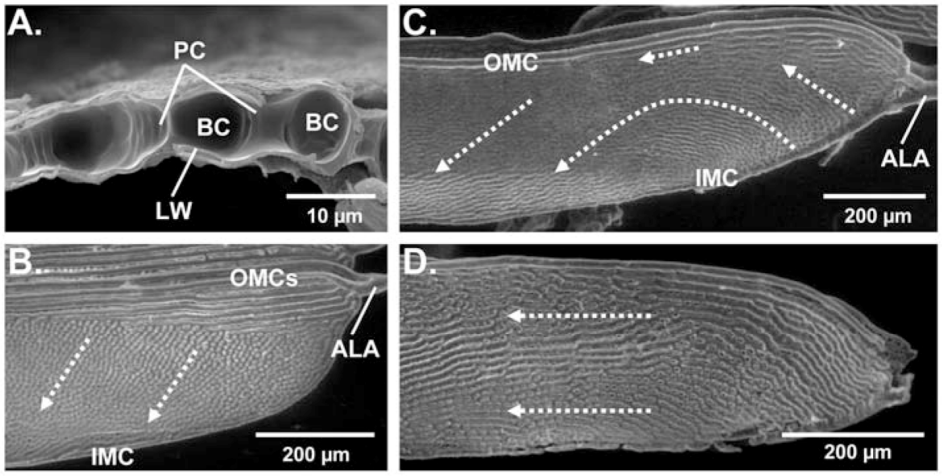

Figure 5. SEM images of the lamellar vasculature. **A:** Cross-section through a striped marlin (45 kg) lamella showing the blood channels formed by pillar cells. Vascular replica casts of the lamellae are shown for **B:** a 4.3 kg yellowfin tuna, **C:** a 45 kg striped marlin, and **D:** a 15.3 kg wahoo. Dotted arrows show the direction of blood-flow through the exchange surfaces. Water flow is from left to right in B–D. Abbreviations: ALA, afferent lamellar arteriole; BC, blood channel; IMC, inner marginal channel; LW, lamellar wall (water-blood barrier distance); OMC, outer marginal channel; PC, pillar cell.

Inter-lamellar Fusions.—The inter-lamellar fusion of the striped marlin extends along the leading lateral edge of adjacent lamellae on the same filament and secures their relative position (Fig. 2). This creates rigid pores similar to those formed by lamellar fusions (compare Fig. 2E with 4B). Although wahoo lamellae are not always completely fused and are thus less rigid, the thick lateral lamellar edges (Fig. 3C,D) may still help to maintain pore integrity.

The major difference between inter-lamellar and lamellar fusions is that inter-lamellar fusions do not connect with the lamellae on the adjacent filament (compare Fig. 2D with 4A). Thus, the inter-lamellar fusion serves solely to secure lamellar pore width, while the lamellar fusion also secures the filament-to-filament distance. Because striped marlin and wahoo have stronger filament fusions [supported by both cartilage and bony epithelial toothplates (Johnson, 1986)], a complete lamellar fusion may be less crucial to secure adjacent filaments. How tuna, striped marlin, and wahoo filament, lamellar, and inter-lamellar fusion patterns compare in their effect on water resistance through the gill sieve is unknown.

The structural composition of inter-lamellar fusions in striped marlin and wahoo is nearly identical to that of tuna lamellar fusions. Both fusions are composed of stratified epithelium with mucous cells comprising the leading edge. A mucus covering of the gill epithelia likely reduces water drag through the gill sieve (Daniel, 1981) and would thus be important for lamellar and inter-lamellar fusions that turn and guide water flow into lamellar pores. Nutrient supply to lamellar and inter-lamellar fusions appears to be from the outer (lateral) lamellar vascular channels, which near the leading (efferent) edge, are embedded within the fusion (Figs. 2L, 3F, 4E).

Our findings suggest that the lateral lamellar edges may play a role in the formation of lamellar and inter-lamellar fusions. In all three species examined, the lateral lamellar edges embedded in the fusion are turned toward the distal end of the

filament, minimizing the distance between neighboring lamellae (Figs. 2L, 3F, 4E). In wahoo, the leading lateral edges of non-fused lamellae are turned toward their neighbors and often possess epithelial extensions, which appear to be bridging the inter-lamellar space (Fig. 3C,D). If the inter-lamellar fusions of wahoo are in the formation process this may explain their irregularity along the length of the filaments. However, we did not observe any notable differences in the frequency of fused lamellae with an increase in wahoo body mass (14.6–24.2 kg). Examination of a larger size range of wahoo may reveal a trend in lamellar fusing and body size.

Finally, some remarks are warranted regarding the apparent similarities between lamellar fusions in tunas and those which occur in the primitive, freshwater, air-breathing bowfin, *Amia calva* Linnaeus, 1766 (Bevelander, 1934; Daxboeck et al., 1981; Olson, 1981). In *Amia*, lamellar fusions appear to maintain gill rigidity during air exposure. *Amia* lamellar fusions are structurally different than those of tunas in that the lateral lamellar edges are bound for their entire length, not just near the leading edge. Also, the outer lamellar vascular channels embedded in the fusion do not appear to turn toward the tip of the filament (Olson, 1981) as seen in tunas.

Tuna Microvasculature.—Tunas have thin lamellae and thin lamellar walls that minimize diffusion distances for effective gas exchange (Table 1; Hughes, 1970; Muir and Brown, 1971). Unlike most teleosts, the configuration of tuna pillar cells forces blood through the lamellae in a unique diagonal progression (Fig. 5B; Muir, 1970; Muir and Brown, 1971; Olson et al., 2003). Pressure drop (δp) through a tube can be minimized by increasing channel diameter or decreasing channel length as shown by the Hagen-Poiseuille equation:

$$\delta p = (32\mu Vl)/d^2 \text{ (dynes cm}^{-2}\text{)}$$

where μ is viscosity, V equals the mean velocity, l is the channel length, and d equals the channel diameter. Muir and Brown (1971) proposed that the short, diagonal vascular channels of tuna lamellae minimize vascular pressure drop while maintaining small channel diameters (short diffusion distances). Other relatively large teleosts (Atlantic cod, *Gadus morhua* Linnaeus, 1758, and Atlantic salmon, *Salmo salar* Linnaeus, 1758) appear to minimize pressure drop though large lamellae by increasing the diameter of the vascular channels, which consequently increases diffusion distances and likely decreases gas exchange efficiency (Muir and Brown, 1971).

The diagonal progression of tuna lamellae also increases the number of respiratory blood channels in parallel. Assuming the blood is fully saturated in these short, oblique channels, this ultimately increases functional gill area for gas exchange (Muir, 1970). Even though lamellar blood flow is diagonal, Brown and Muir (1970) suggested that contours influencing the flow pattern of water passing between adjacent lamellae may still result in a counter-current flow. However, this has not been substantiated.

Striped Marlin and Wahoo Microvasculature.—The thickness of striped marlin and wahoo lamellae and lamellar walls (the water-blood barrier distance) are comparable to measurements determined for yellowfin and other tuna species (Table 1; Hughes, 1970) and are much thinner than those documented for most other fishes (Hughes and Morgan, 1973). Striped marlin have converged with tunas for diagonal lamellar vascular channels, although this characteristic appears more fully developed in the latter (compare Fig. 5B with 5C). Thin lamellar walls may be particu-

larly important to tuna and striped marlin because their oblique channels reduce red blood cell (RBC) residence times through the lamellae (Olson et al., 2003). Although wahoo lamellae appear as thin as those of tunas and striped marlin (Table 1), they do not possess shortened diagonal channels (Fig. 5D). The added resistance of channel length appears to be compensated by larger spaces between the pillar cells. Increased RBC residence times through longer wahoo lamellar channels may account for the slightly thicker lamellar walls than those found in striped marlin and yellowfin (Table 1).

If the main function of oblique lamellar blood flow is to minimize blood pressure drop while maintaining thin lamellae (short diffusion distances) and to increase the number of respiratory blood channels in parallel, it remains unclear why diagonal channels occur in Atlantic mackerel, *Scomber scombrus* Linnaeus, 1758 (Muir and Brown, 1971), but not in wahoo (which possess much larger lamellae and likely have greater aerobic demands). Also unexplained is why yellowfin and striped marlin have diagonal channels in the short lamellae near the filament tips. A more detailed comparative study of channel design in these and other high-performance fishes may provide additional insight into these discrepancies.

Tunas possess the largest relative gill surface areas documented (Muir and Hughes, 1969), and preliminary data indicate that the gill areas of striped marlin and wahoo are also relatively large compared to most marine teleosts (Wegner, unpubl. data). The increase in gill surface area for these high-performance fishes is largely the result of their reduced lamellar thickness which increases the number of lamellae per length filament (Table 1). Thus, the combination of increased gill surface areas, thin lamellae, and thin lamellar walls, greatly enhances gas exchange in these high-performance fishes.

Phylogeny.—The relationship of *Acanthocybium* and the billfishes within the suborder Scombroidei has been controversial, and only a brief account will be presented here. Early osteological studies showed that *Acanthocybium* is more similar to the Scombridae (tunas, bonitos, Spanish mackerels, mackerels) than the billfishes (Istiophoridae + *Xiphias*) (Gregory and Conrad, 1937; Conrad, 1938). Similarly, based on morphological characters, Collette et al. (1984) placed the wahoo within the Scombridae as sister group to *Scomberomorus* (Spanish mackerels) and placed the billfishes as sister group to the Scombridae. Johnson (1986) subsequently proposed an alternative hypothesis, in which billfishes are the sister group to *Acanthocybium* and included in the Scombridae (wahoo + billfishes are proposed as the sister group to *Scomberomorus*). Johnson (1986) based his hypothesis on several synapomorphic traits of *Acanthocybium* and the billfishes including: an elongate beaklike snout, the loss of gill rakers, cartilaginous gill filament fusions, and the investment of the gill filaments with bony epithelial toothplates. Johnson (1986) argued that these characters (with the exception of the loss of gill rakers) are unique among perciforms, and are less likely to occur within separate lines than the skeletal changes that separate the billfishes from the wahoo. The inter-lamellar fusion documented in this study is thus another synapomorphy that links the Istiophoridae to *Acanthocybium*. Despite this finding, recent studies based on both morphological and genetic data call for billfishes to be placed in a separate suborder from the Scombroidei (Orrell et al., 2006).

If the billfishes are in fact the sister group to wahoo, the inter-lamellar fusions of striped marlin and wahoo may be of the same origin as the lamellar fusions of tu-

nas. To our knowledge the status of lamellar and inter-lamellar fusions in the genera separating *Acanthocybium* from the tunas has never been documented. However, we note that lamellar fusions (similar to those of tunas) are present for the Eastern Pacific bonito, *Sarda chiliensis* (Cuvier, 1832) (Wegner, unpubl. data).

Acknowledgments

This research was supported by the California Sea Grant, the William H. and Mattie Wattis Harris Foundation, the University of California, San Diego Academic Senate, the Tuna Industry Endowment Fund at Scripps Institution of Oceanography, the Pfleger Institute of Environmental Research, and the George T. Pfleger Foundation. This work would not have been possible without the help and support of Tom Pfleger. We thank T. Rothery and crew of the Polaris Supreme, S. Aalbers, M. Domeier, J. Donley, T. Fullam, and N. Sepulveda who were instrumental in specimen acquisition. Special thanks are extended to S. Aalbers, N. Lai, and K. Olson who helped in the vascular casting process and E. York who aided in the use of the SEM. We additionally thank D. Johnson and one anonymous reviewer for their comments on this manuscript, and D. Cartamil, B. Collette, and K. Olson who reviewed early versions of the work. Finally, we thank the International Billfish Symposium, its organizing committee, and the Offield Center for Billfish Studies.

Literature Cited

Beerkircher, L. R. 2005. Length to weight conversions for wahoo, *Acanthocybium solandri*, in the Northwest Atlantic. Col. Vol. Sci. Papers ICCAT 58: 1616–1619.

Bevelander, G. 1934. The gills of *Amia calva* specialized for respiration in an oxygen deficient habitat. Copeia 1934: 123–127.

Brill, R. W. and A. E. Dizon. 1979. Effect of temperature on isotonic twitch of white muscle and predicted maximum swimming speeds of skipjack tuna, *Katsuwonus pelamis*. Env. Biol. Fish. 4: 199–205.

Brown, C. E. and B. S. Muir. 1970. Analysis of ram ventilation of fish gills with application to skipjack tuna (*Katsuwonus pelamis*). J. Fish. Res. Board Can. 27: 1637–1652.

Chatwin, B. M. 1959. The relationships between length and weight of yellowfin tuna (*Neothunnus macropterus*) and skipjack tuna (*Katsuwonus pelamis*) from the eastern tropical Pacific Ocean. Inter-Amer. Trop. Tuna Comm. Bull. 3: 305–352.

Collette, B. B., T. Potthoff, W. J. Richards, S. Ueyanagi, J. L. Russo, and Y. Nishikawa. 1984. Scombroidei: development and relationships. Pages 591–620 *in* H. G. Moser, W. J. Richards D. M. Cohen, M. P. Fahay, A. W. Kendell, and S. L. Richardson, eds. Ontogeny and systematics of fishes. Amer. Soc. Ichthyol. Herp. Spec. Pub. No. 1.

Conrad, G. M. 1938. The osteology and relationships of the wahoo (*Acanthocybium solandri*), a scombroid fish. Am. Mus. Novit. 1000: 1–32.

Daniel, T. L. 1981. Fish mucus: In situ measurements of polymer drag reduction. Biol. Bull. 160: 376–382.

Daxboeck, C., D. K. Barnard, and D. J. Randall. 1981. Functional morphology of the gills of the bowfin, *Amia calva* L., with special reference to their significance during air exposure. Respir. Physiol. 43: 349–364.

Freadman, M. A. 1981. Swimming energetics of striped bass (*Morone saxatilis*) and bluefish (*Pomatomus saltatrix*): hydrodynamic correlates of locomotion and gill ventilation. J. Exp. Biol. 90: 253–265.

Gregory, W. K. and G. M. Conrad. 1937. The comparative osteology of the swordfish (*Xiphias*) and the sailfish (*Istiophorus*). Am. Mus. Novit. 952: 1–25.

Hughes, G. M. 1970. Morphological measurements on the gills of fishes in relation to their respiratory function. Folia Morphol. Prague 18: 78–95.

_____. 1972. Morphometrics of fish gills. Resp. Physiol. 14: 1–26.
_____. 1984. General anatomy of the gills. Pages 1–72 *in* W. S. Hoar and D. J. Randall, eds. Fish Physiology. Vol. 10A Academic Press, Orlando. 456 p.
_____ and M. Morgan. 1973. The structure of fish gills in relation to their respiratory function. Biol. Rev. Camb. Philos. Soc. 48: 419–475.
Johnson, G. D. 1986. Scombrid phylogeny: an alternative hypothesis. Bull. Mar. Sci. 39: 1–41.
Jones, D. R. and D. J. Randall. 1978. The respiratory and circulatory systems during exercise. Pages 475–543 *in* W. S. Hoar and D. J. Randall, eds. Fish Physiology Vol. 7. Academic Press, London. 576 p.
Kishinouye, K. 1923. Contributions to the comparative study of the so-called scombroid fishes. J. Coll. Agric. Imp. Univ. Tokyo 8: 293–475.
Lütken, C. F. 1880. Spolia Atlantica. Dansk. Vid. Selsk. Skrift. 12: 409–613.
Muir, B. S. 1969. Further observations on gill modifications of oceanic fishes. Copeia 1969: 629.
_____ 1970. Contribution to the study of blood pathways in teleost gills. Copeia 1970: 19–28.
_____ and C. E. Brown. 1971. Effects of blood pathways on the blood-pressure drop in fish gills, with special reference to tunas. J. Fish. Res. Board Can. 28: 947–955.
_____ and G. M. Hughes. 1969. Gill dimensions for three species of tunny. J. Exp. Biol. 51: 271–285.
_____ and J. I. Kendall. 1968. Structural modifications in the gills of tunas and some other oceanic fishes. Copeia 1968: 388–398.
Olson, K. R. 1981. Morphology and vascular anatomy of the gills of a primitive air breathing fish, the bowfin (*Amia calva*). Cell Tissue Res. 218: 499–517.
_____ 1996. Scanning electron microscopy of the fish gill. Pages 31–45 *in* J. S. D. Munshi and H. M. Dutta, eds. Fish Morphology. Horizon of New Research. Science Publishers Inc., Lebanon. 300 p.
_____, H. Dewar, J. B. Graham, and R. W. Brill. 2003. Vascular anatomy of the gills in a high energy demand teleost, the skipjack tuna (*Katsuwonus pelamis*). J. Exp. Zool. 297A: 17–31.
Orrell, T. M., B. B. Collette, and G. D. Johnson. 2006. Molecular data support separate scombroid and xiphioid clades. Bull. Mar. Sci. 79: 505–520.
Roberts, J. L. and D. M. Rowell. 1988. Periodic respiration of gill-breathing fishes. Can. J. Zool. 66: 182–190.
Stevens, E. D. and E. N. Lightfoot. 1986. Hydrodynamics of water flow in front of and through the gills of skipjack tuna. Comp. Biochem. Physiol. 83A: 255–259.
Trois, E. F. 1883. Osservazioni sull' intima struttura delle branchie del *Xiphias gladius*. Atti Istit. Sci. Venezia. 1: 773–785.

Addresses: (N.C.W, J.B.G.) *Center for Marine Biotechnology and Biomedicine and Marine Biology Research Division, Scripps Institution of Oceanography, University of California, San Diego, 9500 Gilman Dr. La Jolla, California 92093-0204.* (C.A.S.) *Pfleger Institute of Environmental Research, 901-B Pier View Way Oceanside, California 92054.* Corresponding Author: (N.C.W.) *E-mail: <nwegner@ucsd.edu>.*

The appendix chapter, in full, was published as: Wegner NC, Sepulveda CA, Graham JB. 2006. Gill specializations in high-performance pelagic teleosts, with reference to striped marlin (*Tetrapturus audax*) and wahoo (*Acanthocybium solandri*). Bull Mar Sci 79:747-759. The dissertation author is the primary investigator and author of this paper.